3. SITE 582[1]

Shipboard Scientific Party[2]

HOLE 582

Date occupied: 28 June 1982

Date departed: 29 June 1982

Time on hole: 10 hr., 58 min.

Position (latitude; longitude): 31°46.51′N, 133°54.83′E

Water depth (sea level; corrected m, echo-sounding): 4879

Water depth (rig floor; corrected m, echo-sounding): 4882

Bottom felt (m, drill pipe): 4892

Penetration (m): 29.1

Number of cores: 4

Total length of cored section (m): 38.8

Total core recovered (m): 18.18

Core recovery (%): 47

Oldest sediment cored:
Depth sub-bottom (m): 29.1
Nature: Hemipelagic mud and ash
Age: Quaternary

Principal results: See Summary and Conclusions section.

HOLE 582A

Date occupied: 30 June 1982

Date departed: 30 June 1982

Time on hole: 5 hr., 53 min.

Position (latitude; longitude): 31°46.51′N, 133°54.83′E

Water depth (sea level; corrected m, echo-sounding: 4879

Water depth (rig floor; corrected m, echo-sounding): 4882

Bottom felt (rig floor; m, drill pipe): 4892

Penetration (m): 48.5

Number of cores: 2

Total length of cored section (m): 19.4

Total core recovered (m): 16.26

Core recovery (%): 84

Oldest sediment cored:
Depth sub-bottom (m): 48.5
Nature: Hemipelagic mud and silty sand
Age: Quaternary

Principal results: See Summary and Conclusions section.

HOLE 582B

Date occupied: 1 July 1982

Date departed: 7 July 1982

Time on hole: 141 hr., 18 min.

Position (latitude; longitude): 31°46.51′N, 133°54.83′E

Water depth (sea level; corrected m, echo-sounding): 4879

Water depth (rig floor; corrected m, echo-sounding): 4882

Bottom felt (rig floor; m, drill pipe): 4892

Penetration (m): 749.4

Number of cores: 73

Total length of cored section (m): 700.9

Total core recovered (m): 284.7

Core recovery (%): 41

Oldest sediment cored:
Depth sub-bottom (m): 749.4
Nature: Mudstone
Age: Pliocene
Measured velocity (km/s): 1.86

Principal results: See Summary and Conclusions section.

BACKGROUND AND OBJECTIVES

Background

Knowledge of convergent plate boundaries is rapidly increasing, in large part because of the recent International Phase of Ocean Drilling (IPOD) cruises of the Deep Sea Drilling Project. Leg 87 is the last of this series of *Glomar Challenger* cruises devoted to investigation of the problems of active margin tectonic processes. A wide range of mechanical responses, ranging from accretion of incoming sediment to tectonic erosion of the forearc, has been postulated or recognized. Efforts are now being focused on the recognition of the characteristics of the different responses along this spectrum. The gross structure of the accretionary end member is best delineated by high-quality seismic reflection profiles. That internal structure of the predicted accretionary prisms

[1] Kagami, H., Karig, D. E., Coulbourn, W. T., et al., *Init. Repts. DSDP*, 87: Washington (U.S. Govt. Printing Office).

[2] LEG 87A: Hideo Kagami (Co-Chief Scientist), Ocean Research Institute, University of Tokyo, 1-15-1 Minamidai, Nakano, Tokyo 164, Japan; Daniel E. Karig (Co-Chief Scientist), Department of Geological Sciences, Cornell University, Ithaca, New York 14853; William T. Coulbourn (Science Representative), Deep Sea Drilling Project, Scripps Institution of Oceanography, University of California at San Diego, La Jolla, California 92093 (present address: Hawaii Institute of Geophysics, University of Hawaii, 2525 Correa Road, Honolulu, Hawaii 96822); Cynthia J. Bray, Department of Geological Sciences, Cornell University, Ithaca, New York 14853; Jacques Charvet, Sciences de la Terre, ERA 601, Université d'Orléans, 45046 Orléans, France; Hajimu Kinoshita, Department of Earth Science, Faculty of Science, Chiba University, Chiba 280, Japan; Martin Lagoe, ARCO Exploration Company, Denver, Colorado 80217 (present address: Department of Geologic Science, University of Texas at Austin, Austin, Texas 78712); Thomas H. Lang, Department of Geology, Florida State University, Tallahassee, Florida 32306; Gail A. Lombari, Graduate School of Oceanography, University of Rhode Island, Kingston, Rhode Island 02881; Neil Lundberg, Earth Sciences Board, University of California, Santa Cruz, Santa Cruz, California 95064 (present address: Department of Geological and Geophysical Sciences, Princeton University, Princeton, New Jersey 08544); Tsutomu Machihara, Technology Research Center, Japan National Oil Corporation, 3-5-5 Midorigaoka, Hamura-cho, Nishitama-gun, Tokyo 190-11, Japan; Prasanta K. Mukhopadhyay, Institüt für Erdöl und Organische Geochemie (ICH-5), P.O. Box 1913, Kernforschungsanlage Jülich GmbH, D-5170 Jülich 1, Federal Republic of Germany; Alec J. Smith, Department of Geology, Bedford College, University of London, London NW1 4N5, United Kingdom; Carol L. Stein, Earth Sciences, Division 6331, Sandia National Laboratories, Albuquerque, New Mexico 87185; and Asahiko Taira, Department of Geology, Kochi University, Kochi 780, Japan (present address: Ocean Research Institute, University of Tokyo, 1-15-1 Minamidai, Nakano, Tokyo 164, Japan).

has proven difficult to obtain by drilling because commonly it lies beneath very deep water and is characterized by poor hole conditions resulting from the generally clastic and brittle nature of its constituent sediments and sedimentary rocks.

The Nankai Trough (Fig. 1) is considered an accreting trench system and has become an important drilling target for several reasons, the most graphic of which was the production of a processed multichannel reflection profile that very clearly outlined large-scale structural framework of the toe of the landward slope (Fig. 2). The shallow depth of the Nankai Trough, caused by subduction of Miocene crust of the Shikoku Basin, places most of the objectives within range of the drill. Previous deep-sea drilling at Site 298 on the inner slope of the Nankai Trough demonstrated that the relatively fine-grained sediments can produce quite stable hole conditions (Ingle, Karig, et al., 1975b). This drill site also revealed anomalously rapid compaction and development of structural fabric, which suggested that a detailed and more quantitative study of the physical and mechanical properties of this sediment might be scientifically rewarding.

Subduction is proceeding relatively slowly in the Nankai Trough. Previously estimated convergence rates range from 2 cm/yr. based on geologic data (Karig, Ingle, et al., 1975) to over 5 cm/yr. based on seismologically determined slip vectors (Fitch and Scholz, 1971; Seno, 1977). Subduction has occurred along this plate boundary, at least intermittently, since sometime in the Mesozoic. Evidently, the present pulse of subduction began after the opening of the Shikoku Basin (early to middle Miocene), but the exact timing and magnitude of subduction since, as well as the location of the present Eurasian-Philippine pole of rotation, are uncertain. The subduction rate in the Nankai Trough may have increased over the past few million years, producing the discrepancy between geologically and seismologically determined rates.

The sediments entering this trench include about 700 m of (Shikoku) basin strata overlain by trench wedge deposits that vary in thickness along the arc. In the vicinity of the proposed sites, the trench wedge has a maximum thickness of about 0.75 km. The forearc of the Nankai system appears on reflection profiles to be typical of that proposed for "accreting arcs." The lower

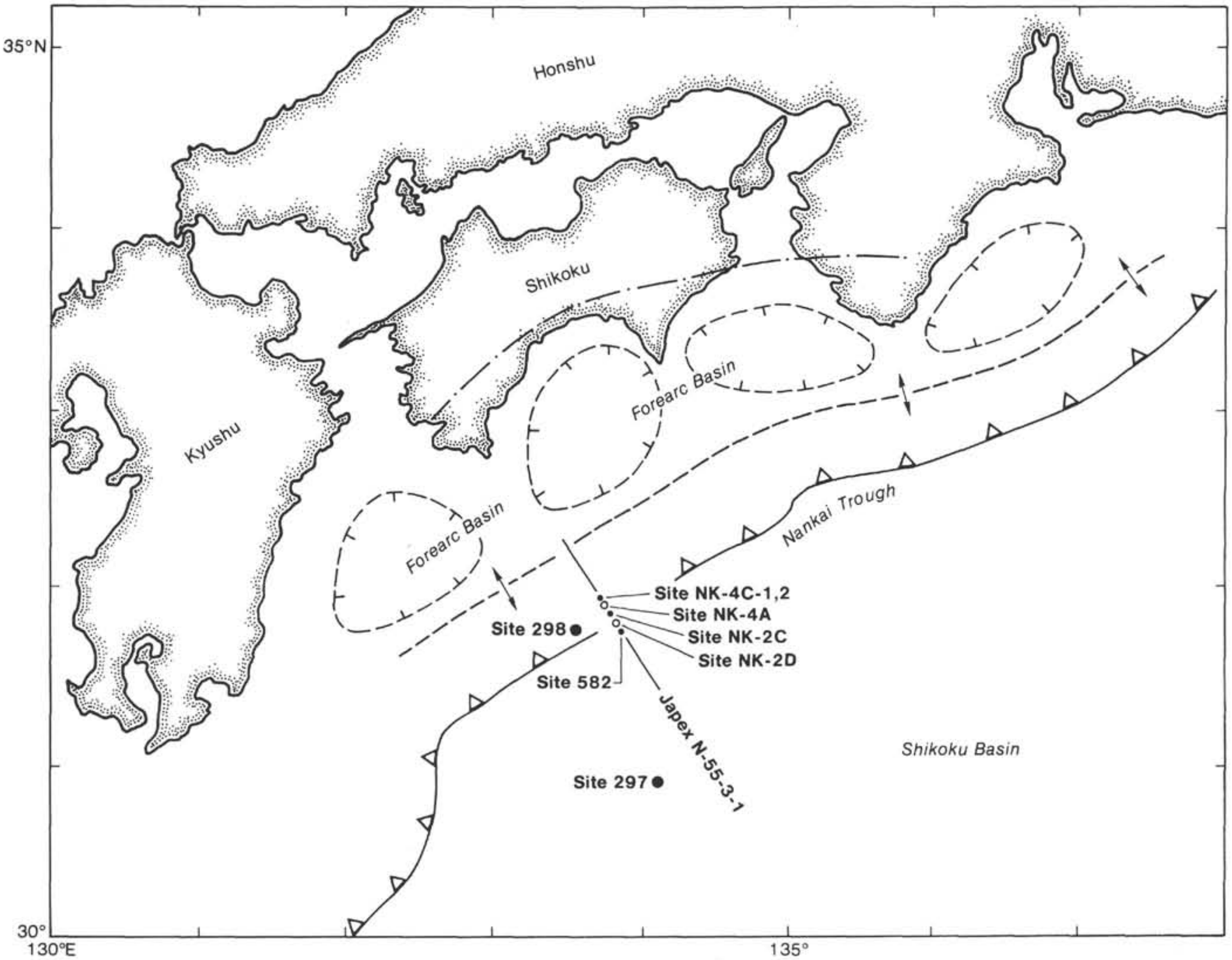

Figure 1. Location of prime (dot) and of alternate (circle) drilling sites proposed for Nankai Trough.

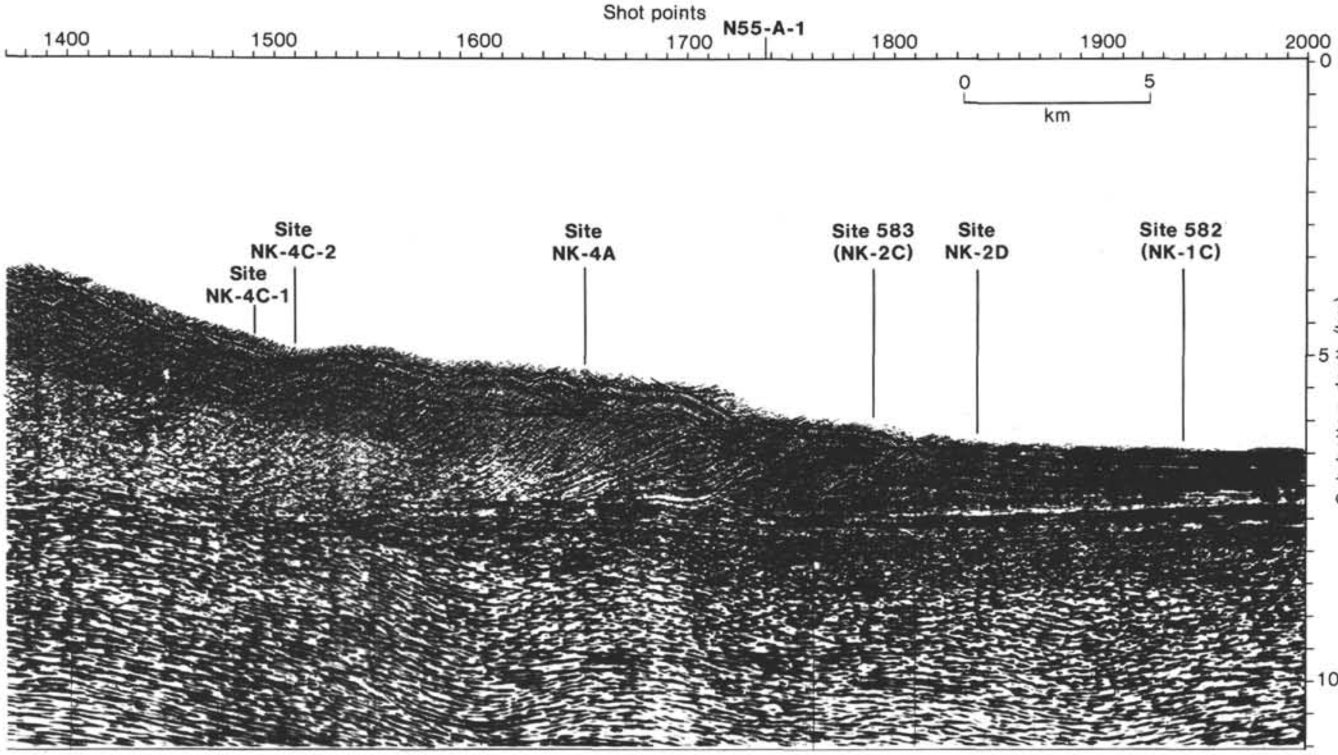

Figure 2. Ocean Research Institute seismic Profile N55-3-1 across the lower part of the inner slope of the Nankai Trough showing locations of proposed drill sites.

trench slope displays well-developed ridges with some small linear slope basins. Behind the trench slope break is the Tosa Terrace, the upper surface of a segmented forearc basin. Flanking this basin to the north is the sharply uplifted Shimanto Terrane, a Cretaceous to Neogene subduction complex, of Shikoku Island.

During DSDP Leg 31, two sites were drilled near the Nankai margin (Fig. 1). Site 297 penetrated most of the sediment fill in the Shikoku Basin just south (seaward) of the trench, and Site 298 was drilled on the first terrace of the inner trench slope (Ingle, Karig, et al., 1975b). Site 297 afforded information about the sediments similar to those now known to underlie the toe of the landward slope (Fig. 2), but Site 298 provided the most interesting information relating to subduction processes. This hole (611 m deep) penetrated only Quaternary sediments. Except for the uppermost 100 m, the drilled sequence was thought to represent trench turbidites. These sediments are of predominantly fine-grained clastics, generally fining downward. The upper 100 m consists of a less consolidated and poorly sampled sequence of pebbly mudstones, sands, and silts. Although they were interpreted as slope sediments, they could also represent a slump apron at the inner edge of the trench floor, as has since been recognized in several other arcs (Moore et al., 1980). The entire section displays a more rapid reduction in porosity with depth than at nearby sites drilled in more slowly deposited, undeformed basinal sections. Because there was no evidence of overburden removal, this assumed anomalously rapid porosity reduction was attributed to some form of tectonic, stress-induced dewatering. A distinct foliation in finer-grained sediments below 300 m was interpreted to represent axially planar or fanning cleavage related to an overturned, nearly recumbent anticline defined by inverted strata below 500 m.

Interest in the Nankai Trough increased dramatically after the acquisition of multichannel reflection profiles, which displayed "accretionary structures" with greater clarity than seen in similar profiles from most other arcs. In particular, Profile N55-3-1 illustrates in detail the style of deformation at the base of the slope (Fig. 2). The migrated sections delineate individual faults and locate the main décollement with precision. Along the décollement, trench-filling strata are selectively sheared off the descending plate as tabular thrust sheets that become part of the overlying mass, thought to be an imbricate stack. Each sheet, bounded by major thrust surfaces, is approximately 1 km thick and 5 km wide but, in addition, is thickened internally by minor thrusts.

The seismic profile suggests that subsequent accretion not only rotates the earlier emplaced thrust sheets but also, in classic thrust-belt style, folds the upper thrust sheet into hanging-wall anticlines. Further upslope, acoustic coherence within the prism is lost, but the slope sediments thicken and form several small basins. The sediments in one such basin show a marked arcward tilt and are delimited on the landward side by a sharp discontinuity, probably a thrust fault.

The profile also reveals that the structure of Site 298 was misinterpreted. Instead of the overturned anticline depicted in the Leg 31 volume (Karig, Ingle, et al., 1975), the section drilled was basically an upright thrust slice. The several indications of overturned beds near the base of that hole might instead have represented small-scale drag folds associated with a thrust that seems to have been penetrated near 500 m. If so, then these slip surfaces could be successfully penetrated by drilling in the Nankai system.

Objectives

The major objectives of drilling at Site 582 cannot be separated from those at Site 583, for which Site 582 will provide a reference section for structure, stratigraphy, and physical properties. These objectives can be summarized as (1) subduction dynamics and mechanics; (2) subduction zone kinematics and evolution; and (3) subduction zone sedimentation.

1. *Subduction dynamics and mechanics.* The existence of a seismic profile on which the structural framework associated with a subduction zone is so clearly delineated provides a unique opportunity to investigate the mechanical and physical properties of the deforming sediments as functions of position in the displacement field. A major goal is to measure porosity, pore pressure, structural fabric, and other physical characteristics of sediments at a pair of drill sites, one located in front of the deformation front (Site 582) and the other drilled through the toe of the landward slope (Site 583). A comparison of experimental work on cores from these sites with results of rock and soil mechanics experiments should narrow down the nature of the stress field and the behavior of pore waters under such circumstances. The holes near the base of the trench are, in large part, vehicles for a series of structural, geophysical, and geochemical experiments.

2. *Kinematics and evolution.* Understanding the mechanical response of the forearc region to convergence requires the calculation of displacements and their distribution across the forearc. Studies of several subduction zones suggest that most of the crustal shortening at a subducting boundary occurs near the trench, but this conjecture remains a qualitative conclusion. Other arguments debate the trajectories of rock and sediment within the subduction zone: how much rock and sediment is accreted, subducted to mantle depths, or subcreted to the base of the prism? What factors govern this distribution?

We had anticipated that a combination of data from the reflection profiles and other geophysical investigations, together with drill hole determination of sediment accumulation rates, rates of uplift, and tectonic setting, would add considerably to our understanding of trench kinematics. We also had hoped to eliminate some of the uncertainties surrounding the Neogene subduction history of the Nankai system through the dating of any accreted material at several points across the prism and by analysis of sedimentation rates in the trench as a function of time.

3. *Sedimentation processes.* The cored section at Site 582 can be converted to horizontal facies distribution from the site southward if steady-state tectonic and sedimentologic conditions over the past 1 Ma are assumed. Variable subduction rates and Quaternary climatic effects are thought to be of secondary importance here, but do temper our steady-state assumption. The acoustic character of strata displayed on Profile N55-3-1 suggests that the facies changes from trench to outer slope and that basinal deposits should dominate (Fig. 2). Site 582 also provides an opportunity to clarify the nature of the unusual fan assemblages represented by trench wedges.

A subsidiary, yet important, sedimentologic objective for Site 582 is to corroborate and expand the tephrochronologic record of the Quaternary in southwestern Japan.

Other objectives that have been identified for the Nankai sector include studies of paleoceanography of the Kuroshio, organic geochemistry of clathrates (which define a strong bottom simulating reflector beneath much of the trench slope), heat flow, and the nature of the pore waters in a zone of deforming and dewatering sediments.

OPERATIONS

The *Glomar Challenger* was scheduled to depart Yokohama, Japan, on 24 June 1982. Difficulty in repairing the thruster and generator motors, however, delayed our departure until 0320Z on 25 June 1982. After steaming southward, we passed between Miyake Island and Nii Jima (island) and started underway geophysical observations including: 12-kHz echo-sounder, 3.5-kHz bottom profiler, seismic reflection profiler using both 120-cu.-in. and 60-cu.-in. Bolt air guns, as well as a total magnetic force recorder. Our track was generally seaward of the axis of the Nankai Trough (Fig. 3). While we were en route to Site 582, at approximately 1500Z, the seismic reflection profile revealed a central rift of the Shikoku Basin plate at Magnetic Anomaly 5C. An offset basement high in the middle of the trough is located approximately between the 2130Z and the 2300Z time lines. At the end of this track, we approached about 6 mi. to the east-northeast (74°) of Site 582 at approximately 0115Z, slowed to 6 knots, received a satellite fix at 0152Z, and dropped the beacon at 0217Z on 27 June. We proceeded another 2 mi. west-southwest (254°), then turned north, retrieved the geophysical gear, and returned to the site. The final location for the drill site is 31°46.51′N, 133°54.83′E, slightly north of the planned position at Shot Point (SP) 1940 on Profile N55-3-1 (Fig. 2), but outside the deformation front of the landward slope of the Nankai Trough (Fig. 4).

Drill pipe run-in began at 0342Z on 27 June, and the first mudline core penetrated the bottom at 2000Z on 29 June (Table 1). Some time was lost because of a premature release of the hydraulic bit. The first core established the mudline depth and indicated a drill-string length of 4882 m, which agreed with the precision depth recorder (PDR) depth to within 3 m. After three cores had been drilled, the bottom-hole assembly (BHA) was lost below the head sub. The loss was probably caused by a strong current that forced the vessel nearly 300 m off site as it made a large heading change to compensate for a sudden wind shift.

The first core of Hole 582A was collected at 0825Z on 30 June. Before spudding Hole 582A, the making-up of the BHA and retorquing of joints of some of the stands resulted in a loss of time. After two cores were

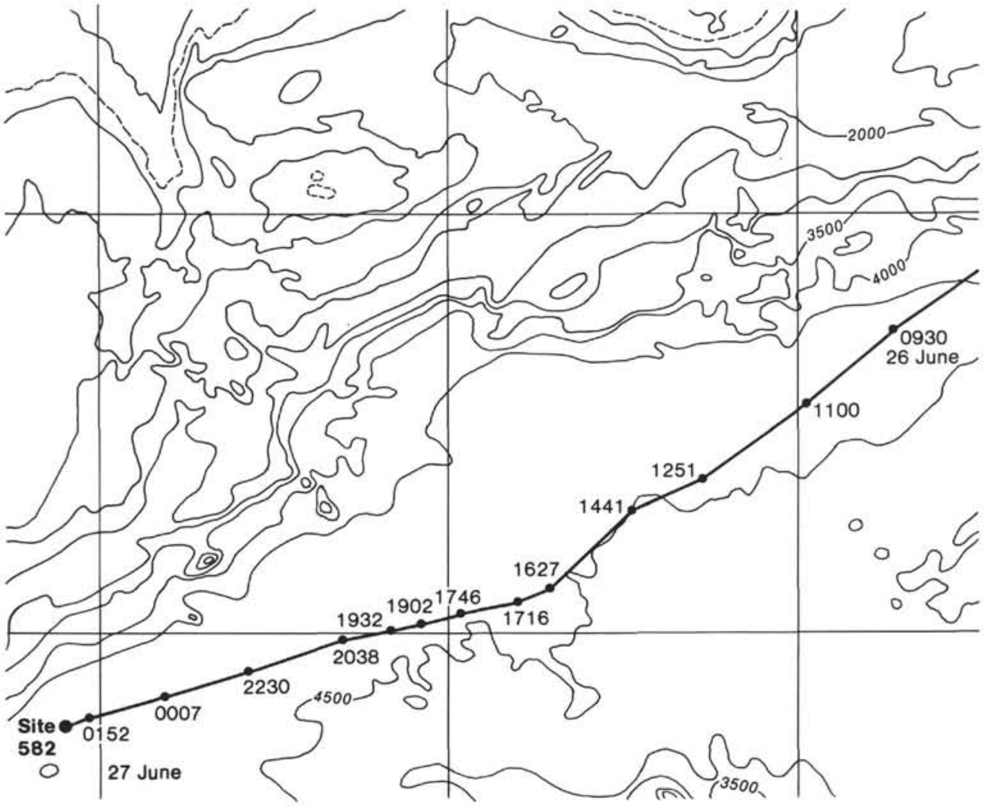

Figure 3. Approach track line of *Glomar Challenger*, en route from Yokohama to Site 582. Numbers along the track line indicate time in GMT.

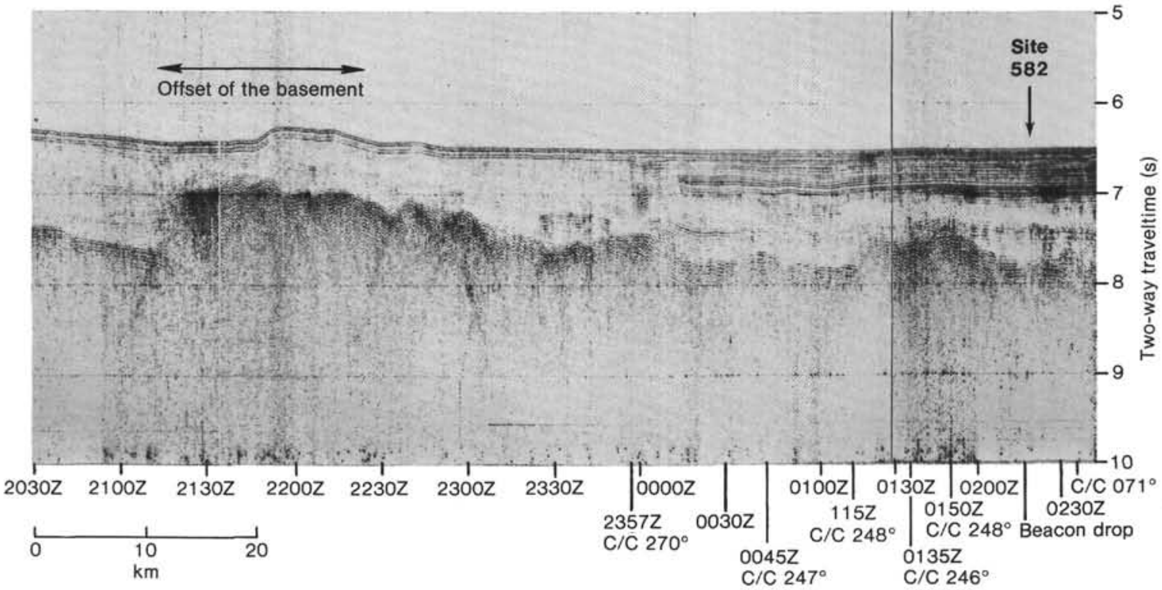

Figure 4. Location of Site 582 on *Glomar Challenger* single-channel seismic reflection profile. C/C = course change.

drilled, the first heat flow–pore water probe was successfully operated, but pore water was not collected because of mashed tubing in the probe. Subsequently, the hole was abandoned for the safety of the BHA during installation of the heave compensator.

The first core of Hole 582B was collected at 1722Z on 30 June after the hole was washed to the total depth of Hole 582A. Heat flow–pore water probes were made between each set of five cores. The third attempt successfully measured heat flow at 145 m sub-bottom, but the pipe stuck at the end of measurement; for safety reasons, heat flow measurements were deferred for a period of time. Thereafter, between each set of ten cores, a single shot was lowered on a wire line to measure the

Table 1. Coring summary, Site 582.

Core	Date (1982)	Time (L)[a]	Depth from drill floor (m)	Depth below seafloor (m)	Length cored (m)	Length recovered (m)	Percent recovered
Hole 582							
1	6/29	0630	4892.0–4901.7	0.0–9.7	9.7	9.14	94
2	6/29	0856	4901.7–4911.4	9.7–19.4	9.7	0	0
3	6/29	1048	4911.4–4921.1	19.4–29.1	9.7	9.04	93
4	6/29		4921.1–4930.8	29.1–38.8	9.7	0	0
					38.8	18.18	47
Hole 582A							
0	6/30		4892.0–4921.1	0.0–29.1	Drilled		
1	6/30	1725	4921.1–4930.8	29.1–38.8	9.7	6.63	68
2	6/30	1912	4930.8–4941.5	38.8–48.5	9.7	9.63	99
					19.4	16.26	84
Hole 582B							
0	7/1		4892.0–4941.5	0.0–48.5	Drilled		
1	7/1	0222	4941.5–4951.2	48.5–58.2	9.7	0.07	0
2	7/1	0355	4951.2–4959.9	58.2–67.9	9.7	6.38	66
3	7/1	0534	4959.9–4969.6	67.9–77.6	9.7	4.68	48
4	7/1	0710	4969.6–4979.3	77.6–87.3	9.7	0	0
5	7/1	0843	4979.3–4988.9	87.3–96.9	9.6	4.07	42
6	7/1	1300	4988.9–4998.5	96.9–106.5	9.7	Trace	—
7	7/1	1445	4998.5–5008.1	106.5–116.1	9.6	10.69	111
8	7/1	1631	5008.1–5017.8	116.1–125.8	9.7	3.98	41
9	7/1	1810	5017.8–5027.5	125.8–135.5	9.7	2.41	25
10	7/1	1950	5027.5–5037.2	135.5–145.2	9.7	8.83	91
11	7/2	0010	5037.2–5046.8	145.2–154.8	9.6	0.14	1
12	7/2	0215	5046.8–5056.4	154.8–164.4	9.6	1.36	14
13	7/2	0400	5056.4–5066.0	164.4–174.0	9.6	0.62	6
14	7/2	0545	5066.0–5075.6	174.0–183.6	9.6	9.62	100
15	7/2	0725	5075.6–5085.2	183.6–193.2	9.6	3.88	51
16	7/2	0855	5085.2–5094.8	193.2–202.8	9.6	3.68	38
17	7/2	1040	5094.8–5104.5	202.8–212.5	9.7	0.45	5
18	7/2	1235	5104.5–5114.2	212.5–222.2	9.7	7.88	81
19	7/2	1415	5114.2–5123.9	222.2–231.9	9.7	8.25	85
20	7/2	1555	5123.9–5133.5	231.9–241.5	9.6	3.94	41
21	7/2	1745	5133.5–5143.1	241.5–251.1	9.6	4.48	47
22	7/2	1935	5143.1–5152.7	251.1–260.7	9.6	6.19	64
23	7/2	2123	5152.3–5162.3	260.7–270.3	9.6	7.61	79
24	7/2	2315	5162.3–5171.9	270.3–279.9	9.6	1.80	19
25	7/3	0115	5171.9–5181.5	279.9–289.5	9.6	7.99	83
26	7/3	0315	5181.5–5191.1	289.5–299.1	9.6	6.31	66
27	7/3	0440	5191.1–5200.7	299.1–308.7	9.6	0	0
28	7/3	0620	5200.7–5210.3	308.7–318.3	9.6	0	0
29	7/3	0800	5210.3–5219.9	318.3–327.9	9.6	2.53	26
30	7/3	0945	5219.9–5229.5	327.9–337.5	9.6	7.31	76
31	7/3	1130	5229.5–5239.1	337.5–347.1	9.6	1.62	17
32	7/3	1330	5239.1–5248.5	347.1–356.5	9.4	3.66	39
33	7/3	1502	5248.5–5257.9	356.5–365.9	9.4	4.97	53
34	7/3	1658	5257.9–5267.3	365.9–375.3	9.4	2.11	22
35	7/3	1850	5267.3–5276.8	375.3–384.8	9.5	0	0
36	7/3	2040	5276.8–5286.3	384.8–394.3	9.5	1.60	17
37	7/3	2240	5286.3–5295.8	394.3–403.8	9.5	2.89	30
38	7/4	0041	5295.8–5305.2	403.8–413.2	9.4	5.28	56
39	7/4	0233	5305.2–5314.6	413.2–422.6	9.4	9.13	97
40	7/4	0430	5314.6–5324.0	422.6–432.0	9.4	2.43	26
41	7/4	0625	5324.0–5333.5	432.0–441.5	9.5	7.02	74
42	7/4	0820	5333.5–5343.0	441.5–451.0	9.5	7.51	79
43	7/4	1015	5343.0–5352.5	451.0–460.5	9.5	Trace	—
44	7/4	1210	5352.5–5362.0	460.5–470.0	9.5	2.39	25
45	7/4	1355	5362.0–5371.5	470.0–479.5	9.5	0.22	2
46	7/4	1705	5371.5–5381.0	479.5–489.0	9.5	0.50	5
47	7/4	2030	5381.0–5390.6	489.0–498.6	9.6	0.97	10
48	7/5	0130	5390.6–5400.2	498.6–508.2	9.6	1.21	13
49	7/5	0355	5400.2–5409.8	508.2–517.8	9.6	Trace	—
50	7/5	0620	5409.8–5419.4	517.8–527.4	9.6	9.60	100
51	7/5	0817	5419.4–5429.0	527.4–537.0	9.6	2.12	22
52	7/5	1005	5429.0–5438.6	537.0–546.6	9.6	5.37	56
53	7/5	1203	5438.6–5448.3	546.6–556.3	9.7	0.15	2
54	7/5	1425	5448.3–5458.0	556.3–566.0	9.7	1.21	12
55	7/5	1620	5458.0–5467.7	566.0–575.7	9.7	6.01	62
56	7/5	1835	5467.7–5477.3	575.7–585.3	9.6	1.66	17
57	7/5	2022	5477.3–5486.9	585.3–594.9	9.6	6.89	72
58	7/5	2250	5486.9–5496.5	594.9–604.5	9.6	8.24	86
59	7/6	0130	5496.5–5506.1	604.5–614.1	9.6	4.71	49
60	7/6	0400	5506.1–5515.7	614.1–623.7	9.6	3.26	34
61	7/6	0600	5515.7–5525.3	623.7–633.3	9.6	5.05	53
62	7/6	0800	5525.3–5534.9	633.3–642.9	9.6	5.52	58
63	7/6	1000	5534.9–5544.5	642.9–652.5	9.6	4.66	49
64	7/6	1240	5544.5–5554.1	652.5–662.1	9.6	9.55	99
65	7/6	1500	5554.1–5563.8	662.1–671.8	9.7	0.92	9
66	7/6	1705	5563.8–5573.5	671.8–681.5	9.7	3.90	41
67	7/6	1929	5573.5–5583.2	681.5–691.2	9.7	2.76	28
68	7/6	2210	5583.2–5592.9	691.2–700.9	9.7	2.34	24
69	7/7	0030	5592.9–5602.6	700.9–710.6	9.7	0.16	2
70	7/7	0245	5602.6–5612.3	710.6–720.3	9.7	2.91	30
71	7/7	0510	5612.3–5622.0	720.3–730.0	9.7	1.18	12
72	7/7	0720	5622.0–5631.7	730.0–739.7	9.7	0.94	10
73	7/7	1010	5631.7–5641.4	739.7–749.4	9.7	2.10	22
					700.9	284.70	41

[a] Time in this table is expressed as local time. To convert to Z time (Zulu times given in text), subtract 9 hours from local time. Dash indicates that only a trace was recovered.

pipe angle. Angles of 5 and 4.5° were recorded at Cores 582B-13 and 582B-23.

By 0805Z on 4 July, the pipe had reached 489.0 m sub-bottom (Core 582B-46) and core recovery had become very low. A bit deplugger was sent down to check the bit condition. When it was retrieved, a drilling mixture of mud and sand was recovered (center bit Core X1, located between Cores 582B-46 and 582B-47). Circulation pressure indicated that the core barrel was seated properly at the bit, and the material recovered undoubtedly represented drill cuttings that had been suspended in the annulus of the hole.

After Core 582B-47 was taken, we decided to run a final heat flow–pore water probe, because the results of the previous measurements were uncertain and because the condition of the hole had improved. The probe was successfully retrieved from 498.5 m sub-bottom and a temperature measurement was obtained, but the pore-water sampler was not used because of the induration of sediment.

When firm distal turbidites were encountered at Core 582B-49 at a depth of 518 m sub-bottom, the hole angle was 8°. While we were drilling from this depth down to 585 m sub-bottom (Core 582B-56), the hole filled with shaly cuttings and sand, and we encountered some difficulties in clearing it. Cutting breccia filled Core 582B-56. Mud flushes were frequently required to clear the hole. Another single shot was lowered to measure the pipe angle, and an angle of 8.5° was recorded at 585 m sub-bottom (Core 582B-56).

After Core 582B-57, the greater proportion of hemipelagic mudstone increased the recovery to more than 5 m per core. Some slight decrease in the diameter of the recovered cores, such as Core 582B-64, led to suspicion of bit damage, but a core of normal diameter was recovered from below.

By 0600Z on 6 July, the pipe reached 671.8 m sub-bottom (Core 582B-65), and the recovery rate decreased, perhaps because of slightly stronger than normal fluid pressure. Large concentrations of drilling breccia persisted, however, and in Core 582B-66 cutting-fill was recovered at the very top of the barrel, preventing normal core samples from entering. This observation (and weight and torque indications) suggested that cuttings had reached a thickness of 10 to 12 m between each coring attempt, adversely affecting recovery rate.

An angle of 7° was recorded in Core 582B-68 at 700.9 m sub-bottom depth, indicating a stable inclination of the pipe. At a depth of 730.0 m sub-bottom nannofossil Zone NN18 was reached, marking the top of the Pliocene; having completed our objectives, we decided to stop drilling at 0110Z on 7 July. The last core, Core 582B-73, penetrated to 749.4 m sub-bottom.

Failure of the hydraulic-bit release after two attempts prevented logging Hole 582B. The drill string was pulled on deck by 1751Z on 7 July, terminating operations at Site 582. When the BHA was retrieved on deck, examination of the hydraulic-bit release mechanism showed that it had been rendered inoperative because of jamming by drill cuttings.

SEDIMENTOLOGY

Description of Lithologic Units

The lithology at the Site 582 reflects the role of the Nankai Trough as a repository for hemipelagic sediments, sediment gravity flows, and eolian deposits from volcanic episodes on the Japanese island arc. We recognize two lithologic units constituting the 749.4 m cored at the three holes drilled at Site 582, and these are summarized in Figure 5. Sand layers are more frequent in the upper 530 m of the column and virtually absent below the boundary between Units 1 and 2. The relative abundance of sand, indicated by such parameters as sand percentage in smear slides and maximum thickness of the sand layer in the core, enable us to subdivide Unit 1 into nine parts: four sandy parts and five muddy parts (see shaded patterns to the right of the Polarity column, Fig. 5). Volcanogenic plagioclase and glass are common throughout the sequence with a slight tendency to increase in frequency in the upper part of Units 1 and 2, reflecting the number of ash layers encountered. The $CaCO_3$ content and total carbon content seem to be slightly higher in Unit 1 than 2, but the organic carbon content is almost constant throughout sequence. Diatoms are present above but virtually absent below 450 m sub-bottom. Calcareous nannoplankton specimens are found throughout the column except in a microfossil-barren zone between 530 and 590 m sub-bottom.

Unit 1: Hemipelagic and Sandy Mud (0 to 566 m sub-bottom)

This unit (Cores 528-1 to 582B-54) consists of dark olive gray (5Y 3/2) hemipelagic mud and sandy mud, including graded beds. This dark gray (5Y 3/2) hemipelagic mud with intercalated sandy and silty intervals is yet another example of a facies common to most circum-Pacific trench axes and landward slopes (see Scientific Party, 1980; Watkins, Moore, et al., 1981; Aubouin, von Huene, et al., 1982). According to DSDP convention (see Explanatory Notes chapter, this volume), hemipelagic sediments are distinguished by a terrigenous component in excess of 30%, a total nonbiogenic component in excess of 40%, and a biogenic silica content in excess of 10%. The sediments of Unit 1 between 450 and 560 m barely meet the latter criterion.

The sediments of Unit 1 are gassy, and the uppermost 50 m emitted a strong odor of H_2S. Spotty concentrations of pyrite attest to a reducing environment; in the uppermost 350 m cracks, bubbles, and numerous gaps and voids are common.

The hemipelagic mud and sandy mud drilled at Holes 582 and 582A and in the uppermost 100 m of Hole 582B was badly deformed by rotary drilling. Well-preserved counterparts of these sediments are perhaps represented in graded beds of Cores 33 to 42 (356 to 451 m sub-bottom). The best preserved cycles show basal layers of pumice-bearing sand or silty sand, grading upward into silt and finally into *Chondrites*-rich clayey intervals (Fig. 6). Apparently, as hemipelagic sedimentation in this basin proceeded, either (1) the "trace-makers" migrated away from a stagnating environment, or (2) diagenesis might not have proceeded far enough to sharply define their structures; it is also possible that drilling-induced deformation obscured their tracks. Irrespective of cause, the uppermost clay-rich layers within each turbidite cycle of this unit are generally barren of lebenspürren, but commonly show parallel dark laminations. Other trends typical of these graded sequences are summarized in Figure 7.

Hemipelagic mud and fine-grained turbidites make up the bulk of this lithologic unit. The mud contains silt-size and clay-size grains and varying amounts of microfossils. Generally, siliceous microfossils are better represented than their calcareous counterparts. Diatoms are present from 0 to 425 m sub-bottom, after which they occur only sparsely. Sponge spicules are concentrated in sporadic white patches (Sample 582B-7-2, 140–141 cm) that at first glance resemble small blebs of volcanic ash. Radiolarians are most common in the muds immediately beneath coarser-grained intervals. Foraminifers and calcareous nannofossils are rare in these deep-water muds, although nannofossils were quite abundant in Sample 582B-42-1, 80–81 cm. The clay also contains white ash layers at Samples 582B-8-3, 30–31 cm; 582B-19-4, 8–9 cm; and 582B-20-2, 90–91 cm. Volcanic ash is disseminated throughout the section in various quantities, reaching a maximum of about 50% in parts of Core 582B-19, and that contribution produces a markedly lighter color. Drilling disturbance erased any fine structures such as cross-bedding, parallel laminations, and any burrows that might have been present in the uppermost 200 m. In contrast, below that depth, particularly beginning with Core 582B-29, *Chondrites*, dark black spots, and laminations are obvious.

Sand and silt beds are common in Unit 1. Sandy intervals are numerous between 25 and 125 m sub-bottom; some show grading. Below Core 582B-8 (125 m sub-bottom), sands give way to silty horizons and the former are not recovered again until Core 582B-29 to 582B-44 (325 to 470 m sub-bottom), where they are abundant and contain large pumice grains. These pumice-bearing sands are generally graded, as shown in Figure 6. Grains within the coarse layers are angular through rounded. Some of the sand-size grains are probably fecal pellets. The sandy and silty intervals of Unit 1 contain a variety of heavy minerals; a partial list includes hornblende, biotite, apatite, epidote, glaucophane, pyroxenes, and zircon. The center bit core (Core 582B-X1), located between Cores 582B-46 and 582B-47, contained abundant red volcanic fragments. Foraminifers are the most common biogenic components of these coarse-grained intervals, but even these are not abundant. Calcareous benthic foraminifers indicate a variety of depths, all of considerably shallower character (even including transported fresh-water diatoms) than the 4882 m depth of their present location (see Biostratigraphy section).

Smear-slide estimates of the percent of the sand fraction within the coarse-grained beds suggest a general downhole decrease in sand content from Cores 582-1 to 582B-26 (0–300 m sub-bottom). Migration of submarine channels in the Japanese margin, Pleistocene climatic fluctuations, plate motion, or a combination of these

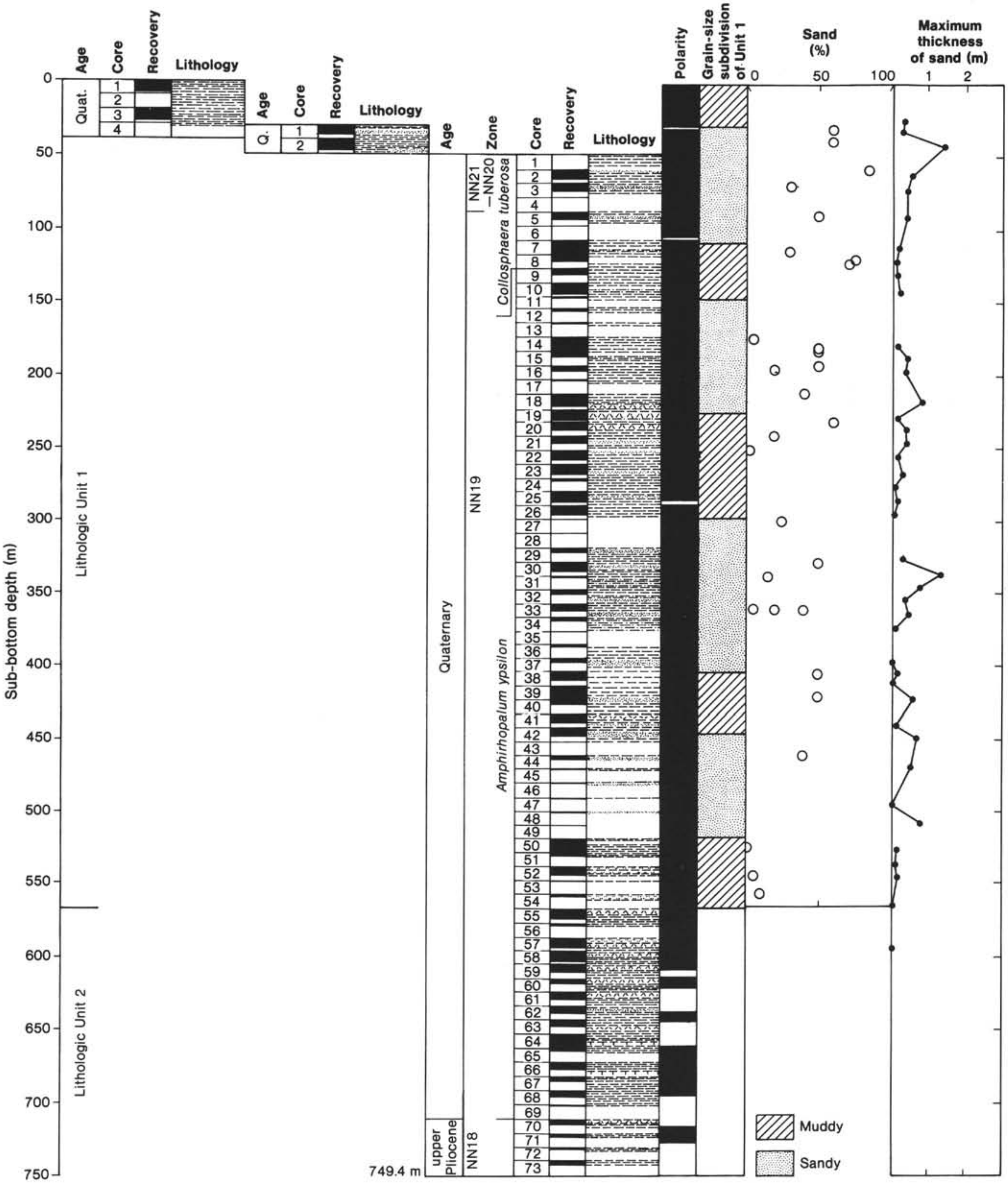

Figure 5. Summary lithology, magnetic polarity, and smear-slide estimates for Site 582. For lithologic symbols, see Explanatory Notes chapter (this volume). Shaded patterns indicate Unit 1 subdivisions based on grain size. In last four columns ▲ = trace. This figure was constructed by the Scientific Party of Leg 87B (see Footnote 2, site chapter, Site 584, this volume).

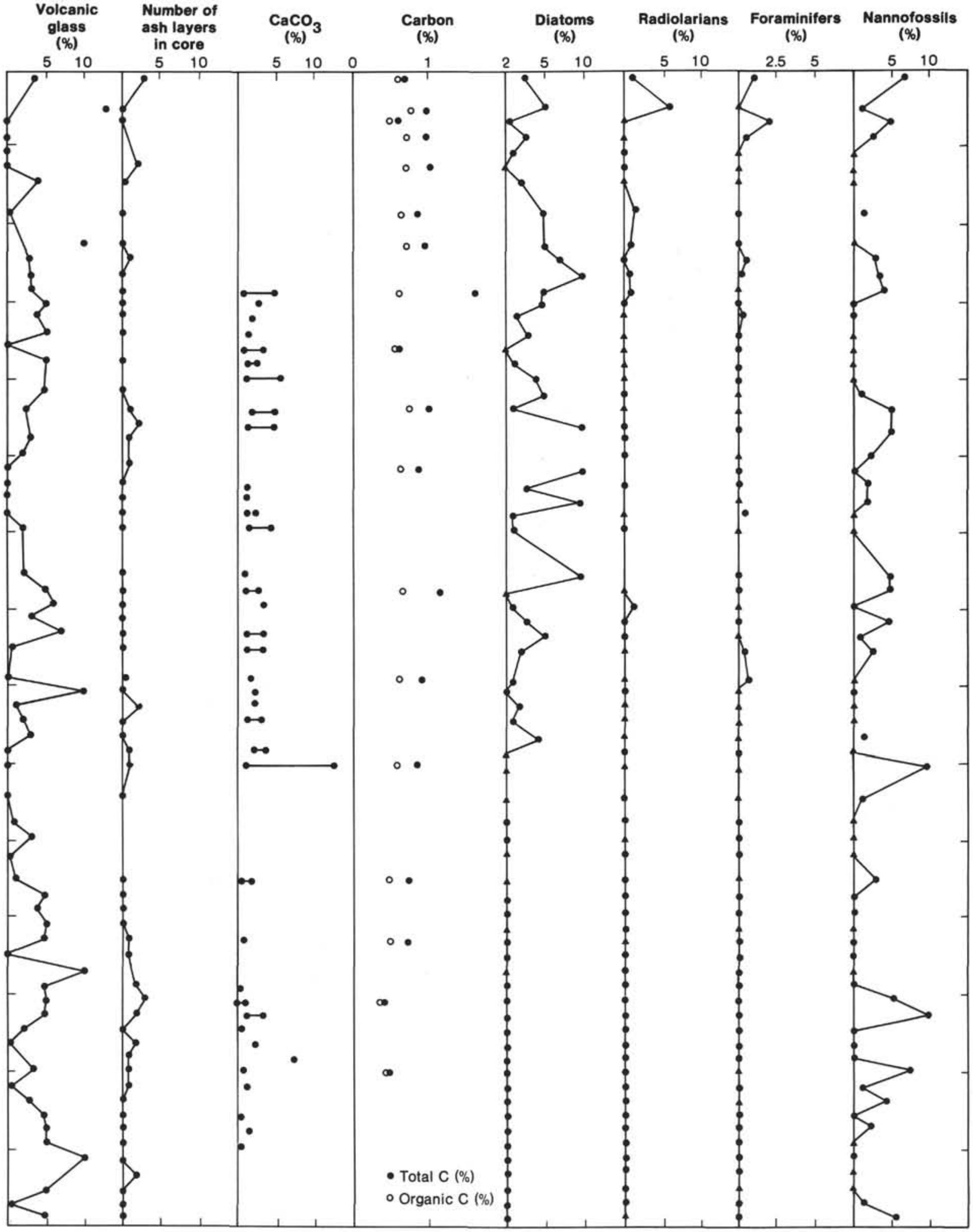

Figure 5. (Continued).

and other factors might have produced this fining-downward trend. Plate motion, however, is the least likely cause because coarser-grained layers reappear in Cores 582B-29 to 582B-44 (300–462 m sub-bottom).

Sporadic recovery at Site 582 may have been related to the lithology and lack of induration of Unit 1. Sediment was firm enough to begin saw-cutting at Core 582B-22 (254 m sub-bottom), and at that depth details previously obscured by wire-cutting became apparent. Incipient fissility, *Chondrites*, and laminations are recorded downhole, beginning at Core 582B-22. Drill biscuits were first apparent in Core 582B-26 (295 m sub-

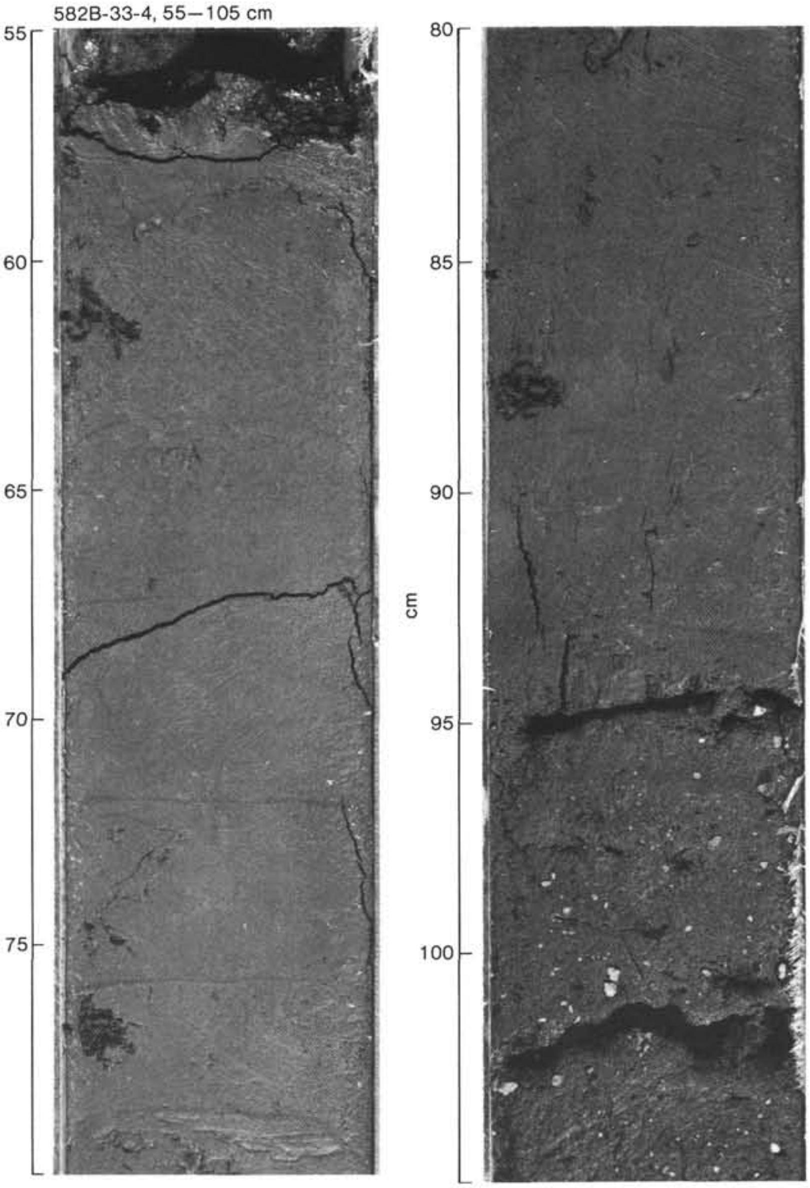

Figure 6. Pumice-bearing turbidite of Core 582B-33.

bottom), immediately preceding an interval of poor recovery (Cores 582B-27 and 582B-28, 299 to 318 m sub-bottom) and became common beneath Core 582B-36 (400 m sub-bottom). Drill breccia first appeared in Core 582B-44 (460 m sub-bottom) and constitutes the bulk of the sediment in Cores 582B-46 and 582B-47 (480 to 499 m sub-bottom), an interval of very poor recovery. After a total lack of recovery in Core 582B-49, Core 582B-50 (518 m sub-bottom) was the first to contain sample sufficiently indurated to merit the designation mudstone. Prominent seismic reflectors occur near 200, 300, 410, 490, and 570 m sub-bottom. The 300 and 490 m reflectors correspond to the induration contrasts noted above. They also correspond to intervals of poor recovery, which may indicate sandy intervals lost during the coring process (see Seismic Stratigraphy section).

Unit 2: Hemipelagic Mudstone (566 to 749.4 m sub-bottom)

Unit 2 (Cores 582B-55 to 582B-73) consists of dark gray (5Y 3/2 to 4/1) hemipelagic mudstone.

A seismic reflector, placed between 540 and 580 m sub-bottom, may mark the top of Unit 2. The lithologic change occurs between Cores 582B-52 and 582B-55 (537 to 566 m sub-bottom), but, because it falls in an interval of poor recovery, the exact nature of the contact remains unknown. We use the modifier "hemipelagic" in a broad sense because Unit 2 lacks the coarse-grained constituents of Unit 1, imparting a more pelagic aspect to it in spite of low concentrations of siliceous microfossils. Details of the facies of Unit 2 are summarized in Figure 8. Sediments of Unit 2 differ from those of Unit 1 in their

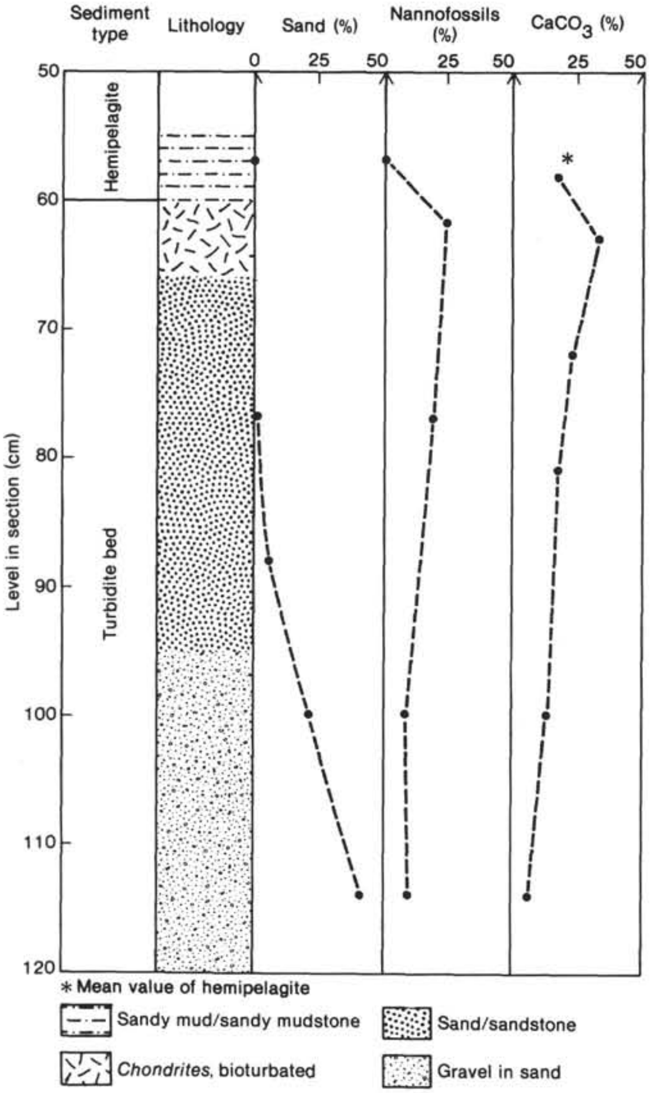

Figure 7. Example of a typical Site 582 turbidite (Section 582B-33-4).

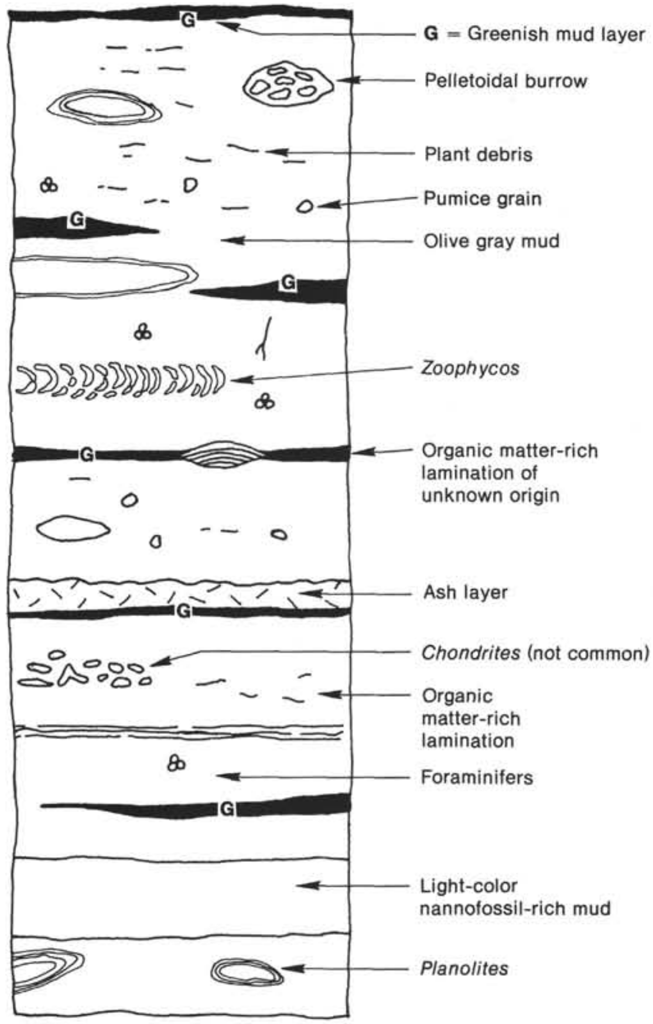

Figure 8. Idealized summary sketch of features observed in Lithologic Unit 2 of Site 582.

slightly green tint and color alternations, lack of coarse silt and sand layers, lack of graded-bed *Chondrites* sequences, abundance of zoophycid and planolitid traces, abundance of green laminations, presence of numerous pumice clasts isolated in a mudstone matrix, and the sparse occurrence of lighter-colored, nannofossil-rich blebs and intervals.

Quartz is generally present in excess of 10% and volcanic glass is disseminated throughout the unit. Only locally is glass present in sufficient concentration to produce easily recognizable white layers; an exception is the ash layer in Core 582B-61 (626 m sub-bottom). Alternations of color are common in Unit 2. These 2-to-5-cm thick cycles of dark greenish gray (5G 5/1) and dark brownish gray (5GY 4/1) staining are best developed in Core 582B-64 (652.5–662.1 m sub-bottom).

The most prominent secondary structures in Unit 2 are normal faults (Fig. 9) and dewatering conduits. The former are best seen in Cores 62, 63, and 64 of Hole 582B, where they offset burrows. (See Structural Geology section for details).

Provenance of Site 582 Turbidites

The sediments studied from Holes 582 and 582A, and particularly the coarse fraction of these sediments, were rich in lithic fragments up to 40% of silt-size and sand-size particles. Inspection of smear slides and thin sections prepared of unconsolidated coarse sands indicates that the main components of these lithic fragments are chert, argillite, and volcanic rock, especially andesites. In the heavy mineral component, volcanic derivatives such as pyroxene and hornblende are also common. These minerals and rock assemblages suggest some constraints for the sediment provenance of Nankai Trough turbidites.

The Outer Zone of southwestern Japan is composed of three major geologic terranes: metamorphic rocks in the Sambagawa Belt; sandstone, shale, chert, limestone, and basalt in both the Chichibu and the Shimanto belts. The lithic components, such as chert and argillite, and a part of heavy mineral suits, such as epidote and glaucophane, were possibly derived from these terranes. The volcanic components, which probably compose 30 to 40% of total lithic fragments, however, could not be derived

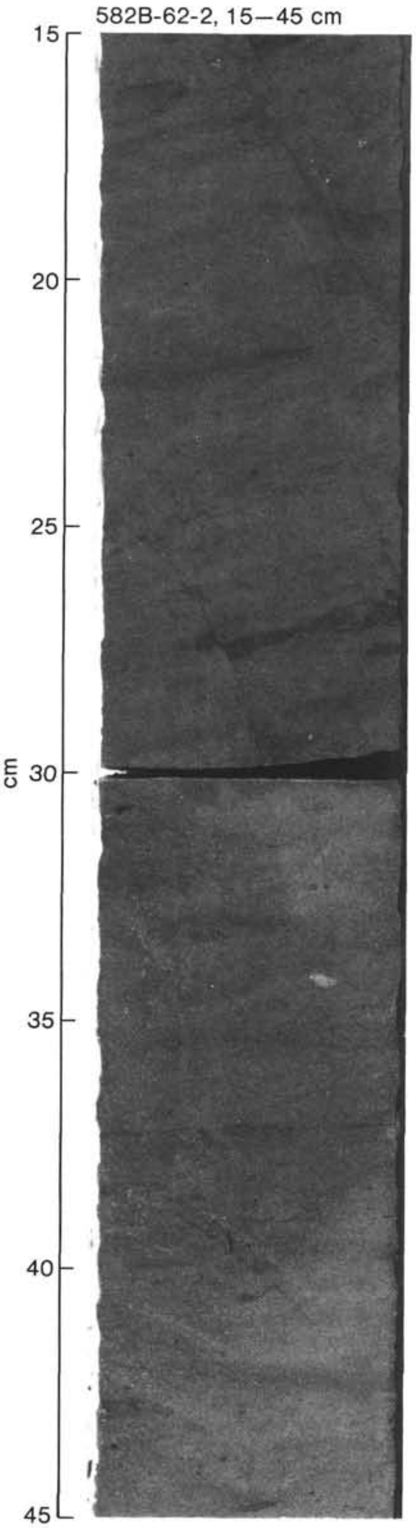

Figure 9. Burrow offset by healed normal fault, Core 582B-62.

from terranes. Pumice grains are abundant in the basal portions of the turbidites but rare in intercalated hemipelagic sediments, suggesting that the turbidites were transported from a volcanically active region.

The most obvious provenance for the Nankai Trough turbidites is, therefore, the Tokai drainage basin, which includes all three major geologic terrains and is one of the most active areas (both tectonically and volcanically) in Japan. The Tenryu, Ohi, Fuji, and Kano rivers drain parts of the Sambagawa, Chichibu, and Shimanto belts as well as the Cenozoic volcanic terranes of Izu, Tanzawa, and Yatsugatake regions. These rivers have not developed coastal plains; instead they form fan delta systems that connect directly with the submarine canyon systems at the head of the Suruga Trough and Tenryu submarine canyon. The Suruga Trough and the Tenryu submarine canyon link directly into the Nankai Trough (see Fig. 10), offering the most likely pathway for the lithic particles found at Site 582.

The bulk of the trench wedge of Nankai Trough is probably formed by axial transport of sediments from central Japan beginning in the Pleistocene, as the Izu collision process began to control the Quaternary tectonics of the region (Matsuda, 1977). This concept is supported by evidence on land in Shizuoka, where deposition of the Ogasayama conglomerates reflects a high rate of uplift of the Akaishi Mountains. Micropaleontologic evidence supports this conclusion: the emplaced fauna of foraminifers and radiolarians in turbidites are a mixture of Kuroshio and Oyashio assemblages. The turbidites are perhaps derived from within the zone of Kuroshio and Oyashio mixing, such as off central Japan, although fluctuations throughout the Quaternary period may be expected.

Comparison with Sites 297 and 298 of Leg 31

The age range of sediments at Site 297 (30°52.36′N; 134°09.89′E) is from Miocene to late Pleistocene (Ingle, Karig, et al., 1975a). The floor of the basin was probably above the calcite compensation depth (CCD) until the middle Miocene. In the late Miocene(?), hemi-

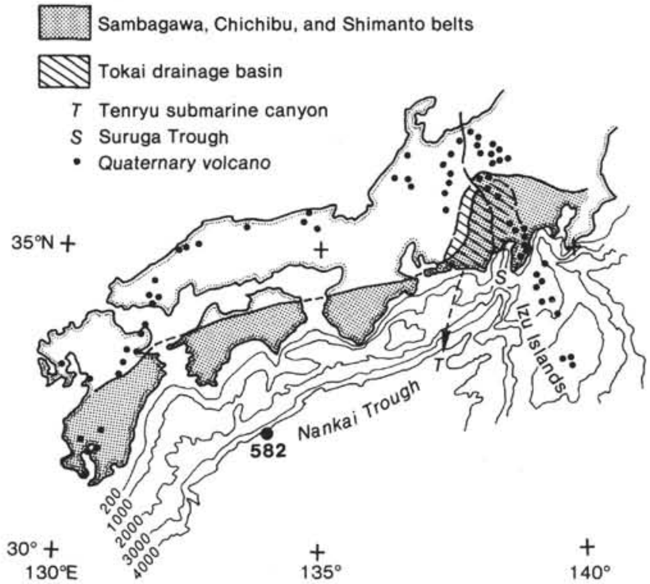

Figure 10. Sketch map showing location of selected features of Japanese geology. Tokai Basin is the most probable source of the suite of rock fragments and minerals observed in the graded beds of Site 582.

pelagic sedimentation gave way to turbidites, then terminated in the Pliocene (about 3.5 Ma). These turbidites may mark the uplift of southwestern Japan; they continued to reach Site 297 until an intervening sediment trap, a precursor to the Nankai Trough, developed. The turbidite layer creates a distinct seismic reflector between Sites 297 and 582, permitting correlation between the post-turbidite hemipelagic sediments of the upper transparent layer of Site 297 and Unit 2 of Site 582, though at the latter site the reflector was not cored.

At Site 582, the equivalents of the upper transparent layer are less porous and thinner than at Site 297. Their lower porosity at Site 582 results from their loading by turbidites, of Unit 1, which began arriving at the site about 0.7 Ma. Their thinning at Site 582 may not be entirely due to compaction.

The two units of Site 298 (31°42.93′N; 113°36.22′E) do not correlate directly with Site 582 (Ingle, Karig et al., 1975b). Set in the lower inner slope of the Nankai Trough, they are said to demonstrate marked compaction and deformation. The lower unit of Site 298 (Unit 2, early Pleistocene) is said to show the changing loci of sedimentation, and it represents trench fill. The upper unit (Unit 1, late Pleistocene to Holocene[?]) is probably also trench fill but contains semilithified cobbles and thus may indicate deposition influenced by the slope apron. Site 582 represents a different depositional setting, and hence direct comparisons are not possible.

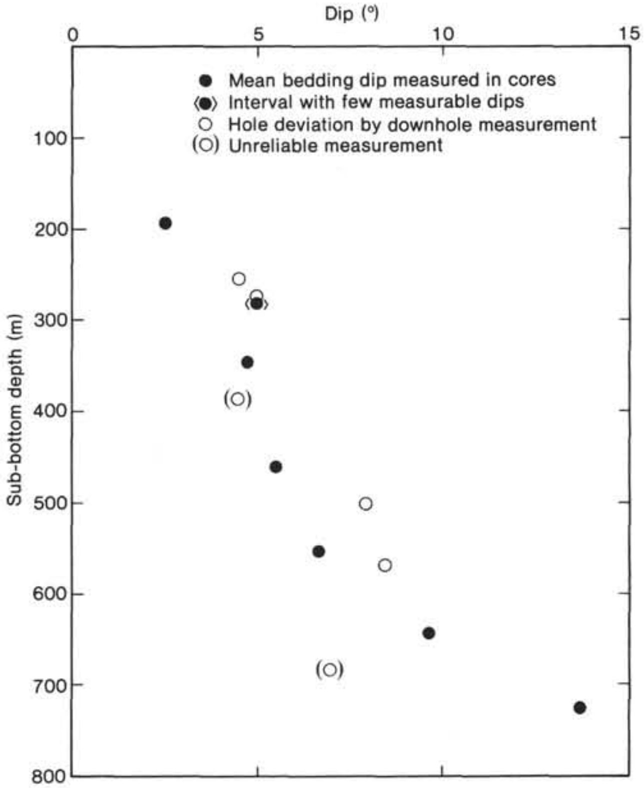

Figure 11. Horizontal bedding as an indicator of hole deviation, Site 582.

STRUCTURAL GEOLOGY

Sediments and sedimentary rocks recovered at Site 582 exhibit very little structural deformation; we had located the site seaward of seismically defined thrust faulting. Of particular interest, Site 582 cores lack the "fracture cleavage" and kink folds of cores from Site 298 (see Ingle, Karig, et al., 1975b). Drilling deformation in these cores is apparently limited to readily identified features, such as swirled and bowed bedding in soft to stiff mud in the upper part of the section, followed by drilling laminations, and finally drill biscuits and artificial open fractures in mudstone. The upper part of many cores contains drill cavings (or fill) of angular fragments derived from shallow levels in the hole.

Bedding dips measured in cores from Unit 1 agree very closely with downhole determinations of angular deviation from vertical, reflecting the flat-lying nature of the trough fill (Fig. 11). Measured dips from the underlying Unit 2, however, average 2 to 4° greater than hole-deviation measurements. This difference is small, but may represent downbowing of the Philippine Plate seaward of the Nankai Trough (see Fig. 2).

The only pervasive secondary fabric we observed in cores from Site 582 is a fissility defined by very planar parting surfaces parallel to bedding, some of which were open when the cores were split. Incipient fissility was noted in the first core cut by the circular power saw (Core 582B-22, 254 m sub-bottom) and so is likely present at somewhat shallower depths as well. Fissility becomes more pronounced with depth and by Core 582B-52 (537 m sub-bottom) approaches a truly shaly fabric that splits mudstone into thin wafers. Fissility is not developed in bioturbated intervals and is interpreted as a product of depositional alignment of platy minerals, accentuated by compaction caused by burial.

Five healed faults are defined by high-angle (52 to 80°), thin, dark shear zones in Cores 62 to 64 of Hole 582B (635 to 661 m sub-bottom, Fig. 12). Visible offset and/or drag features suggest normal-fault displacement along each of these faults. A planar, open fracture in Core 582B-51 (528 m sub-bottom) is also interpreted as normal fault, on the basis of dip-slip slickenlines and marked steps along a polished, planar fracture surface. All other fractures are tentatively interpreted as artifacts of drilling or handling, following guidelines suggested by Arthur and others (1980) and Lundberg and Moore (1981).

Thin veinlike structures are developed in mudstone at several horizons in Core 582B-62 (634 to 638 m sub-bottom), as very faint, dark surfaces crudely perpendicular to bedding (Fig. 13). These surfaces are curviplanar and locally anastomose, and are present in parallel sets confined to specific horizons and as long, solitary features. Although poorly developed, they appear to be incipient stages of features reported in various forearc regions as dewatering veins, vein structure, and spaced foliation (Arthur et al., 1980; Ogawa, 1980; Lundberg and Moore, 1981; Cowan, 1982; von Huene, Aubouin, et al., 1985). These features have previously been recognized only in trench slope environments. They apparently form early and serve as dewatering conduits, but their origin remains unclear. The association of "pseudoveins" with the healed normal faults in Core 582B-62, and the ab-

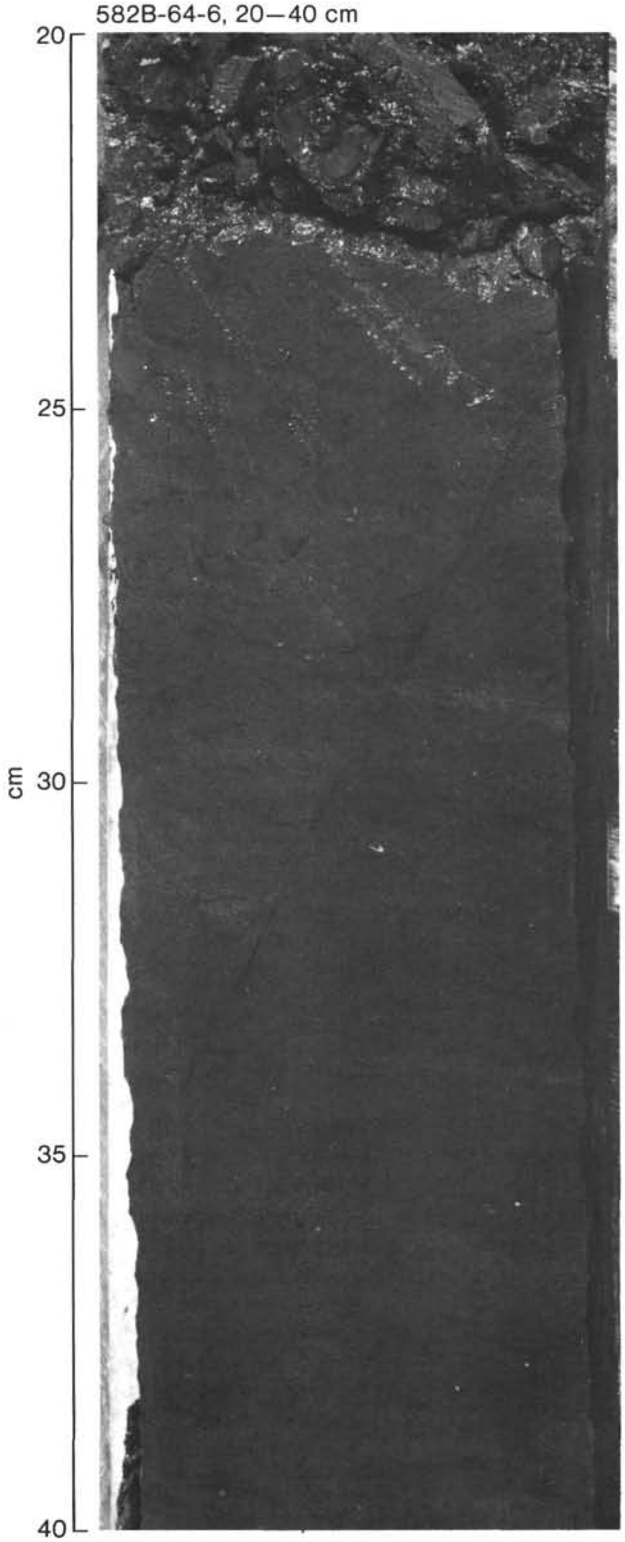

Figure 12. Healed normal fault, Lithologic Unit 2, Site 582.

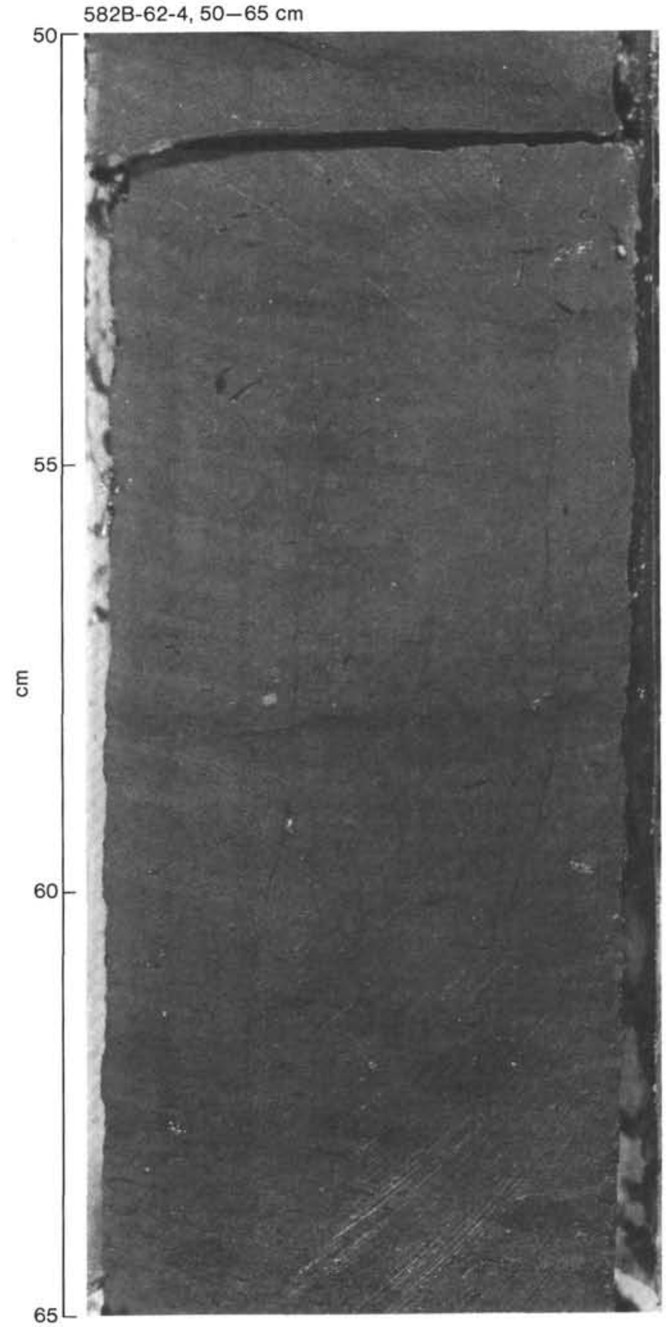

Figure 13. Curviplanar, locally anastomosing "pseudo-veins," Core 582B-62, Unit 2.

sence of both features elsewhere in the section, substantiate the suggestion that they are related to horizontal extension (Ogawa, 1980; Lundberg and Moore, 1981; Cowan, 1982). This extensional strain has likely been caused by downbowing of the Philippine Plate at the outer swell seaward of the Nankai Trough. Brittle rupture is facilitated by reduced effective confining pressure resulting from the presumed high pore pressures that accompany rapid deposition of the overlying trough-fill turbidites of Unit 1.

BIOSTRATIGRAPHY

The sediment recovered in the upper 560 m at Site 582 is a sequence of gray hemipelagic, Quaternary to uppermost Pliocene sediments alternating with coarser turbidite sequences in the upper 570 m (Fig. 14). Calcareous nannofossils are the most consistently occurring mi-

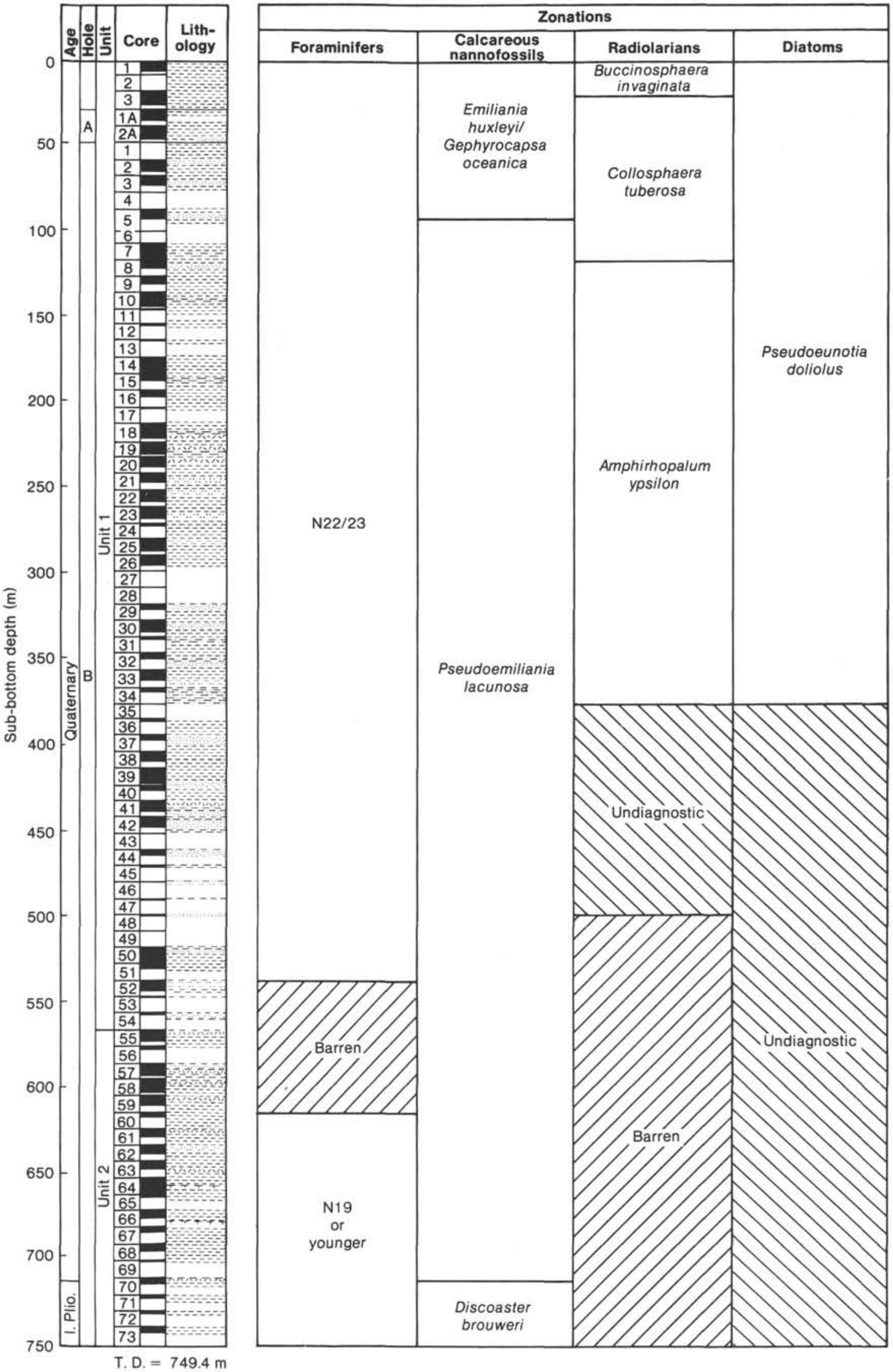

Figure 14. Summary biostratigraphy of Site 582. For lithologic symbols, see Explanatory Notes chapter (this volume). T. D. = total depth.

crofossils, foraminifers are less abundant (common to rare above Core 582B-33 and more sporadic below this level). Radiolarians are common only through Core 582-3. They occur intermittently throughout the remaining samples in varying abundances.

Faunal diversity is high in much of the sediment because of two major factors. Mixing of deep-dwelling and shallow-dwelling foraminifers is due to downslope transport by turbidity flows. Also, the position of Site 582, near the mixing front of the Kuroshio and Oyashio, accounts for the presence of subtropical and cool-temperate foraminifers and radiolarians in the assemblages. Age determinations were relatively consistent when all three fossil groups were present; slight discrepancies may be explained by the possibility of downhole contamination.

Benthic foraminifers, where present, indicate a mixed assemblage of bathyal and shelf species. The deepest elements in these assemblages are lower bathyal (2000 to 4000 m). Radiolarians, although not as reliable as depth indicators, also provide evidence of transported fauna.

All microfossil groups were absent in the core catcher samples from Cores 49, 50, 52, 53, 54, 61, 64, and 65 in Hole 582B.

Sediment accumulation rates were difficult to calculate based on the microfossils alone. The following data were tabulated:

1. Base of the *Collosphaera tuberosa* Zone (radiolarians) 370,000 yr. in 125.8 m for a rate of 340 m/Ma.
2. Base of the *Gephyrocapsa oceanica* Zone (nannofossils) 440,000 yr. in 90.7 m for a rate of 206 m/Ma.
3. Base of the *Pseudoemiliania lacunosa* Zone (nannofossils) 1.65 Ma in 721.1 m for a rate of 437 m/Ma.
4. Base of the *Pseudoeunotia doliolus* Zone (diatoms) 640,000 yr. in 366 m for a rate of 572 m/Ma.

If the sediment accumulation rate is averaged between the two nannofossil events, the 630.4 m recovered represents 1.21 Ma—a lower Quaternary rate of 521 m/Ma. As stated before, discrepancies may be due to downhole contamination and/or reworked older sediments.

Foraminifers

Introduction

The composition and distribution of foraminiferal faunas at Site 582 reflect the interplay of latest Neogene depositional and oceanographic processes in the Nankai Trough. Assemblages of both planktonic and benthic foraminifers are products of original biogeographic distributions and subsequent postmortem transport and dissolution.

Site 582 was drilled at 4882 m water depth, beneath the present CCD. Continuous coring penetrated a largely Quaternary section composed of two primary lithofacies: (1) interbedded hemipelagic mud and sandy turbidites (0 to 566 m sub-bottom) and (2) bioturbated, hemipelagic mudstone (566 to 749.4 m sub-bottom). The foraminiferal faunas are slightly different in the two lithofacies: the former contain an important input from postmortem displacement of faunas downslope and the latter is significantly affected by dissolution.

Planktonic Foraminifers

Planktonic foraminifers occur frequently, though sporadically within the sequence of hemipelagic mud and sandy turbidites (Unit 1). Generally, samples from the hemipelagic mud interbeds contain very rare or no foraminifers. Samples from turbidites contain rare to common planktonic and benthic foraminifers, as well as other biotic components (e.g., echinoid spines and plates, ostracodes, mollusk fragments, and bryozoan debris).

The planktonic foraminifers from these samples (above Core 582B-51) indicate a Quaternary, Zone N22/23 (modified from Blow, 1969) assignment. Diagnostic species include *Globorotalia truncatulinoides*, the modern form of *G. inflata* and *Neogloboquadrina eggeri* (sensu Saito, Thompson, and Berger, 1981). Important associates include *N. pachyderma, Pulleniatina obliquiloculata, Globigerina falconensis, Globigerinoides ruber, G. trilobus, G. cyclostoma, Orbulina universa*, and *Globigerinita glutinata*.

This fauna is a mixture of subtropical (e.g., species of *Globigerinoides, P. obliquiloculata*, rare menardiform globorotalids) and cool-temperate (e.g., *Globorotalia inflata*, dextral *N. pachyderma, Globigerina falconensis*) species. This mixture reflects the position of Site 582 near the confluence of the cold Oyashio and warm Kuroshio. The assemblages also represent a mixture of dissolution-resistant and dissolution-susceptible species. In particular, the presence of common species of *Globigerinoides* in assemblages now at or below the CCD is evidence that these assemblages were transported and rapidly buried by turbidity flows. Reworking of some specimens is also indicated by their dark yellow to orange color, but the bulk of the assemblage is white. Samples from Cores 52 to 59 yielded no foraminifers.

The planktonic foraminifers in the hemipelagic mudstones (Unit 2) below Core 60 show the effects of dissolution. These low-diversity assemblages are dominated by *Globorotalia inflata* and *Sphaeroidina dehiscens*, both dissolution-resistant species. In addition, fragments and partly dissolved specimens are frequently found. Clearly, these assemblages were not buried as rapidly as those in the turbidite sequence above. Species rarely associated in these assemblages include *Orbulina universa, Globigerinita glutinata, Globigerinoides cyclostoma*, and *Globorotalia tumida*. The age of this assemblage is Pliocene or Pleistocene, N19 or younger. A more precise age is not evident from the initial examination of these faunas.

Benthic Foraminifers

Benthic foraminifers are rare to common in sandy samples of the turbidite sequence (Core 582B-51 and above) and rare to absent in the hemipelagic mudstones (Core 582B-60 and below). Within the upper interval, the assemblages are diverse and well-preserved mixtures of shallow-water and deep-water species. Shelf species include *Ammonia beccarii, A. japonica, A.* cf. *stachi*, several species of *Elphidium, Florilus* cf. *costiferum*, and several species of *Quinqueloculina*. The deepest elements within these assemblages are lower bathyal to abyssal and include *Melonis pompilioides, M. barleanum, Cibicides weullerstorfi, Stilostomella* spp., and costate-to-hispid uvigerines. Agglutinated species, characteristic of sub-CCD environments in other parts of the Pacific Ocean, are very rare to absent in most of the samples, including those from hemipelagic interbeds.

The hemipelagic muds below Core 582B-60 contain rare benthic foraminifers, mostly deep-water species such as *Melonis pompilioides, Pullenia bulloides*, and hispid uvigerines. The benthic assemblages in Site 582 show no detectable bathymetric changes in the section penetrated.

In summary, the assemblages of foraminifers found at Site 582, their distribution, and their mode of preservation reflect several important depositional and oceanographic processes. Assemblages in the upper turbidite sequence are mixed subtropical and cool-temperate faunas, orginating from an area near the confluence of major surface-current systems. They were rapidly buried by turbidity flows at an area near the present CCD. This rapid burial protected them from dissolution and incorporated a mixed assemblage of shallow-water and deep-water benthic species as well.

Assemblages from the hemipelagic mudstones below Core 582B-60 show evidence of slower deposition, significant dissolution, and little displaced benthic fauna.

Radiolarians

Hole 582

Common to abundant Quaternary radiolarians are contained throughout Hole 582 with moderate preservation. Nigrini's (1971) tropical radiolarian *Buccinosphaera invaginata* Zone was recognized throughout Core 1, and the *Collosphaera tuberosa* Zone in Core 3.

Hole 582A

Samples examined from this hole did not contain enough diagnostic taxa to make a zonal assignment. However, a typical Quaternary assemblage, moderately preserved, was observed, including *Spongaster tetras tetras, Pterocanium praetextum praetextum*, and *Didymocyrtis tetrathalamus tetrathalamus*.

Hole 582B

The boundary of the *Collosphaera tuberosa* Zone and Nigrini's *Amphirhopalum ypsilon* Zone could not be definitely determined until Core 8. Radiolarians are few to rare until Core 23, which is also assigned to the *A. ypsilon* Zone. In Core 25, *Stylatractus universus* is present, as well as species diagnostic of the *A. ypsilon* Zone. Both the tropical zonation of Nigrini (1971) and the high-latitude zonation of Hays (1970) (*S. universus* Zone) could be applied through Sample 582B-34-1, 99–100 cm, which was the last sample examined that had sufficient radiolarians to determine a zonal age. Radiolarians abundance decreases downhole to Core 40, and beneath Core 46 samples from this site are barren.

Where radiolarians are common to abundant, the fauna is relatively diverse with over 100 taxa identified. Cooler-water species, such as *Theocalypta davisiana, Spongotrochus glacialis, Actinomma antarcticum, Spongurus* sp., *Styptosphaera spumacea*, and *Ceratocyrtis borealis*, are present in the same intervals as warmer-water species, such as *Siphonosphaera polysiphonia, Spongurus* cf. *elliptica, Liriospyris reticulata*, and *Phormospyris stabilis scaphipes*. This faunal diversity arises from mixing at the front of the Kuroshio and Oyashio. Subsequently, this assemblage was transported to the area of Site 582. Radiolarians are absent in lowermost sediments, those in which turbidite sequences were not observed.

Relative sediment accumulation rates were calculated using radiolarian and calcareous nannofossil events for the upper 100 m of sediment. The *Buccinosphaera invaginata* Zone spans approximately 0.21 Ma and is represented by only 10 to 20 m of sediment, indicating an approximate accumulation rate of 50 to 100 m/Ma. Sediment accumulation rates based on the calcareous nannofossils are comparable. This accumulation rate resembles rates of pelagic sedimentation, a surprising result because the turbidite sequences at Site 582 should have accumulated much faster. The *Collosphaera tuberosa* Zone has a duration of close to 0.16 Ma and is represented by 80 to 106 m of sediment. These values yield an approximate rate of 400 to 500 m/Ma of sediment accumulation. The contrast in rates suggests that a portion of the Holocene sediments are missing or that Holocene rates are anomalously low.

Calcareous Nannofossils

Hole 582

The three cores retrieved from Hole 582 contained common, well-preserved calcareous nannofossils of the latest Quaternary. *Gephyrocapsa oceanica* and *Emiliania huxleyi* dominate the assemblages. Other species present in varying degrees include *Helicopontosphaera kamptneri, Calcidiscus leptoporus, Umbilibosphaera mirabilis*, and *Coccolithus pelagicus*.

It is not clear why *G. oceanica* is so dominant even in the earliest sediment recovered. Possible loss of the uppermost sediment caused by drilling disturbance may be partially responsible.

Hole 582A

As at Hole 582, common, well-preserved nannofossils were encountered, dominated by *Gephyrocapsa oceanica* and *Emiliania huxleyi*. The associated species are the same as in Hole 582. The only apparent difference between flora in these two holes is a relative decrease in overall abundance of nannofossils in Hole 582A.

Hole 582B

Abundant to rare calcareous nannofossils were recovered from a sequence characterized at least in the upper 560 m by turbidites. Preservation fluctuates from very good in two nannofossil-rich muds to moderate to poor in the great majority of samples.

Sediments in the first several cores contain nannofossil assemblages identical to those found in Holes 582 and 582A. These sediments fall within the *Gephyrocapsa oceanica* to *Emiliania huxleyi* Zones (Martini and Worsley, 1970). The first common *Pseudoemiliania lacunosa* occurs in Core 5 (582B-5-2, 44–55 cm) placing this sample within the *P. lacunosa* Zone (Martini and Worsley, 1970). The abundances of *P. lacunosa* remain fairly constant throughout the rest of the section, rising only within conspicuously nannofossil-rich intervals. Samples below Core 23 exhibit a change in the dominant *Gephyrocapsa* component from *G. oceanica* above to *G. caribbeanica* below. Transitional forms that have a central crossbar orientation between that of these two forms are also common below Core 23.

Assemblages in Cores 26 to 36 vary in preservation and abundance in response to deposition within turbidites. One turbidite sequence (582B-36-1, 71–91 cm) was sampled at various intervals, and these samples were examined for nannofossils. Both abundance and preservation decrease upward within that sequence. Rapid burial of the nannofossils in the basal section of the turbidite explains the higher concentrations found there. In the more slowly deposited finer sediment above, dissolution effects are more pronounced.

Cores 42 (582B-42-1, 65–66 cm) and 57 (582B-57-4, 143–144 cm) contain nannofossil-rich muds with some of the most abundant and well-preserved nannofossils in the section. *P. lacunosa*, which is generally few to rare in abundance elsewhere in the section, becomes common in both of these intervals.

The first Pliocene sediment (582B-70-2, 66–67 cm) was dated by calcareous nannofossil assemblages including *Calcidiscus macintyrei*, and *Discoaster brouweri*, and a lack of Pleistocene species of *Gephyrocapsa*. The Pliocene/Pleistocene boundary occurs between Samples 582B-70-2, 66–67 cm and 582B-69,CC. Recovery in this interval was incomplete, and drilling disturbance was particularly severe. All other samples examined to total sub-bottom depth (749.4 m) are upper Pliocene.

Diatoms

For this shipboard study, diatoms of Site 582 were examined using smear slides prepared for calcareous nannofossils. Samples from Hole 582B were analyzed only down to Sample 582B-42-5, 80–81 cm, because sedimentologic examination of samples below that level revealed very few diatom remains.

Upper Quaternary diatoms were recovered from Holes 582, 582A, and 582B. Biostratigraphic zonation of these holes is difficult; few samples contain age-diagnostic species, both because of low productivity of diatoms in the area and because of dilution of age-diagnostic marine planktonic species by displaced marine benthic and nonmarine diatoms. Holes 582, 582A, and 582B (Cores 2 through 34), however, are safely assigned to the *Pseudoeunotia doliolus* Zone (0 to 0.64 Ma) of Burckle (1972, 1977), because *P. doliolus* (base; 1.8 Ma) was found and because *Nitzschia reinholdii* (top; 0.64 Ma) does not occur at all in the interval.

Samples from these holes contain few to rare diatoms, and in general their preservation is poor. Abundance of diatoms varies from sample to sample and bears no general relationship with increasing depth, except for a sudden decrease near Core 582B-42.

Diatom assemblages in these holes represent three different habitats: marine planktonic, marine benthic, and nonmarine diatoms, the first being the predominant element. The latter two are evidently displaced flora introduced to the site by turbidity currents. Displaced diatoms account for more than half of the total assemblage in several samples. In general, the lower diversity assemblages contain no displaced elements whereas the highly diverse ones contain many. Preservation of nonmarine diatoms is generally better than that of marine ones. Marine planktonic species are predominantly composed of warm-water forms such as *Coscinodiscus nodulifer, Nitzschia marina, Pseudoeunotia doliolus* and so forth, and no typical cold-water forms were found. The low-latitude diatom zonation of Burckle (1972, 1977) was applied to these holes, therefore, instead of the high-latitude scheme of Koizumi (1973).

SEDIMENT ACCUMULATION RATES

The biostratigraphy for Site 582 indicates an accumulation rate of 206 to 340 m/Ma for the uppermost 126 m of the axial turbidites (Fig. 15). The high rates of about 886 m/Ma for the deeper portion of Lithologic Unit 1 are expected, because of the site's position in the Nankai Trough. These rates approach an unlikely 1338.5 m/Ma if the paleomagnetic dates rather than the microfossil control for the Shikoku Basin strata are accepted.

Why are the rates for the upper section so much lower than those derived for the mid-section of the Trough fill? Assuming that the biostratigraphic control warrants the accuracy implicit in these numbers, there are a variety of explanations to consider. Most of these depend on submarine morphology; therefore, a brief discussion of the major bathymetric features of the region is presented.

A block diagram (Fig. 16), constructed from a preliminary bathymetric map of the Leg 87A study area, illustrates some of the principal features of the northwestern slope of the Nankai Trough. The trough itself shallows to the southwest, just beyond the front border of the diagram, with maximum depths between 4900 and 5000 m occurring in a closed depression between the area shown on front edge of the diagram and the location of Site 582 (the topographic gradient is too low to show on the illustration, Fig. 16). The seaward side of the Nankai Trough slopes gently upward to the Shikoku Basin. A series of low ridges, which are generally linear at the resolution afforded by the existing bathymetry, border the northwest flank of the trough. The two-dimensionality of this topographic grain gives way upslope to a general tendency of the bathymetric contours to parallel the strike of the topography of Shikoku Island. Ashizuri Canyon is the major bathymetric feature crossing the slope and a less distinct depression parallels to the northeast. The continuity of the latter feature and the possibility that the Ashizuri Canyon reaches the Nankai Trough are also beyond the resolution afforded by the available bathymetric chart. Numerous small catchments and local sediment ponds are scattered across the slope. Beyond the back-edge of the diagram marked by the Ashizuri Knoll

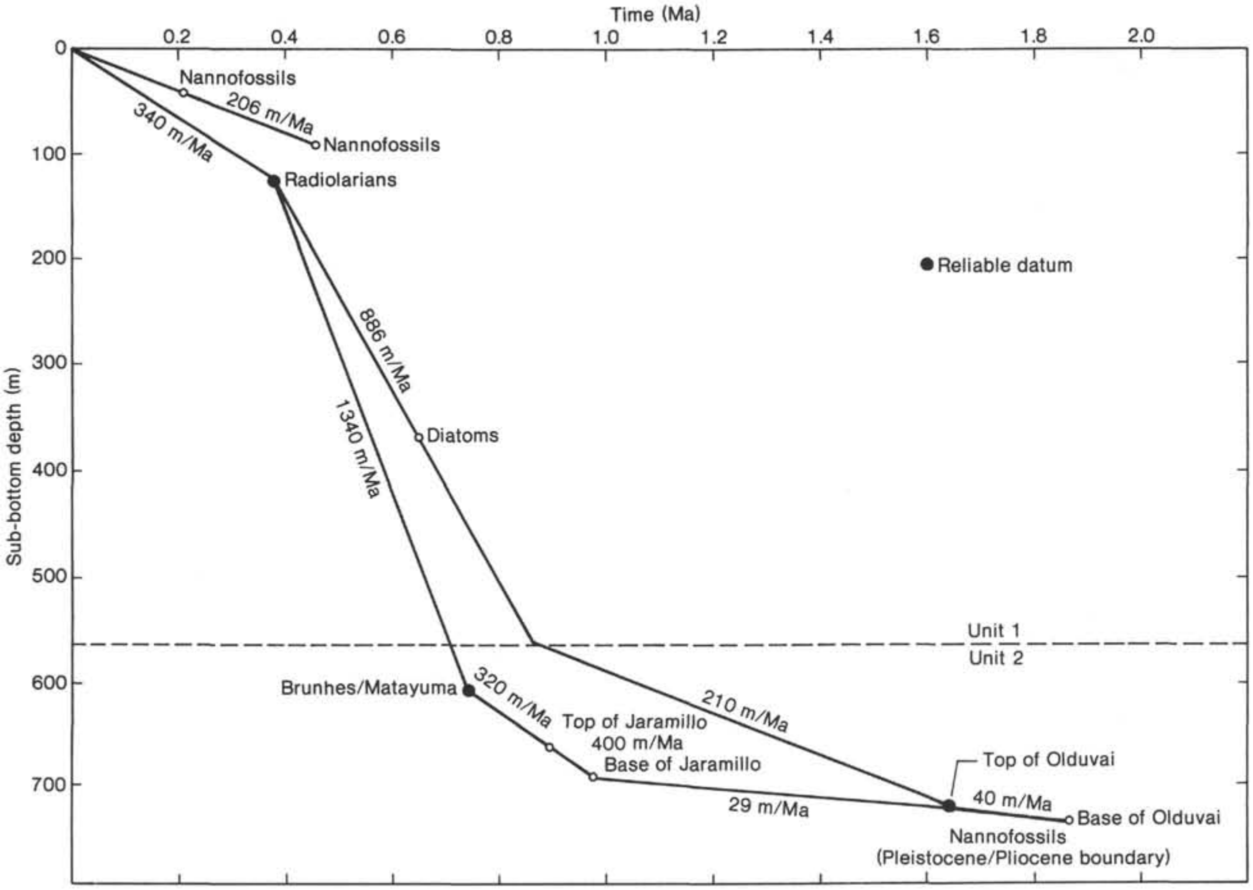

Figure 15. Sediment accumulation rates, Site 582. Other sediment accumulation rates (for comparison): trench wedge (Site 298), 900 m/Ma; Shikoku Basin (Site 297), 91 m/Ma for Quaternary, 147 m/Ma for Pliocene.

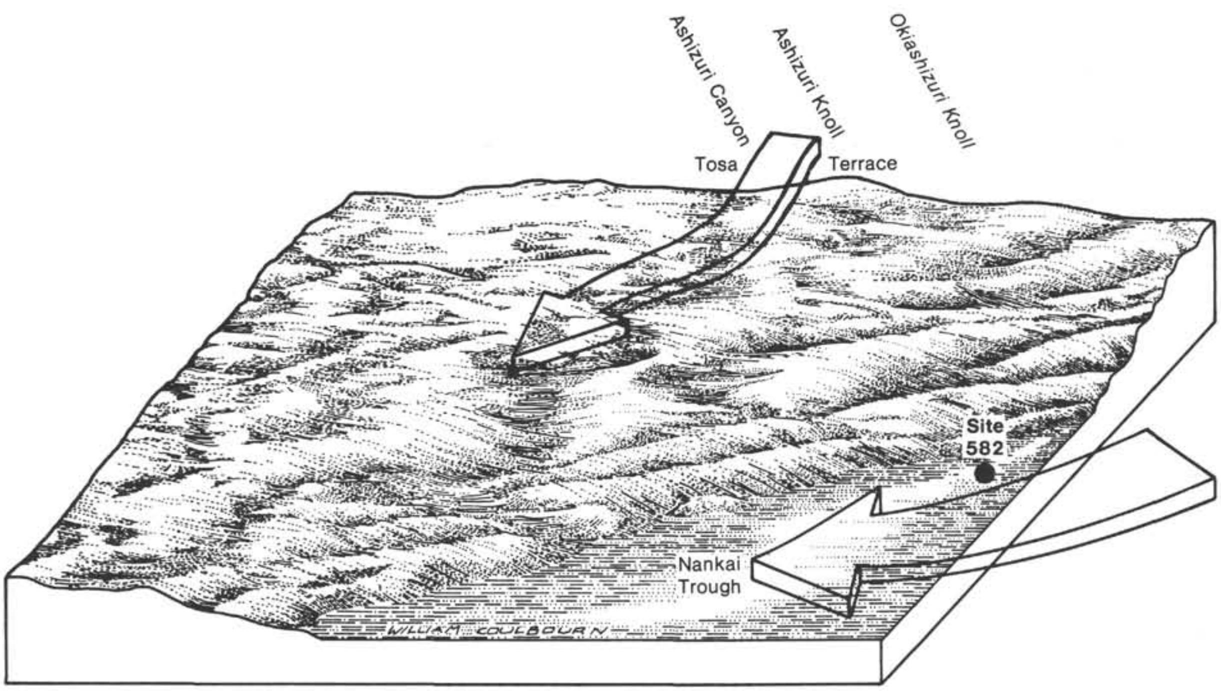

Figure 16. Block diagram showing bathymetric features of the Nankai Trough and northwestern slope, near the Leg 87 study area. Arrows represent possible directions of sediment transport, and their relative width indicates the importance of that transport to the sediments accumulated at Site 582.

is the large, subhorizontal surface of the Tosa Terrace (Fig. 16). The bulk of the sediment shed from Shikoku Island is trapped or at least temporarily ponded in this basin. In all likelihood, the ridges, canyons, gullies, and catchments charted on the present-day slope are representative of similar features that occupied the slope throughout the Pleistocene; in geologic terms they are short-lived and therefore have migrated through the course of time.

Ash falls blanketed swaths of the offshore region in punctuated events, but their total thickness is only on the order of 1 to 2 m at Site 582, compared to the total of 749 m drilled. Hemipelagic mud rains out of the surface water of the region at a rate that is relatively constant in comparison to the rate of accumulation caused by episodic deposition, nondeposition, and erosion by turbidity and gravity flows. Factors controlling the frequency, magnitude, and pathway of these events also control the sediment accumulation rate at locations like Site 582. Bathymetry, the composition of heavy minerals, and the presence of pumice grains in the axial turbidites indicate that the most important route of transport to Site 582 is from the Tokai Basin via the Suruga Trough and Tenryu Canyon to the Nankai Trough (for details, see Provenance subsection of Sedimentology section). At the present time, the depocenter for these flows should be the bathymetric depression to the southwest of Site 582. Accumulation rates would vary depending on the paleolocation of that depocenter with respect to Site 582, the existence of other depocenters between Suruga-Tenryu and Site 582, the velocity of individual turbidity flows crossing or even not reaching the site, and the amount of overshoot necessary to reach base level. Given sufficient velocity and gradient, flows with a large overshot might erode sediment previously deposited at Site 582. Alternatively, given the coincidence of the depocenter and the drill site, accumulation rates could be extremely rapid. Accompanied by local, relatively rapid sinking of the seafloor with respect to adjacent segments of the trough, high accumulation rates could be sustained for an extended period of time.

Other sources, each subject to changes through time, augment the fluctuations in accumulation rate produced by the axial flows. Certainly, sediment reaches the Nankai Trough by surface creep, gullies, and submarine canyons crossing the slope. The arrows in Figure 16 illustrate some potential pathways. The migration of submarine canyons across the slope would dramatically increase discharge at specific points directly downstream. Such accumulations could themselves hinder the flow of sediment along the trough or, by acting as a barrier, encourage deposition uptrough from them. The supply of sediment to these canyons depends in turn on the changing efficacy of the upper slope basin as a sediment trap, in this case, the Tosa Terrace. More efficient entrapment upslope decreases the supply of sediment bypassed through canyons to greater depths and starves those catchments of fill. That starvation generates a type of feedback mechanism, requiring greater overflow upslope before lower slope basins fill to the brim and in turn pass sediment further downslope.

In general terms, then, low accumulation rates in the uppermost section at Site 582 are due to the absence of episodic deposition, particularly by axial turbidity flows. These fluctuations may act in concert with, but do not require, local tectonic uplift of Site 582 relative to adjacent areas.

INORGANIC GEOCHEMISTRY

X-Ray Mineralogy

Mineralogic composition of sediments at Hole 582B was determined by bulk sample X-ray diffraction using the shipboard diffractometer. In general, mineralogy does not change with depth, and no particular characteristics or trends distinguish episodes of turbiditic versus hemipelagic sedimentation. Major minerals present are quartz, plagioclase, feldspar, kaolinite, and illite; minerals occurring in minor or trace amounts are calcite, montmorillonite-smectite, chlorite, pyrite, and K-feldspar. There is no evidence of diagenetic reactions at the depth reached at this site. Of possible significance is the complete absence of any swelling clay below a depth of approximately 566 m sub-bottom.

Interstitial Water

Data collected as a part of the DSDP shipboard inorganic geochemistry program are listed in Table 2 and plotted in Figure 17. Unfortunately, key values between the interval of 60 to 175 m sub-bottom, those that might have been very important in our interpretation of the presence or absence of clathrate, are missing. The values we do have indicate an alkalinity maximum at 175 m sub-bottom. Previous experience on *Glomar Challenger* voyages has shown that high alkalinities, especially when they are coupled with low salinities and chlorinities, suggest the presence of gas hydrate. The relatively constant values for salinity and chlorinity shown in Figure 17, and the lack of physical evidence of clathrate in Site 582 samples, indicate that if clathrate is present, it is disseminated in the sediment.

The concentration of calcium is nearly constant, but the magnesium concentration decreases with increasing sub-bottom depth.

ORGANIC GEOCHEMISTRY

Introduction

The main objective for this site was to monitor the light hydrocarbons (in hydrate or nonhydrate form) for safety reasons and to evaluate the hydrocarbon content of the turbidite and hemipelagic sediments.

Gas samples were obtained by punching vacutainers into the core liner in gas pockets occurring in the first 670 m drilled. No head-space gas analysis was done on these sediments. For the first 193 m sub-bottom, gas pockets in the core liner showed high pressure, and the gases bubbled out of the core liner along with the mud when the core liner was punched. Sediments swelled in some cases. The gases were studied first by a Carle Gas Chromatograph (GC) with a thermal conductivity detector and later by a Hewlett-Packard GC with a flame

Table 2. Summary of shipboard interstitial water data, Site 582.

Hole	Core-Section (interval in cm)	Sub-bottom depth (m)	pH	Alkalinity (meq/l)	Salinity (‰)	Calcium (mM/l)	Magnesium (mM/l)	Chlorinity (‰)
IAPSO			7.31	2.34	35.2			
Surface seawater			7.17	2.32	34.1	10.47	52.03	18.55
582	1-3, 143-150	4.5	7.79	21.122	33.8	6.22	46.58	19.78
	3-5, 120-130	26.9	7.19	16.265	33.0	5.49	41.51	19.99
582A	1-5, 0-10	35.1	7.50	19.529	33.6	5.30	46.97	19.78
	2-5, 0-10	44.8	7.71	24.642	33.8	4.74	42.44	19.07
582B	2-2, 140-150	61.2	7.81	28.33	33.8	4.76	42.12	19.58
	14-5, 138-150	181.5	7.98	45.62	34.6	4.78	46.65	19.68
	18-3, 140-150	217.0	7.78	36.433	34.1	6.92	43.47	19.37
	23-1, 140-150	262.2	7.86	23.477	33.6	6.51	40.25	19.34
	30-5, 137-150	335.4	7.89	20.36	33.0	5.15	33.71	19.10
	33-4, 140-150	362.5	7.95	20.21	32.2	5.79	35.52	18.89
	38-3, 140-150	408.3	7.76	20.08	33.8	5.34	38.07	19.10
	50-3, 135-150	522.3	7.89	21.336	33.6	8.05	29.55	19.07
	54-2, 135-150	559.3	7.91	25.36	33.3	9.65	28.61	19.37
	61-2, 135-150	626.7	7.70	20.62	33.3	9.78	27.82	19.20
	66-2, 135-150	674.8	7.64	18.00	33.0	10.96	25.44	18.04

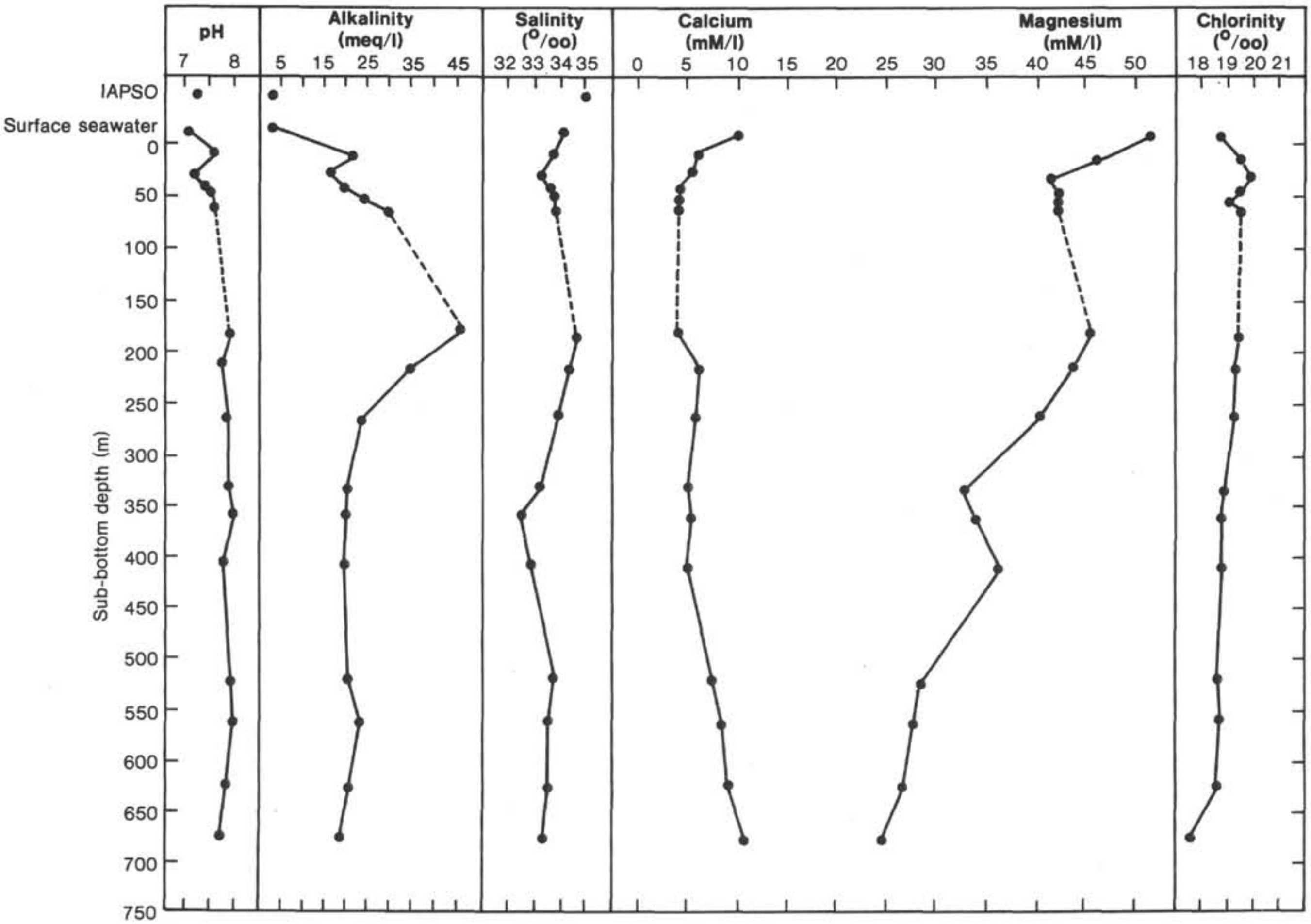

Figure 17. Interstitial water chemistry, Site 582.

ionization detector (FID) system. The procedures and instrumentation are the same as described by previous shipboard geochemists (see Sheridan, Gradstein, et al., 1983; Hinz, Winterer, et al., 1983; von Huene, Aubouin, et al., 1984).

The hydrocarbon evaluation of these sediments is done by Rock-Eval, and organic carbon was determined for the first time by the LECO carbon analyzer. The standards used in both cases are Samples 27251 and SDO-1. The instrumentation and procedures followed for Rock-Eval are the same as those cited earlier (Hinz, Winterer, et al., 1983). Because the LECO carbon analyzer is widely known to organic geochemists, the description of the instrumentation is not given here. As usual, for organic carbon analysis, samples were first treated with 4N HCl and dried at 110°C before analysis by the LECO. The CHN analyzer was not used, but the Haliburton fluorescence box was used four times at this site.

Results and Discussion

Fluorescence

Samples from Sections 582-3-2, 582B-18-4, 582B-30-3, and 582B-42-2 were analyzed in the Haliburton box. No liquid hydrocarbon fluorescence was detected.

Organic Carbon

Table 3 shows the amount of total carbon and organic carbon in the 21 samples analyzed at Site 582. Except for three samples (Fig. 18), all the cores studied have more than 0.5% C_{org}, the minimum level of organic carbon for a clastic source rock (Tissot and Welte, 1978). The values recorded in Table 3 indicate no correlation between carbonate carbon and organic carbon. Only one or two samples (e.g., 582B-10-1, 1-2 cm) have more than 1.00% carbonate carbon, and in most values are less than 0.3%. In Hole 582B, three samples were analyzed from Core 36 and two samples from Core 42. These cores represent different depositional regimes, the former is a turbidite and the latter is hemipelagic mud. Generally, the organic carbon content in these two different depositional regimes does not show any difference. Organic carbon decreases with depth beyond 500 m sub-bottom (Fig. 18).

Rock-Eval Pyrolysis

Eight core samples from the Pleistocene sediments of the three holes at Site 582 were analyzed for (1) occurrence of migrated or *in situ*-generated hydrocarbons—S_1, (2) pyrolysable hydrocarbons, i.e., hydrocarbon potentiality—S_2, (3) maturation of these sediments—T_{max} (°C), (4) migration index study-transformation ratio, (5) amount of oxygen in the sediment—S_3, and (6) nature of the kerogen—HI and OI.

Table 3. Organic carbon analysis, Site 582.

Hole	Core-Section (interval in cm)	Total carbon (%)	Organic carbon (%)
582	1-1, 74–76	0.65	0.63
	3-6, 70–76	0.94	0.74
582A	1-3, 70–76	0.61	0.47
	2-3, 70–75	0.96	0.70
582B	2-4, 26–29	1.01	0.70
	5-1, 110–112	0.86	0.62
	7-1, 36–39	0.93	0.70
	10-1, 29–31	1.59	0.60
	14-1, 18–20	0.64	0.58
	18-4, 16–19	0.97	0.75
	22-1, 69–72	0.86	0.63
	30-3, 135–137	1.16	0.66
	36-1[a], 95–96	0.68	0.60
	36-1[b], 102–103	0.91	0.61
	36-1[b], 116–117	0.90	0.57
	42-2[b], 10–12	0.88	0.62
	42-5[a], 85–87	0.88	0.64
	50-6, 80–81	0.75	0.53
	54-1, 72–73	0.75	0.52
	58-5, 40–42	0.45	0.40
	63-2, 80–82	0.52	0.45

[a] Hemipelagic mud.
[b] Turbidite.

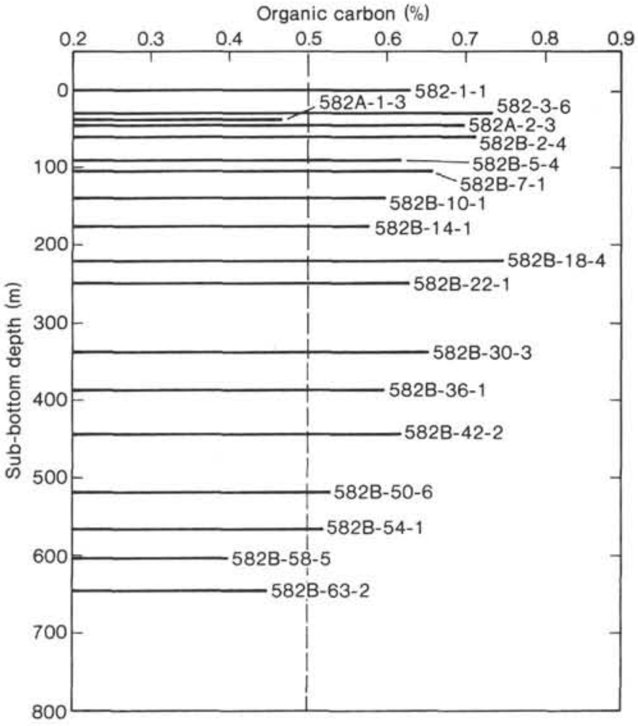

Figure 18. Amount of organic carbon in the 21 samples analyzed from Site 582.

S_1 (mg HC already generated/g of sediment) in all the analyzed samples is negligible and cannot be measured (Table 4). S_2 (mg HC generatable/g of sediment) is also very minor. S_3 (mg CO_2/g of sediment) is also comparatively low for the turbidites. T_{max} (°C) in most sediments shows double peaks, one around 424°C and another around 550°C. The transformation ratios ($S_1/[S_1 + S_2]$) could not be measured because there is no detectable S_1 peak. The hydrogen indexes (HI) in all three holes (Table 4) are very low, and all are below 50, except in Cores 42 and 58 of Hole 582B. Oxygen index (OI) varies from 53 to 363. The hydrogen index (HI) and oxygen index (OI), when plotted against each other, indicate that these kerogens are either type III (vitrinite rich) or between types III and IV (inertinite rich) (Fig. 19, Espitalié et al., 1979—type IV not shown). The T_{max} (°C) peak at 550°C and the double peak may also indicate that a part of the pyrolysable portion of these sediments is derived from recycled terrestrial organic matter. Because of erratic T_{max} data, no exact maturation prediction can be made, but the absence of S_1 peak and one series of low T_{max} (°C) may suggest immaturity and absence of migrated hydrocarbons.

Gas Analysis

Because gases are present at 0 m sub-bottom at Site 582 and because gas hydrates were assumed to occur at this site, we monitored gases throughout these holes. Tables 5 and 6 show the amount of C_1, C_2, C_3, C_4, and

Table 4. Organic geochemistry data, Site 582.

Sample number	Hole-Core-Section (interval in cm)	Sub-bottom depth (m)	S_1	S_2	S_2/S_3	S_2 Pk. temp. (°C)	$\frac{S_1}{S_1 + S_2}$	Organic carbon (wt.%)	CO_3 carbon (wt.%)	Hydrogen index $\left(\frac{\text{mg HC}}{\text{g } C_{org}}\right)$	Oxygen index $\left(\frac{\text{mg } CO_2}{\text{g } C_{org}}\right)$
1	582-1-1, 74–76	1.5		0.24	0.44			0.63	0.02	38	86
2	582-3-6, 70–71	29.0		0.12	0.075	416		0.74	0.20	16	215
3	582B-2-4, 26–29	59.7		0.13	0.05	414		0.70	0.31	19	363
4	582B-5-1, 110–112	88.0		0.22	0.23	550/424		0.62	0.24	35	157
5	582B-14-1, 110–112	174.5		0.14	0.14	550		0.58	0.06	24	175
6	582B-30-3, 135–137	333.2		0.14	0.21			0.66	0.50	21	100
7	582B-42-5, 85–87	450.0		0.38	0.90	550/421		0.64	0.24	59	66
8	582B-58-5, 40–42	604.0		0.22	1.04	550		0.40	0.05	55	53

Note: Pk. temp.: peak temperature. See text for definitions of S_1, S_2, and S_3.

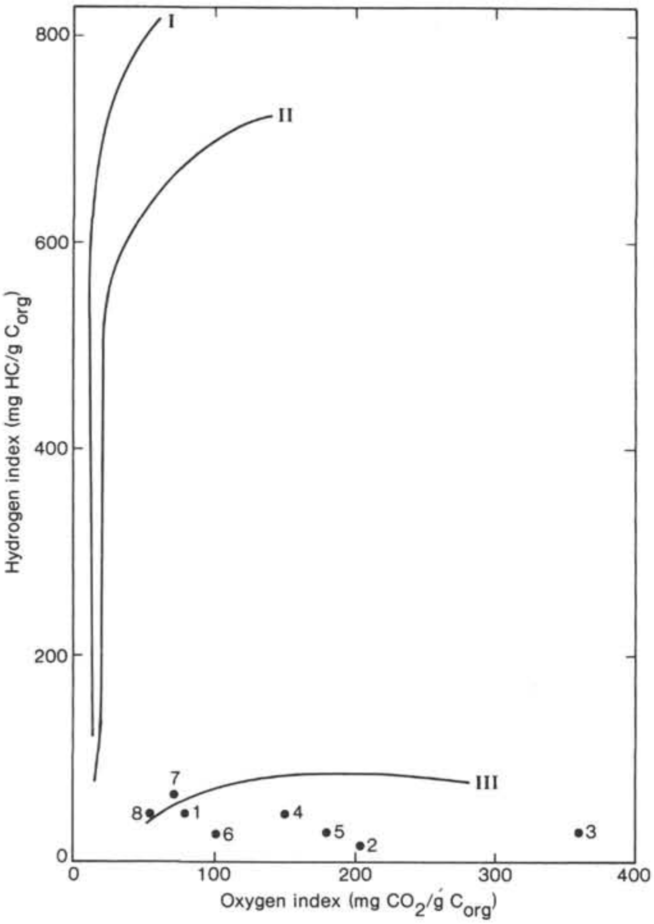

Figure 19. Hydrogen index versus oxygen index (after Espitalié et al., 1979). Roman numerals are kerogen types. Arabic numbers correspond to numbers in "Sample number" column of Table 4.

Table 5. Carle gas data from Site 582.

Hole	Core-Section	Methane (C_1 in vol. %)	Ethane (C_2 in ppm)	C_1/C_2 ($\times 10^3$)	CO_2 (%)	H_2S
582	1-6	6.54	3.11	21.000	0.18	Tr.
	3-3	68.4	4.79	143.000	1.23	Tr.
582A	1-2	23.6	1.54	148.400	0.35	Tr.
	2-3	84.1	2.56	328.500	1.14	Tr.
582B	2-2	86.2	2.68	373.200	1.38	Tr.
	3-3	86.0	2.78	369.100	1.14	
	5-2	84.3	2.02	417.300	1.10	
	7-5	90.8	1.76	515.900	0.79	
	9-3	73.7	1.47	501.400	0.83	
	14-4	90.7	2.48	365.700	1.32	
	15-2	84.3	2.45	344.100	1.70	
	16-2	66.7	5.81	114.800	0.40	
	18-4	18.6	8.16	22.790	0.35	
	19-4	85.7	3.97	215.900	2.12	
	20-4	86.6	12.2	71.220	0.41	
	21-2	87.2	3.87	225.300	0.84	
	22-5	76.4	4.20	181.900	0.81	
	23-5	90.9	4.40	206.600	0.48	
	25-6	90.6	5.37	168.700	0.77	
	30-5	87.5	9.03	96.900	0.74	
	31-1	82.0	6.51	126.000	0.63	
	32-2	83.8	10.4	54.400	0.47	
	33-4	79.1	10.2	77.700	1.08	
	36-6	59.4	16.2	36.640	1.20	
	37-2	61.7	13.4	45.980	0.93	
	38-1	84.2	13.3	63.310	1.06	
	39-2	85.8	13.4	62.630	1.13	
	40-1	66.8	11.3	59.120	1.09	
	41-1	81.9	12.8	63.790	1.64	
	43-3	87.0	12.3	70.730	1.17	
	44-1	82.9	12.0	69.198	1.74	
	48-1	46.4	6.66	69.670	0.47	
	50-2	84.5	13.3	63.530	1.96	
	52-2	9.57	1.90	50.370	0.39	
	54-2	73.9	12.7	57.870	1.67	
	55-4	57.1	10.2	55.940	1.35	
	57-4	67.1	10.7	63.270	1.61	
	58-1	29.0	4.78	56.520	0.83	
	59-2	2.86	2.35	12.170	0.34	
	60-2	16.4	4.00	41.000	0.46	
	61-2	1.70	0.50	34.000	0.26	
	62-4	1.05	0.23	46.100	0.35	
	63-3	3.15	0.64	49.070	0.48	
	64-4	0.01	Tr.		0.15	
	66-3	4.47	Tr.		0.50	
	71-1	0.00	Tr.		0.18	

Note: Tr.: trace.

C_5. The concentration of methane and the trends of C_1/C_2 are plotted against sub-bottom depth (m) in Figures 20 and 21. Sections 582-1-6, 582-3-6, and 582A-1-2, 582A-2-3, and 582B-2-2 emitted an intense odor of H_2S, but only a trace quantity was detected by GC (Table 5). H_2S probably forms by sulfate reduction of bacteria near the sediment/water interface. Methane concentration (vol.%) is very high throughout except in some shallow sediment and in Core 582B-18. Preferential diffusion of C_1 in the zone of microbial production may cause the low C_1 values of the shallow sediment. Beyond Core 57 (595 m sub-bottom), the volume of gases suddenly decreases and becomes negligible beyond Core 63 (650 m sub-bottom). CO_2 is present almost continuously throughout the sediment section and in some cases (e.g., Core

Table 6. Hewlett-Packard gas data (in ppm), Site 582.

Hole	Core-Section	Ethane (C_2)	Propane (C_3)	Isobutane (i-C_4)	Butane (C_4)	Neopentane (neo-C_5)	Isopentane (i-C_5)	Pentane (C_5)
582	1-6	1.67	N.D.					
	3-3	3.35	N.D.					
582A	1-2	1.59	Tr.	N.D.				
	2-3	2.56	0.926	N.D.				
582B	2-2	2.68	1.65	N.D.				
	3-3	2.79	1.58	Tr.	N.D.			
	5-2	2.02	1.38	Tr.	N.D.			
	7-5	1.76	1.68	Tr.	N.D.			
	9-3	1.47	1.35	Tr.	N.D.			
	14-4	2.48	2.85	Tr.	N.D.			
	15-2	2.45	2.39	Tr.	N.D.			
	16-2	5.81	1.67	0.33	0.27	N.D.		
	18-4	8.16	1.84	2.13	1.86	0.93	Tr.	0.80
	19-4	3.97	3.46	0.69	N.D.	N.D.	N.D.	N.D.
	20-4	12.2	1.47	0.21	N.D.			
	21-2	3.87	3.04	0.43	N.D.			
	22-5	4.20	2.38	0.60	N.D.			
	23-5	4.40	2.60	0.88	N.D.	N.D.	Tr.	N.D.
	25-6	5.37	3.30	0.83	N.D.	N.D.	0.41	N.D.
	30-5	9.03	3.10	1.03	N.D.	N.D.	0.52	N.D.
	31-1	6.51	4.44	1.11	N.D.	N.D.	1.10	N.D.
	32-2	15.4	3.21	0.64	N.D.	N.D.	0.77	N.D.
	33-4	10.2	5.19	1.30	0.43	0.21	1.31	Tr.
	36-6	16.2	4.14	1.38	N.D.	N.D.	1.38	N.D.
	37-2	13.4	4.63	1.54	N.D.	N.D.	0.80	N.D.
	38-1	13.3	4.58	1.15	N.D.	N.D.	0.38	N.D.
	39-2	13.4	5.11	1.02	N.D.	N.D.	1.00	N.D.
	40-1	11.3	4.60	1.15	N.D.	N.D.	0.23	N.D.
	41-1	12.8	6.34	2.10	N.D.	N.D.	0.30	N.D.
	43-3	12.3	6.25	2.10	Tr.	0.26	0.05	N.D.
	44-1	12.0	5.79	2.00	0.40	Tr.	3.00	N.D.
	48-1	6.66	2.87	0.96	N.D.	N.D.	Tr.	N.D.
	50-2	13.3	5.03	0.84	N.D.	N.D.	N.D.	N.D.
	52-2	1.90	0.95	N.D.				
	54-2	12.7	3.77	0.90	N.D.			
	55-4	10.2	3.40	0.85	N.D.			
	57-4	10.7	3.65	1.04	N.D.			
	58-1	4.78	1.77	0.59	N.D.	0.29	0.30	N.D.
	59-2	2.35	1.56	Tr.	Tr.	N.D.		
	60-2	4.00	2.67	0.67	0.89	N.D.	0.89	N.D.
	61-2	0.50	Tr.	Tr.	N.D.			
	62-4	0.23	N.D.					
	63-3	0.64	0.50	N.D.				
	64-4	N.D.						
	66-3	Tr.	N.D.					
	71-1	Tr.	N.D.					

Note: Tr.: <0.2 ppm; N.D.: <0.1 ppm.

582B-50, 517 to 527 m sub-bottom), it is about 2%. The presence of CO_2 and high methane content indicate an early diagenetic stage for this sediment (Hunt, 1979). The formation of bubbles and gas pockets within the core liner indicates high absolute concentrations of gases, particularly methane. The C_1/C_2 ratio (Table 5, Fig. 21) is low (10^4) in the sample cored; increases sharply to maximum values of 515,900 and 501,400 between 110 to 130 m sub-bottom; declines gradually between 130 and 193 m; fluctuates between 215,900 and 22,790 between 193 and 413 m; and remains low and constant (10^4) between 413 and 595 m sub-bottom. Beyond 595 m sub-bottom, the amount of gases decreases sharply. Above 347 m sub-bottom, ethane content is generally less than 10 ppm by volume; between 347 and 595 m it generally exceeds 10 ppm; and beneath 595 m it decreases sharply. Propane content varies from trace quantities in the near-surface zone to 6.5 ppm at 440 m sub-bottom (Core 582B-41). Normal pentane is very minor in all the cores. Neopentane is almost absent, and isopentane is present sporadically.

Gas Hydrate

The existence of gas hydrate within the analyzed section is problematic. Gas hydrates are crystalline compounds in which the ice lattice of water expands to form cages that contain the gas molecules (Hunt, 1979). Gas hydrates are solid under particular pressure-temperature conditions (von Huene, Aubouin, et al., 1985). They can accommodate organic molecules as large as isobutane like structures penned in a cage, but pentanes and *n*-butanes are too large for this cage. Near gas-hydrate horizons, the salinity of the interstitial water is greatly reduced, and alkalinity and seismic velocity are increased. Gas hydrate generally occurs between 21 and 27°C (Hunt, 1979). Considering the above facts and the geothermal gradient of about 5.6°C/100 m at the present site, we may consider the gas zones between 10 to 193 m and between 231 to 260 m sub-bottom to be possible gas-hydrate zones. No frozen icelike material occurred in the core liner in these zones, and salinity of the pore waters was not low. Considering the high quantity of methane,

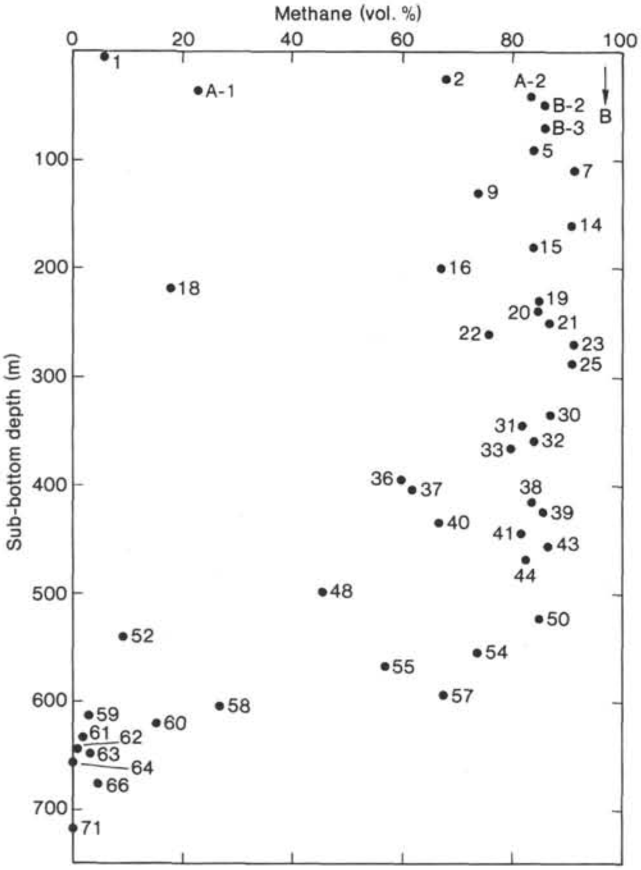

Figure 20. The concentration of methane versus sub-bottom depth, Site 582. Numbers and letter-number combinations indicate core numbers of samples (3 is Core 3 of Hole 582, B-3 is Core 3 of Hole 582B, any core number greater than 3 is from Hole 582B). See Table 5 for corresponding section numbers.

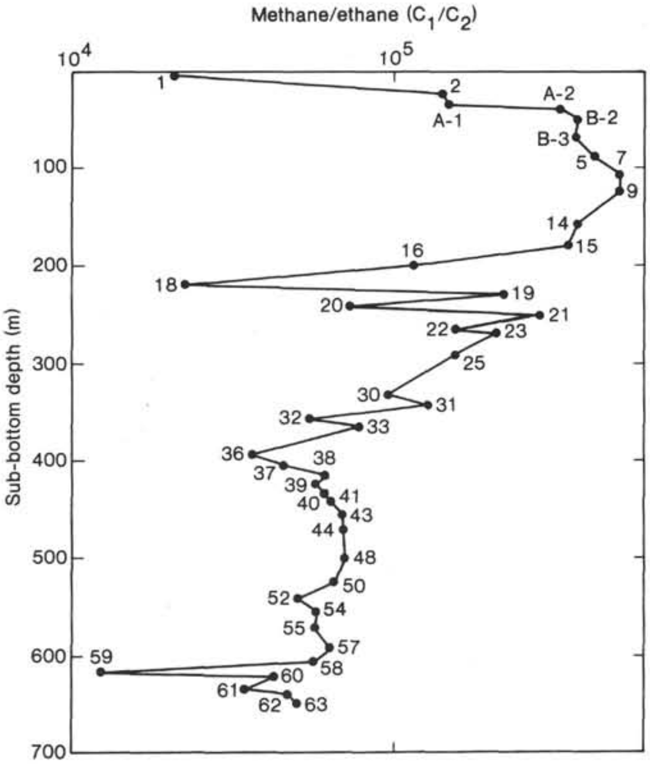

Figure 21. The methane/ethane ratio versus sub-bottom depth, Site 582. Numbers and letter-number combinations as in Figure 20.

the high C_1/C_2 ratio, and the uniformity of the gas composition, the zone between 10 to 193 m sub-bottom could be a gas-hydrate zone with hydrate dispersed within the sediments.

The origin of these gases remains problematic. Considering the presence of high methane, C_1/C_2 ratio, and presence of CO_2 and H_2S, we assume that these gases may have originated from biogenic early diagenetic sources and not from a late catagenetic stage.

PHYSICAL PROPERTIES

Introduction

Physical properties measured during Leg 87 include wet-bulk density, water content, porosity, shear strength, and sonic velocity. Grain densities of representative samples were measured postcruise. Sampling frequency was high in order to produce a well-constrained reference set for this sediment sequence, in which little or no tectonic deformation has occurred.

All samples were taken from the least-disturbed, most-coherent intervals of the recovered core; thus, sampling frequency depended on the core condition. Disturbances of several origins are apparent at different intervals within cores. Gas expansion and accompanying cracks occur within the upper 260 m. Convex-upward laminations and churned sediment produced by drilling remolding are present to a depth of 290 m. Drilling biscuits first appear in Core 582B-26. Local incipient subhorizontal fissility hampered physical property measurements in Cores 23 through 30 of Hole 582B.

The data are tabulated in the Appendix at the end of this volume. Additional plots and discussion of the data are included in Bray and Karig (this volume).

Wet-Bulk Density

Wet-bulk densities, which were determined from the analog GRAPE records, were adversely affected by the cracking and volume increase caused by gas expansion upon pressure release during sampling. As a result, only the maximum sustained wet-bulk densities from the GRAPE are considered reliable.

Special 2-minute GRAPE counts were made on 105 samples from Cores 7 through 73 of Hole 582B. The upper 100 m of this section were either too soft to allow preparation of high-quality samples or too gassy to yield reliable data. Samples selected for this technique exhibited the least gas-induced cracks and minimal drill disturbance.

Samples were taken in Boyce cylinders from Cores 7 through 48, and chunk specimens from Cores 50 through 56 were cut and trimmed with a razor blade. These samples were used both for 2-minute GRAPE counts and water-content determinations. Increased sediment induration allowed minicores to be cut for the remainder of the 2-minute GRAPE and water-content samples. For the chunk and minicore specimens, gamma-ray attenuation was measured both parallel and perpendicular to bedding. The scatter in both sets of wet-bulk density data was considerable but showed a slight increase from an average of 1.80 to an average of 1.95 Mg/m^3 at the base of the section.

Water Content

Water content (percentage of wet weight) was determined for all samples used for special 2-minute GRAPE. Water content decreases from 35% at the sediment/water interface to 22% at 350 m and then remains nearly constant with depth throughout the remainder of Unit 1. In Unit 2, the water content reaches a maximum of 28.1% at 640 m and then declines to 24% in the final core.

Porosities

Porosities were calculated from the maximum sustained GRAPE wet-bulk densities, 2-minute GRAPE wet-bulk densities, and water-content measurements, using grain densities as listed in the Appendix at the end of this volume. The porosity distribution with depth follows a similar trend to that of the water content (Fig. 22). The maximum porosity occurs at the sediment/water interface with an estimated value of 60%. A minimum porosity of 37% occurs at 200 m sub-bottom, after which values increase to 50% at 250 m. At 350 m the porosity is 43% and remains constant again to 575 m. The increase in porosity at 575 m is coincident with the contact between Lithologic Units 1 and 2.

Shear Strength

In an attempt to produce the most complete shear strength data possible utilizing the shipboard equipment, shear strengths were measured with the Wykeham Farrance Vane Shear, two Soiltest CL600 Torvanes, and a Soiltest CL700 pocket penetrometer. Measurements were recorded from each instrument until the sediment shear strength exceeded the equipment capacity.

Undisturbed and remodeled vane shear tests were performed on 32 intervals of silty clay to a depth of 300 m sub-bottom. The undisturbed shear strength increases from a minimum 2.6 kPa at 15 m to a maximum 73.3 kPa at 190 m sub-bottom (Core 582B-15). During testing of Cores 9 through 26 of Hole 582B, horizontal cracks occasionally occurred before shear failure and caused anomalously low undisturbed and remolded strengths. Use of

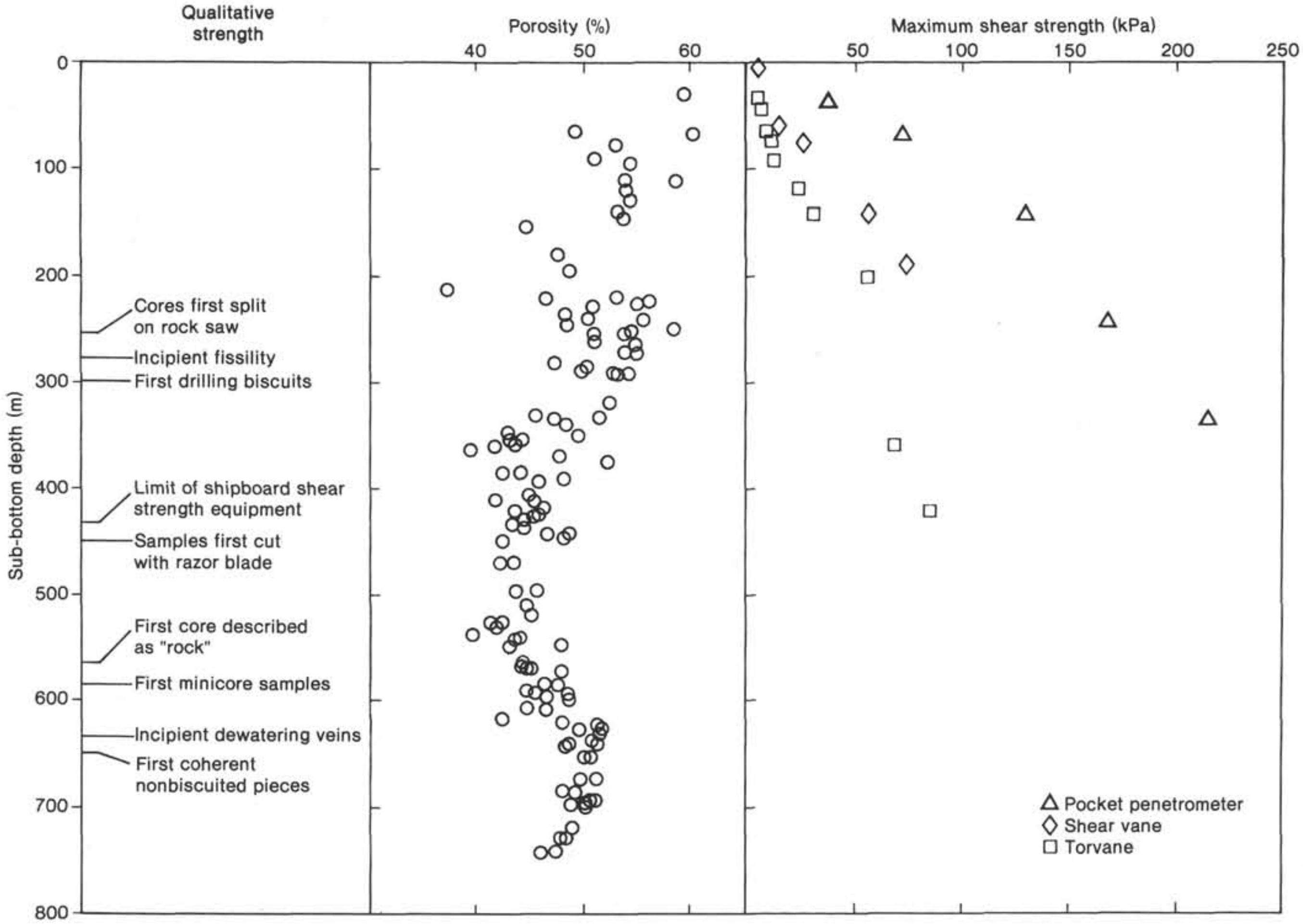

Figure 22. Porosity versus depth (Site 582) as calculated from water-content measurements using grain densities listed in Appendix at the end of this volume. Maximum shear strength versus depth measured with a CL700 Pocket Penetrometer, Wykeham Farrance Shear Vane, and CL600 Torvane.

the vane shear apparatus was discontinued after Core 26, when it became impossible to produce shear failure on a cylindrical surface without surface fractures. Despite the wide scatter in the data, the general trend suggests an increase in shear strength on the order of 0.40 kPa/m.

Sensitivity (ratio of undisturbed shear strength to remolded shear strength) within the two lithologic units of Site 582 is variable and ranges from 1.3 to 5.8. The average sensitivity is 3.2. Sensitivity correlates neither with depth, undisturbed shear strength, nor remolded shear strength.

The CL700 pocket penetrometer was used on Cores 2 through 39 of Hole 582B to measure bearing capacity, which is a function of shear strength unconfined compressive strength. Shear strengths derived from these data range from 36 kPa at 40 m to 216 kPa at 328 m (Fig. 22). These values are somewhat higher than those measured by the vane shear apparatus, and suggest an increased in shear strength to approximately 0.6 kPa/m. At greater depth, sediments are too hard to permit penetration, qualitatively showing a further increase in strength above the limits of the equipment.

Shear strengths measured with the two Soiltest CL600 Torvanes are variable, but show a continuous increase with depth—approximately 0.21 kPa/m. Values range from 2.5 kPa at 40 m to 85 kPa at 420 m, at which point the tests were discontinued because of excessive cracking. Figure 22 shows the maximum shear strengths obtained from each of the three techniques versus depth in the section.

Sonic Velocities

Compressional-wave velocities were measured with the Hamilton Frame velocimeter; shear-wave velocities were obtained with the new sonic viewer provided by H. Kinoshita. Very few sonic velocity measurements were possible in the upper 500 m of the section because of high attenuation caused by high gas content and associated expansion cracks. Frequent measurements were possible in Cores 52 through 73 of Hole 582B. Throughout the section, compressional-wave velocities increase from approximately 1.78 km/s in Core 52 to approximately 1.9 km/s within Core 73. Shear-wave velocities are more variable but also show an increase from about 0.35 to about 0.60 km/s at the base of the section.

When compared to interval velocities calculated from seismic reflection profiles (see Seismic stratigraphy section), the laboratory compressional-wave velocities are lower in four of the six seismic units identified.

PALEOMAGNETICS

Mean and standard deviation of intensities of all samples after the 15-mT alternating field (AF) demagnetization (J_{15}) are 3×10^{-4} and $\sim 1 \times 10^{-1}$ A/m, strong enough to be measured with the shipboard and shore-based magnetometers, at a noise level of 4×10^{-4} and 1×10^{-4} A/m, respectively. The ratio of J_{15} and intensity of natural remanent magnetization (NRM) is 0.693 ± 0.270. The high ratio means that the sediments contain fine magnetic minerals that have a single magnetic domain structure. The intensity of magnetization varies with stratigraphy. In Unit 1, the uppermost 30 m of Hole 582, magnetization is quite weak (3×10^{-4} A/m). From 30 to 560 m sub-bottom, intensity is bimodally distributed; turbidite sands and silts are strongly magnetized ($2 \times 10^{-2} \pm \sim 2 \times 10^{-1}$ A/m), whereas hemipelagic intercalations are weakly magnetized ($5 \times 10^{-3} \pm \sim 1 \times 10^{-2}$ A/m). Samples from Unit 2 are very weakly magnetized (intensity is about 5×10^{-4} A/m). The direction of remanent magnetization after 15-mT AF demagnetization is the basis for this discussion of paleomagnetism.

Inclinations of samples taken from Holes 582 and 582B are bimodal, and these modes are consistent with the inclination of normal and reverse axial dipole field for this area. Their inclinations are therefore indicators of polarity and are used to form the magnetostratigraphic record shown in Figure 5. Above 607 m sub-bottom, the sedimentary sequences have normal polarity except for horizons at 28.42 and 106.67 m sub-bottom. Below 607 m, the sediments are dominantly of reversed polarity. Within this interval, however, sediments from 662 to 693 m and at 721 m sub-bottom are normally polarized. The upper normal interval is correlated with the Brunhes Epoch and lower reversed polarity interval with the Matuyama Epoch. The short normal polarity interval within the Matuyama Epoch represents the Jaramillo Event. These magnetostratigraphic correlations are supported by biostratigraphic data. Isolated horizons of reversed polarity at 28.42 and 106.67 m sub-bottom match one of the short events in the Brunhes Epoch (either the Blake or Biwa I, II, or III) and possibly correlate with the similar events at Site 583.

HEAT FLOW

The Uyeda probe was used to measure sub-bottom temperatures at Site 582. Three of the four runs attempted were successful, and the temperature data (Table 7) were calculated using DSDP calibration tables for the thermistor resistance versus temperature (T). Deviations of the data from the T values given by the table were significant; therefore, the thermistor resistance of the probe was recalibrated for better data reduction.

Thermal conductivities of cores were measured by means of a needle probe. Thirty-six conductivity measurements were made on nine cores. The mean thermal conductivity for the depth interval 0–500 m sub-bottom was calculated to be $3.24 \pm 0.50 \times 10^{-3}$ cal/(cm · deg · s) (0.50 is the standard deviation).

Table 7. Temperature (T) and its gradient with respect to sub-bottom depth (Z) at Site 582.

Sub-bottom depth (m)	T (°C)	dT/dZ (°C/cm)
0	1.75 ± 0.25[a]	
96.9	9.3 ± 0.3	7.68 ± 0.5 ($\times 10^{-4}$)
145.2	12.9 ± 0.5	
508.2	28.8 ± 0.05	4.38 ± 0.15 ($\times 10^{-4}$)

[a] Assumed mudline temperature.

The values for heat flow were calculated upon the assumption that heat flow occurs vertically and only by conductive heat transfer. The average heat flow value for the depth interval 0–500 m sub-bottom at Site 582 is 1.49 HFU[3]. Figure 23 shows the plot of temperature versus sub-bottom depth, and Figure 24 illustrates the distribution of heat flow in the Leg 87 area.

SEISMIC STRATIGRAPHY

High-quality, 48-channel, 24-fold multichannel seismic reflection profiles were made across Site 582 (SP 1940) during the 1980 cruise of *Kaiyo-maru* of the Japan Petroleum Exploration Company, and the migrated depth sections were published in 1982 as part of the Japanese IPOD activities (Nasu et al., 1982).

Figure 25 is the migrated time section of Profile N55-3-1. Stacking velocities at SP 1901 were used to construct Figure 25. These values are 1.69 km/s for the upper Pleistocene turbidites (above Horizon C), 2.13 km/s for the lower Pleistocene turbidites (between C and E), 2.59 km/s for hemipelagic "basin" strata (between E and H), and 2.39 km/s for the Pliocene turbidites (between H and L). A velocity inversion from "basin" strata to the Pliocene turbidites has been used for multichannel data processing. The physical property studies for Site 297 showed a density decrease in their Lithologic Unit 5 (Ingle, Karig, et al., 1975a).

Revised interval velocities are shown for Profile N55-3-1 (Fig. 26), but no velocity inversions are recognized (Y. Aoki, 1982, pers. com.). These velocities were used to calculate the depths to the various reflectors. All the regionally mappable reflection horizons and ocean basement (B, C, E, H, and L) are shown as marker horizons (Fig. 25, Table 8).

The marker horizons of this site are described as follows:

B: bottom-simulating reflector. BSR-type reflectors occur above Horizon B, an acoustically weak reflector produced by velocity and lithology contrast.

C: acoustically strong reflector found within trench-fill sediments.

E: a marker horizon. This reflector is traced across the trench fill and on to the landward slope, but is very faint at Site 582, suggesting that the surrounding sediment has changed to hemipelagic basin strata. The trench-filling sediments at Site 582 start to develop approximately 50 m above this horizon.

H: a physical break and a lithologic change between hemipelagic mudstone above and the turbidite sequence below. Stacking velocity increased slightly from 2.31 to 2.43 km/s.

L: acoustic basement. One of the characteristics of this reflector is a relatively smooth surface lacking horst and graben. Offsets of basement are limited in number. This reflector and H were not penetrated at Site 582.

Continuous coring in Site 582 has provided new results regarding the interpretation of the seismic stratigraphy. Most of the seismic horizons, however, are found within the interval of very little or no core recovery (Table 9, and refer to Table 1). Important for seismic correlation near Site 582 is the discovery of the pumice-bearing sandy turbidite found in Core 582B-27 (300 m sub-bottom). Also, the lack of core recovery and drilling characteristics observed on the rig floor are indications of other sandy intervals. The seismic signature of the sedimentary facies is uniform from Cores 27 down through 31 of Hole 582B and is typified by the turbidite shown in Figure 27. This horizon, Reflector C, may also be a very good marker for Site 583. When drilling through the lower part of the Pleistocene formation, we encountered sandy and silty turbidite sequences with very thin intercalations of dark gray hemipelagites. Apparently, the increased content of coarse-grained sand is responsible for the increase in reflectivity of the 6.90 and 6.99 s reflection horizons. Combined with the C horizon, these three reflectors are characteristic markers of lithologic contrasts indicated in the seismic profile. Between these horizons, interval velocities are 2.13 and 2.33 km/s (Table 10). This range includes the 2.31 km/s velocity determined from the revised values shown in Figure 26.

The turbidite sequences below the 6.99 s reflection horizon (489 m sub-bottom) are distal facies consisting of laminated silty mudstone and a thick accumulation of hemipelagic mudstone. The hemipelagites gradually become more dominant downsection. The lower boundary of the turbidite sequence, as defined in the reflection profile, is placed at the 7.06-s reflection horizon at Site 582.

Correlation of reflectors between this site and Site 297 of Leg 31 is carried out using Line 22-23 of the Geological Survey of Japan. Velocity assumptions are made from shipboard measurements at Site 297 of Leg 31 (Ingle, Karig, et al., 1975a) and from the values listed in Table 11.

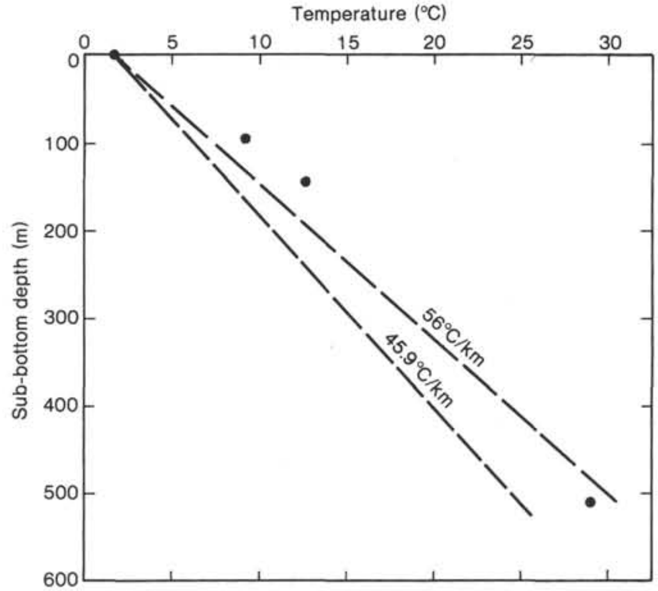

Figure 23. Temperature versus sub-bottom depth (Site 582). Temperatures of the bottom of the hole were measured by inserting heat-flow spearhead probe into sediment. Mudline temperature is assumed to be 1.75 ± 0.25 based upon the oceanographic data of this area.

[3] HFU = heat flow units = × 10^{-6} cal/(cm^2 · s).

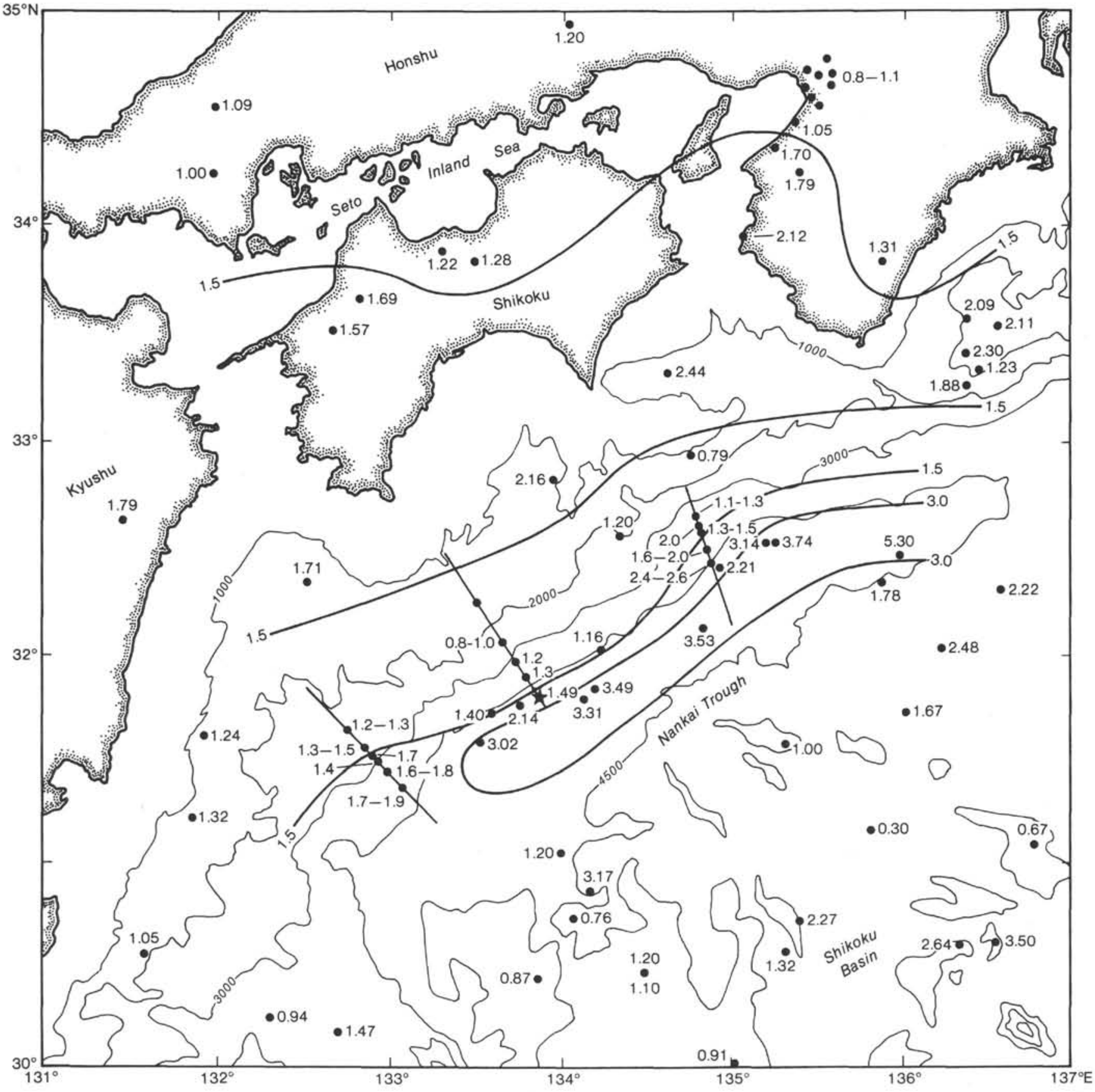

Figure 24. Distribution of heat flow in the Leg 87 study area. * shows the location of the Site 582 value.

Using these values, the sub-bottom depths of reflectors were calculated and generally matched with the drilling results at Site 297 (Table 12). A fairly strong reflector with reverberant layers occurs at 340 m (0.4 s) sub-bottom on the profile across Site 297 (Fig. 28). That reflector may correspond to the top of the Pliocene turbidite sequence drilled at Site 297 and is easily traced toward Site 582.

Based on the calculated interval velocity (Table 8) and the lithology at Site 582, the seismic stratigraphic units are divided as follows (Table 10):

1. Interval between 6.47 and 6.60 s (0 to 107 m sub-bottom). Velocity is 1.65 km/s, and sandy turbidites characterize the lithology.

2. Interval between 6.60 and 6.70 s (107 to 202 m sub-bottom). Velocity of this interval averages 1.90 km/s, unusually high for normally compacted marine sediments of such young age, although again sandy turbidites characterize the lithology. Careful examination of Profile N55-3-1 indicates a patchy occurrence of BSR-type reflectors above marker Horizon B. Also, the velocity inversion calculated below B is unusual for normally com-

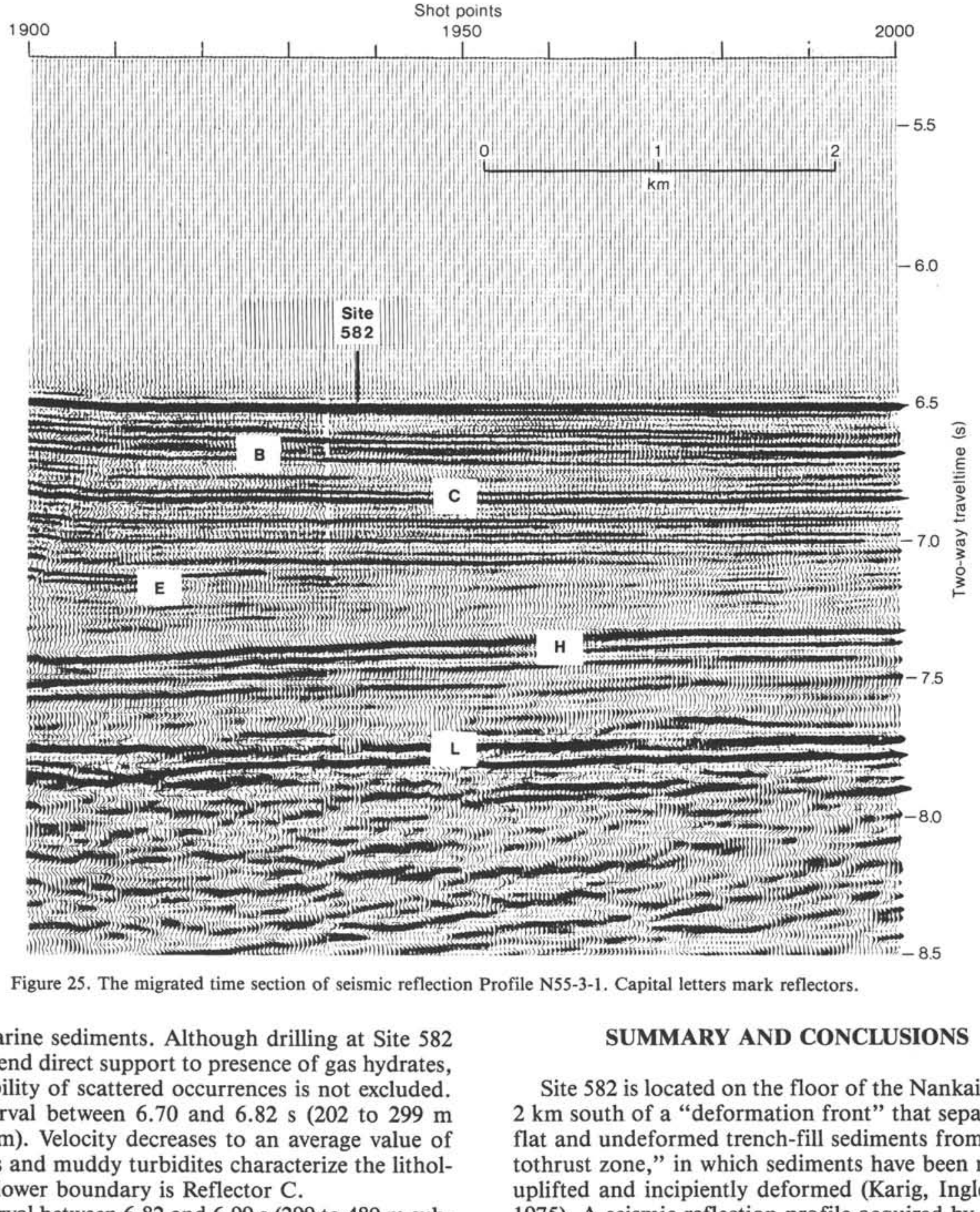

Figure 25. The migrated time section of seismic reflection Profile N55-3-1. Capital letters mark reflectors.

pacted marine sediments. Although drilling at Site 582 does not lend direct support to presence of gas hydrates, the possibility of scattered occurrences is not excluded.

3. Interval between 6.70 and 6.82 s (202 to 299 m sub-bottom). Velocity decreases to an average value of 1.58 km/s and muddy turbidites characterize the lithology. The lower boundary is Reflector C.

4. Interval between 6.82 and 6.99 s (299 to 489 m sub-bottom). Velocity increases markedly to an average value of 2.23 km/s, and coarse-grained sandy turbidites with pumice characterize the lithology.

5. Interval 6.99 to 7.06 s (489 to 556 m sub-bottom). Velocity decreases to an average value of 1.92 km/s and distal turbidites dominate in this interval. Towards land, turbidite facies develop in the deeper horizons, which can be traced to this site as deep as 7.10 s (604 m sub-bottom depth). This horizon is regarded as Reflector E.

6. Interval between 7.06 and 7.36 s (556 to 919 m sub-bottom). This interval represents the hemipelagic mudstone of the Shikoku Basin strata.

SUMMARY AND CONCLUSIONS

Site 582 is located on the floor of the Nankai Trough, 2 km south of a "deformation front" that separates the flat and undeformed trench-fill sediments from a "protothrust zone," in which sediments have been relatively uplifted and incipiently deformed (Karig, Ingle, et al., 1975). A seismic reflection profile acquired by the *Glomar Challenger* upon departure from Site 583 (Fig. 29), combined with the reference seismic profile (Fig. 2), shows that the sediment fill of the Nankai Trough near Site 582 is slightly over 16 km wide and, at the deformation front, it is between 700 and 750 m thick.

This wedge of trench-fill sediments overlies a lower Pleistocene and older basin plain sequence deposited in the Shikoku Basin, which varies very little in acoustic character between Sites 582 and 297. At Site 297, this sequence was shown to consist dominantly of hemipelagic sediments, but with a strongly reflecting mid-Pliocene turbidite sequence between 330 and about 550 m (Ingle,

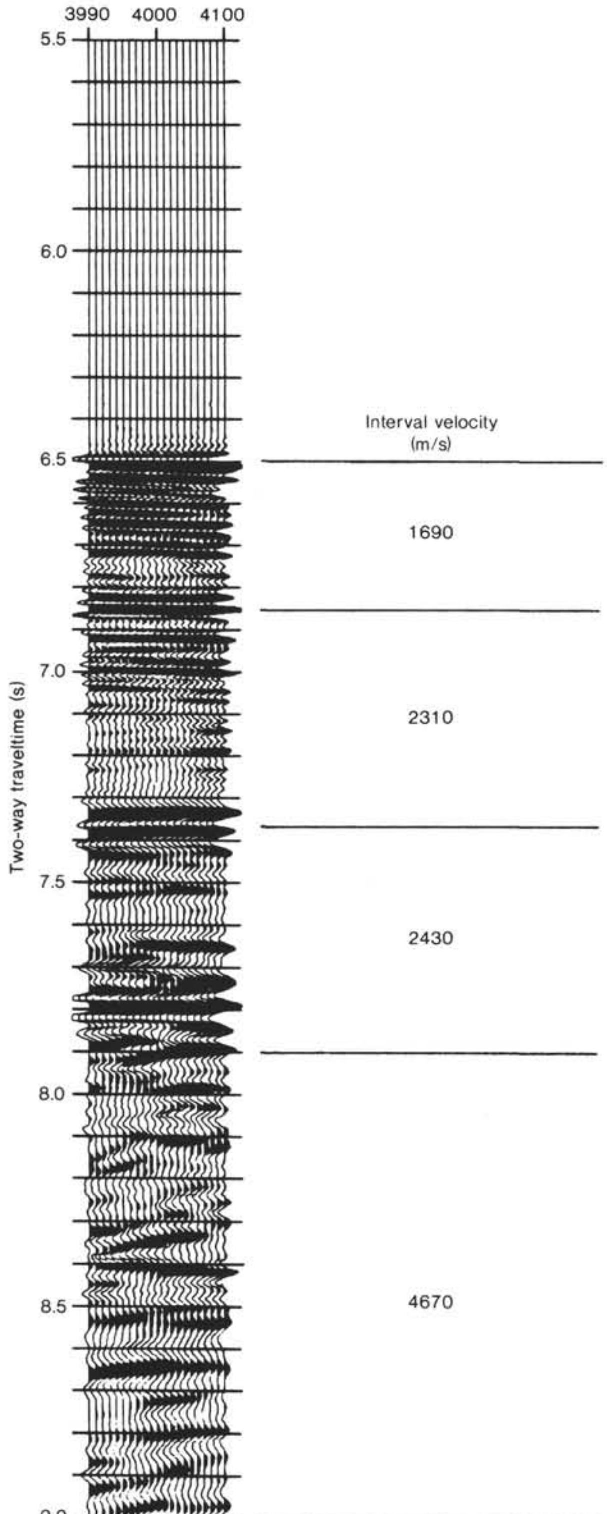

Figure 26. Interval velocities for seismic reflection Profile N55-3-1. The CDP number 3990 corresponds to SP number 1901.

Karig, et al., 1975a). This sequence, assumed to have been deposited horizontally, now dips nearly 3°N beneath the trench wedge and supplies the most reliable measure of the flexure of ocean crust beneath the Nankai Trough.

Table 8. Comparison of interval velocities based on seismic reflection Profile N55-3-1 (Ocean Research Institute, Tokyo) and velocities measured directly on Site 582 samples.

Seismic unit	Average interval velocity (km/s)	Average laboratory velocity (km/s)
1	1.65	1.78
2	1.90	1.70
3	1.58	1.73
4	2.23	1.78
5	2.08	1.83
6	2.31	1.87

Table 9. Seismic reflectors predicted at Site 582.

Reflection time (s)	Interval velocity (km/s)	Calculated sub-bottom depth (m)	Marker horizon	Remarks
6.47		0		Sea floor (4879 m)
	1.69			
6.60		109.9		
6.62		126.8		Faint reflectors in
6.65		152.1		apron sedi-
6.70		194.4	B	ments and
6.78		262.0		trench fill sediments
6.82		295.1	C	Strong reflector
	2.31			
6.90		387.5		Faint reflectors in
6.99		491.5		trench fill
7.02		526.1		sediments
7.06		572.3		Unit 1/Unit 2
7.10		618.5	E	boundary (hemapelagite)
7.36		918.8	H	Top of Pliocene turbidite
	2.43			
7.73		1368.4	L	Top of ocean crust
	4.67			

At Site 582 the thickness of the trench wedge is between 560 (as defined by lithologic change) and 600 m (as defined on the seismic profile). The sediment fill comprising the wedge includes both turbidites and hemipelagic sediments. Because of the low (41%) core recovery in Hole 582B and the inability to log the holes, interpretation of the section is highly subjective and relies on the assumption that the zones with the lowest recovery, and with characteristics that the drillers thought were symptomatic of sand, represent intervals in which sands were washed away. This assumption is strengthened by the good correlation of presumed sand-rich zones with major seismic reflectors (see Seismic Stratigraphy section) and often by trace recovery of sand in cores through these zones.

As predicted by interpretation of the reference seismic profile (Fig. 2), the sediment column sampled at Site 582 consists of two lithologic units: the Nankai Trough axial turbidites and the underlying hemipelagic mud that accumulated in the Shikoku Basin (see Sedimentology section for details). The trench turbidites include both sand and silts rich in volcanic and lithic fragments, in heavy minerals, and in red volcanic fragments. The To-

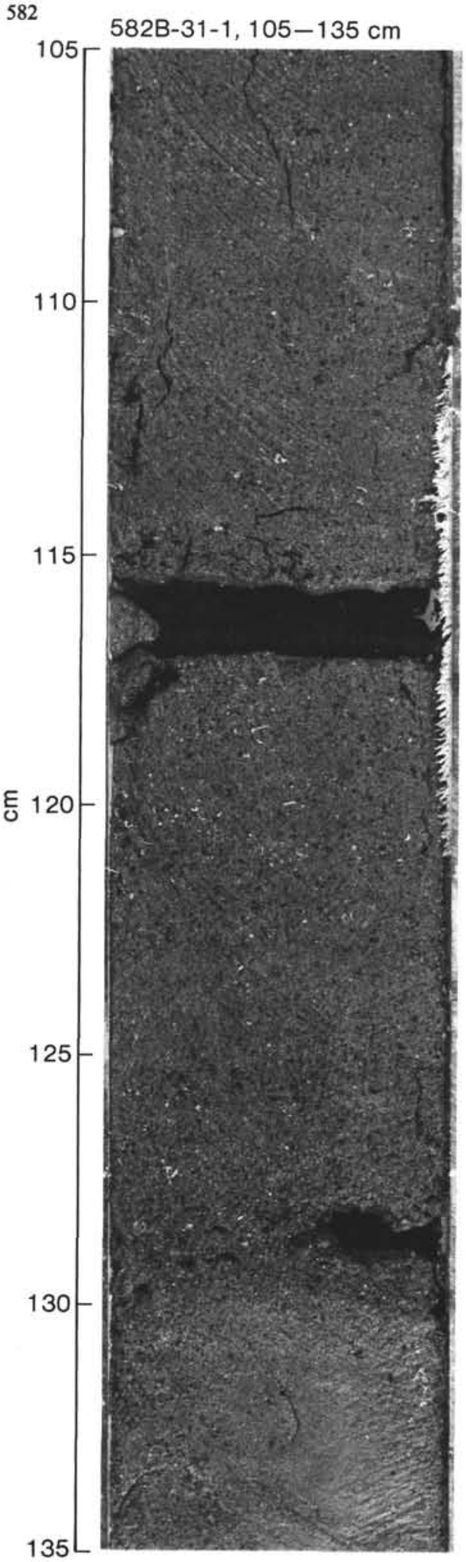

Figure 27. A sandy turbidite from Core 582B-31 showing the type of sediment represented by Reflector C (see Fig. 25).

kai drainage basin, near the Izu Peninsula and considerably to the north of Site 582, contains this range of lithic components, and submarine bathymetry indicates a direct link to the Nankai Trough. It is, therefore, a most likely source for the Site 582 turbidites, although a combination of other-source terranes might produce the same mixture. Within the upper lithologic unit, the sandy intervals decrease in number downward in the section, but a very coarse unit near 300 m sub-bottom marks their reappearance. The latter contain large pumice grains, again indicating a source area in the volcanic rock-bearing terrane of Izu. The migration of channels on the

Table 10. Correlation of drilled seismic horizons at Site 582.

Reflection time (s)	Drilled depth (m)	Calculated average velocity (km/s)	Calculated interval velocity (km/s)	Marker horizon	Seismic unit
6.47	0				
		1.65	1.65		1
6.60	107				
		1.68	1.90		
6.62	126				
		1.71	1.87		2
6.65	154				
		1.75	1.92		
6.70	202			B	
		1.74	1.70		
6.78	270				3
		1.71	1.45		
6.82	299			C	
		2.13	2.13		
6.90	384				4
		2.51	2.33		
6.99	489				
		2.19	1.93		
7.02	518				
		2.14	1.90		5
7.06	556				
		2.18	2.40		
7.10	604			E	
		(2.31)			
7.18	720				6
7.36	(919)			H	

Note: Parentheses indicate not drilled.

Table 11. Velocity assumptions for the lithologic section, Site 297.

Velocity (km/s)	Depth in hole (m)	(s)
1.6	250	0.31
1.8	560	0.65
2.0	660	0.75
2.5	780	0.85

Note: Data from Ingle, Karig, et al., 1975a.

Table 12. Correlation of reflectors at Site 297 (GSJ Line 22-23).

Sub-bottom depth of reflectors (s)	(m)	Remarks
0.2	160	
0.4	340	Top of Pliocene turbidites
0.85	785	Ocean basement

Note: GSJ = Geological Survey of Japan.

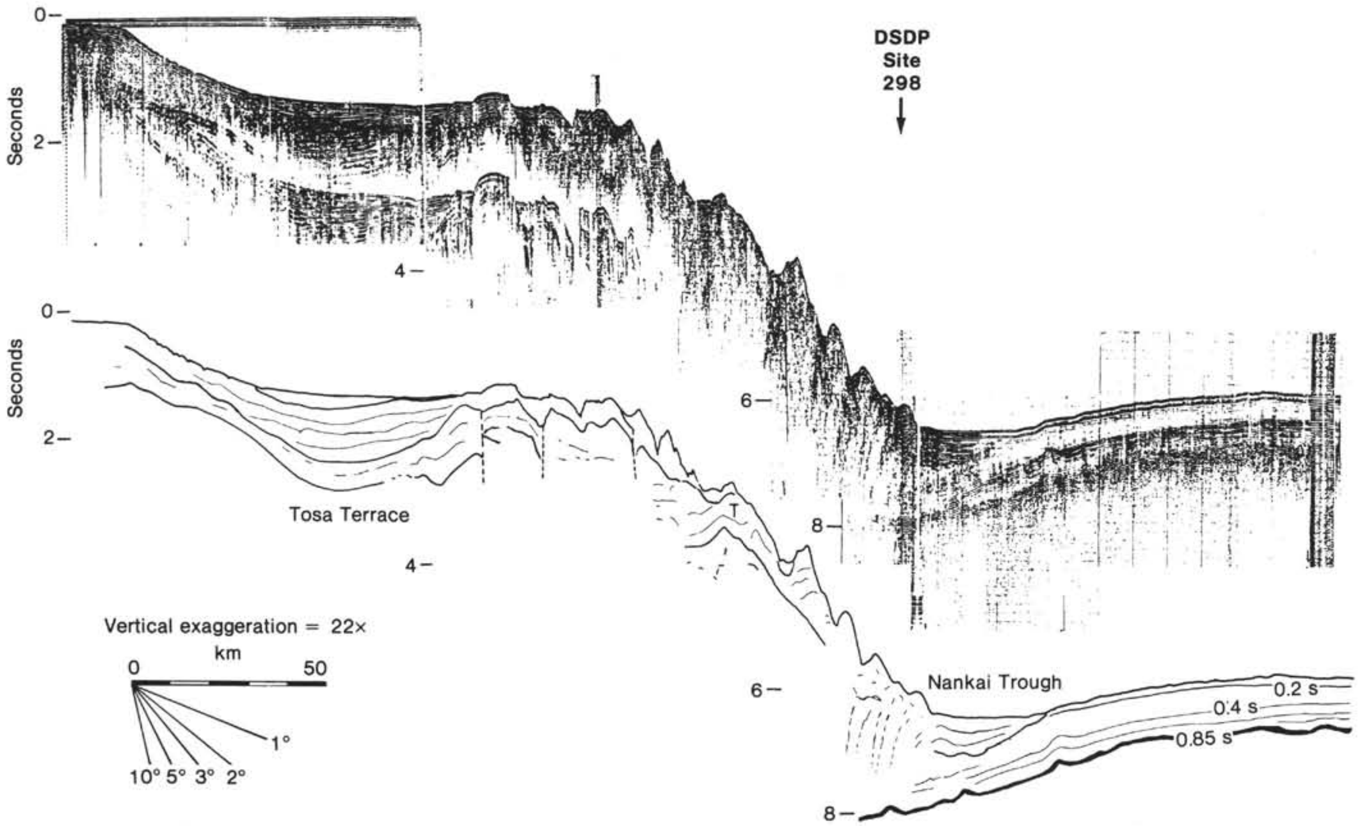

Figure 28. Seismic reflection profiles (Line 22-23) obtained during the GH75-4 cruise to the Tosa Terrace–Shikoku Basin (after Inoue, 1978). Numbers are two-way traveltime in seconds.

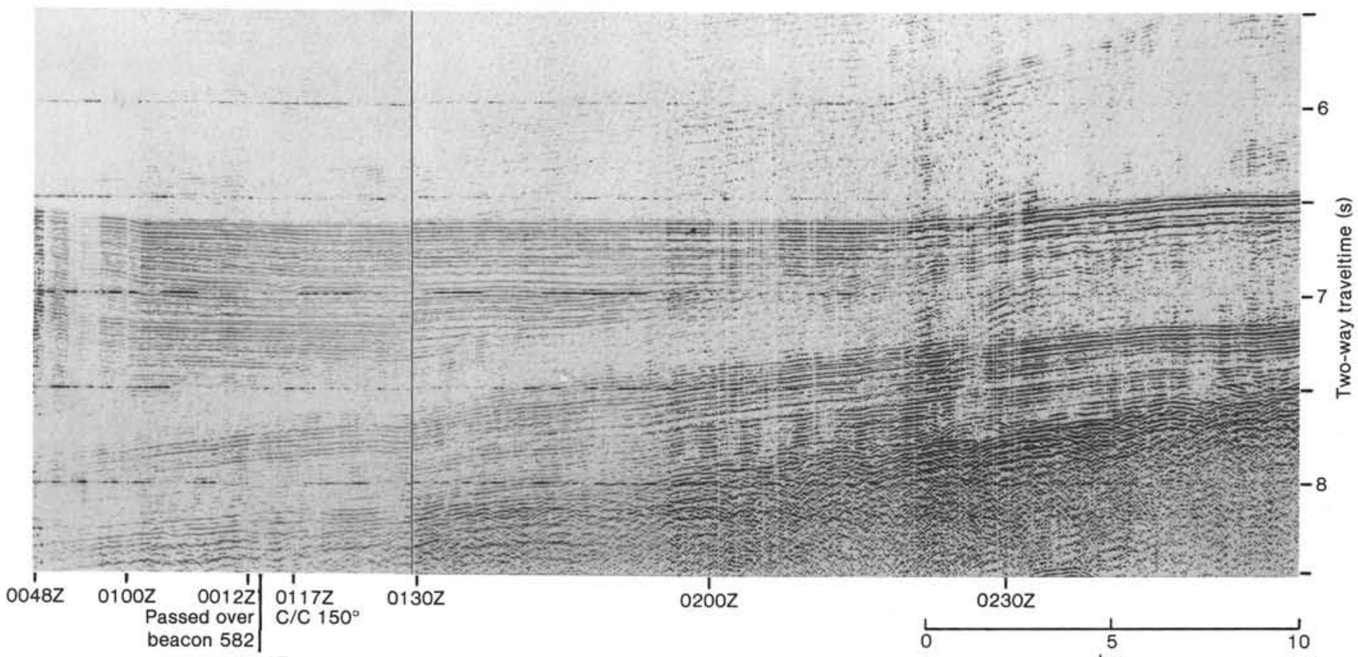

Figure 29. *Glomar Challenger* single-channel seismic reflection profile from a point between Sites 582 and 583, southeastward across the Nankai Trough. This profile extends the reference seismic profile and illustrates the relationship between the trench fill and the underlying section of the Shikoku Basin. C/C = course change.

Japanese margin and depocenters both on the slope and within the Nankai Trough are the most likely causes for the changes recorded in the sandy layers.

The contact between axial turbidites and underlying strata of the Shikoku Basin is near 560 m sub-bottom. These sediments differ from the axial turbidites in their gray to green gray color alternations, their lack of graded-bed *Chondrites* sequences and coarse silt and sand layers, their abundance of green laminations, *Zoophycos* and *Planolites* traces, and the presence of nannofossil-rich intervals and of pumice clasts isolated in a mudstone matrix.

Both the turbidites and the hemipelagic sediments of the axial deposits have an organic carbon content between 0.5 and 0.7%, and that level decreases to less than 0.5% in the hemipelagites beneath. Hydrocarbon gases (mainly methane with very minor CO_2, C_2, C_3 and i-C_4 and traces of H_2S, isopentane, and neopentane) are present throughout the section as gas pockets. No solid gas hydrate was encountered.

Seismic stratigraphy indicates that not only the total thickness of trench fill but also the thickness of individual seismic interval increases toward the inner trench slope. Most of the increase in thickness of units, which ranges up to 20%, occurs beneath the protothrust zone and is primarily attributed to tectonic thickening, because successively younger horizons have been uplifted relative to the Nankai Trough floor by increasing amounts. Uplift resulting from this thickening has raised the protothrust zone relative to the trough floor, depriving it of turbidite fill. On the reference seismic profile, shallow reflectors beneath the trough axis pinch out toward the deformation front, although the details of this feature cannot be resolved. Our 3.5-kHz profile, however, clearly shows onlap (Fig. 30) and either nondeposition or, more likely, slow deposition rather than erosion over the protothrust zone.

At Site 582, calculated sediment accumulation rates (uncorrected for compaction) are poorly constrained and locally contradictory, chiefly because of the paucity of datum levels resulting from very high sediment accumulation rates but also because of solution effects on the microfossils. The average sediment accumulation rate to the Pliocene/Pleistocene boundary is about 440 m/Ma (see Biostratigraphy section), but this area included 130 to 160 m of Shikoku Basin hemipelagic sediments, which were deposited at a much slower rate than the trench fill (Ingle, Karig, et al., 1975a). The average sediment accumulation rate for the trench fill is estimated to be between 670 and 865 m/Ma. This rate appears to decrease upward to less than half the average rate in upper 100 m (0 to 0.5 Ma). The age of the base of the trench fill, calculated both downward in Site 582 and upward from the top of the turbidite sequence in Site 297, which was estimated to be 2.9 Ma old, is about 0.7 Ma. There are, however, complicating effects of differential sedimentation rates and compaction in the Shikoku Basin sequence between Sites 297 and 582, as discussed later in this section.

The estimation of the subduction rate in the Nankai Trough near Site 582 was an important objective not only because it is a critical parameter for mechanical analyses of subduction complexes, but also because seismologic investigations (Seno, 1977; Molnar et al., 1979) suggest much higher subduction rates (4 to 8 cm/yr.) than did drilling at Site 298 (Ingle, Karig, et al., 1975b). One approach to the determination of subduction rates is to use the geometry of the trench fill and the average sedimentation rate to balance the volume influx (sedimentation rate × trench width) against the outflux (subduction rate × thickness). Despite variants on this approach, all such calculations assume either implicitly or explicitly that both sedimentation and subduction rates remain constant for a sufficient time to produce a steady-state trench geometry. The duration necessary to satisfy this assumption is several times the residence period of sediment in the trench wedge.

If the influx and outflux to the Nankai Trough are equated, the subduction rate is near 1 cm/yr. A second approach is to determine the rate of arcward migration

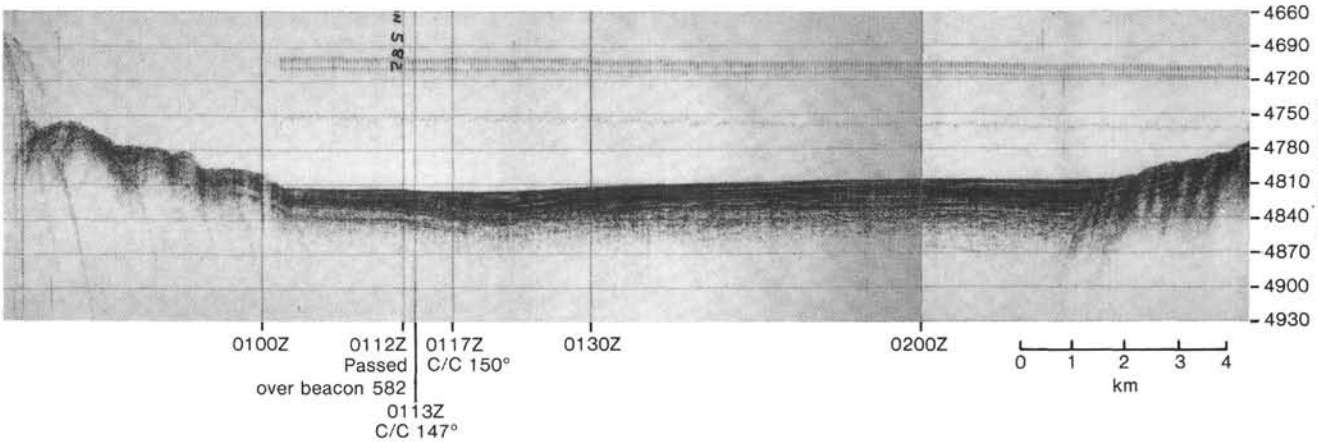

Figure 30. *Glomar Challenger* 3.5-kHz profile across the Nankai Trough from Site 583 southeastward along and beyond the reference seismic profile. The geometry of reflectors on this profile suggests slow, hemipelagic deposition across the protothrust zone and the possible indication of a buried channel. Depths are in meters (assumed velocity = 1.5 km/s). C/C = course change.

of the distinctive facies boundary between the trench-fill sequence and the Shikoku Basin sediments. Because of differences in opinion concerning the seismic definition of the base of the trench wedge, this approach yields values ranging from about 1.0 to 2.5 cm/yr. In short, the steady-state assumption leads to very low calculated subduction rates. Also, these calculations give the rate of migration of the trench wedge with respect to the descending plate, which includes both the perpendicular component of the plate convergence rate and the rate of outbuilding of the inner trench slope.

The geometry of the trench fill in the Nankai Trough is probably not a steady-state feature. The sedimentation rate as measured at Site 582 has decreased over the past 1 Ma by more than half its previous value. Furthermore, if the subduction history of the present Nankai system is short and this trench lies close to the pole of rotation (Seno, 1977), then rapid changes in subduction rates are to be expected.

Determination of subduction rates when geologic conditions are changing is difficult because it requires knowledge of rates of changes in parameters. If total influx and outflux rates are to be compared, then changes of not only sedimentation rates but also of trench widths and thicknesses must be measured. These latter are effectively impossible to measure in most cases because of the destruction of past geometries by deformation beneath the inner trench slope. Moreover, because masses rather than volumes are compared, accurate assessment of porosity changes must also be made.

A seemingly more promising approach to the problem of "instantaneous" subduction rates is the examination of changes in the influx rate of sediment over some relatively short increment of time (t) (Fig. 31). The geometry of this influx increment is a function of width, sedimentation rate, and subduction rate and of their time derivatives. If I is the influx rate in km^3/km per Ma, SD is trench sedimentation rate in km/Ma, SB is subduction rate in km/Ma, and w is trench width in km from deformation front to outer edge of the flat turbidite plain, then

$$\frac{dI}{dt} = SD \frac{dw}{dt} + w \frac{d(SD)}{dt} .$$

The subduction rate is related to w through the migration of the inner edge of the trench floor.

A detailed analysis of this approach is not within the scope of a site report and is described elsewhere (Karig and Angervine, this volume), but several derived constraints can be applied to the subduction rate in the Nankai Trough during the past 0.5 Ma. First of all, $d(SD)/dt$ is negative. Interpretation of the available seismic reflection profiles indicate the width of the Nankai Trough is decreasing (dw/dt is negative). The width through Site 582 is presently 16.3 km, but reflectors from trench fill deposited about 0.6 Ma can be traced on the two profiles (Figs. 2 and 29) for more than 21 km, from the outer facies change, arcward across the basal thrust before they can no longer be resolved because of structural disruption. Thus dw/dt is less than or equal to 7 km/Ma

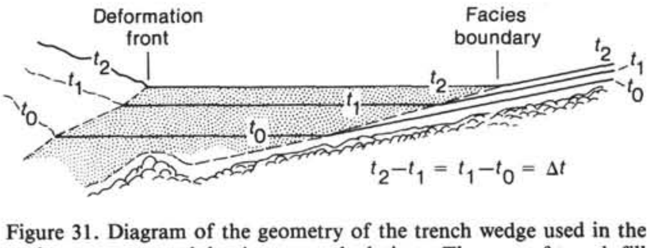

Figure 31. Diagram of the geometry of the trench wedge used in the instantaneous subduction rate calculations. The area of trench fill (stippled pattern), bounded by time lines, represents the amount of sediment influx to the trench wedge during the short time interval Δt. The deformation front (dashed line) delineates the migration path of the minor edge of the trench floor and has no relationship to thrust geometries.

over the past 0.5 Ma. If the decrease is a constant differential over this time increment, then the subduction rate is at least 1.5 cm/yr. If the geometry of the deformed sediments beneath the inner trench slope could be better resolved, the precision of this value might be improved. However, the nonuniform migration of the deformation front, which is tacitly assumed to parallel the subduction rate, begins to pose further limitations to the method.

The primary objective of Site 582 was to produce a reference base with which to compare the results of the following site in an equivalent section on the inner trench slope. As expected, therefore, the structures and physical properties found at Site 582 were not particularly anomalous. The most notable structures are the few small normal faults and veinlike dewatering features in the Shikoku Basin hemipelagites (Unit 2). Similar structures were previously noted only in holes on inner trench slopes and were attributed to subduction-related dewatering and/or extension (Scientific Party, 1980; Watkins, Moore, et al., 1981; von Huene, Aubouin, et al., 1982a, b). The normal faults in the Site 582 cores are most likely due to extensional strain caused by flexure of the outer trench slope and aided by reduced effective confining pressure resulting from the presumed high pore pressures that accompany rapid loading by trench-fill sediments. Concomitant dewatering of the hemipelagic sediments would also account for the close association of the faults and veinlike structures, if, in fact, the latter are caused by dewatering.

A pervasive, subhorizontal fissility that increases in intensity downward occurs in clay-rich, but nonbioturbated, units and is interpreted as a compaction feature accentuating primary mineral alignment. The opening of these fractures may have been intensified by the rapid change of σ_1 (maximum principal stress direction) from vertical to horizontal during drilling, causing failure, or may simply reflect gas expansion and reduced confining stress during the raising of cores.

As expected, porosity at Site 582 decreases downhole (the rate of decrease slows with increasing sub-bottom depth), from about 70% at the surface to 43% at total depth (Fig. 22). Several minor inflections and reversals in the porosity gradient occur, which are considered to be real because of the large number of data collected. The largest reversal occurs near 560 m and can be correlated with the contact between Shikoku Basin hemipelagites and trench fill.

Although the porosity of the Shikoku Basin hemipelagites is higher than that of the overlying trench-fill unit, it is much lower at Site 582 than in the correlative and lithologically similar section at Site 297. This northward decrease in porosity, from more than 70% (Ingle, Karig et al., 1975a) to 45% or less, should result in a reduction in thickness of the upper hemipelagites in Site 582 to less than half that at Site 297. Single-channel seismic profiles (Fig. 29; Ingle, Karig, et al., 1975a) show that this thinning occurs beneath the trench wedge, implying that it is a result of the superincumbent sediment load. The observed thinning is less than that calculated, because the hemipelagic unit, before entering the trench, thins southward away from the source area.

The porosity fluctuations at shallower sub-bottom levels at Site 582 (between 150 and 350 m sub-bottom) are more subtle and less explicable. A sharp downward increase in porosity near 200 m correlates with seismic Reflector B. Coupled with the downhole decrease in interval velocity at this point, the porosity increase would result in a sharp impedance contrast.

Comparison of porosity curves at Sites 582 and 298, drilled in very similar sediment sections, is surprising in that the more reliable water-content values in Site 298 are virtually identical to those in Site 582 down to the base of the trench wedge. This observation brings into question the earlier conclusion (Moore and Karig, 1976) that anomalously rapid dewatering occurred at Site 298 with respect to the undeformed trench section.

Shear strength, as measured by three testing methods, increases continuously downward at Site 582. Although each method gives a different curve (see Physical Properties section), making the absolute values questionable, the relative strength versus depth curve is thought to be valid. The strength of the sediments below 420 m exceeds the capacity of all the instruments, but continues to increase, on the basis of gross physical characteristics, as manifested by the methods used to prepare samples (Fig. 22). This increase in strength is not at all correlative with the porosity curve, which is, below 300 m, nearly constant with depth. No evidence of cementation, diagenesis, or systematic changes in lithology could be found in sedimentologic or X-ray studies of the section, so the cause for the downward increase in strength remains unexplained.

Although the temperature gradient for Site 582 is controlled by only four points, there is a clear downward decrease in heat flow from 2.43 HFU (above 150 m or deeper) to 1.49 HFU (as an average in the measured interval between 160 and 510 m). The reason for the downward decrease is unclear, but the large decrease in porosity of the hemipelagic sediments beneath the trench wedge suggests upward expulsion of this relatively warm water during loading and compaction.

REFERENCES

Arthur, M. A., Carson, B. and von Huene, R., 1980. Initial tectonic deformation of hemipelagic sediment at the leading edge of the Japan convergent margin. *In* Scientific Party, *Init. Repts. DSDP*, 56, 57, Pt. 1: Washington (U.S. Govt. Printing Office), 569-613.

Aubouin, J., von Huene, R., et al., 1982. *Init. Repts. DSDP*, 67: Washington (U.S. Govt. Printing Office).

Blow, W. H., 1969. Late middle Eocene to Recent planktonic foraminiferal biostratigraphy. *In* Brönnimann, P., and Renz, H. H. (Eds.), *Proc. First Int. Conf. Plankt. Microfossils:* Leiden (E. J. Brill), pp. 199-421.

Burckle, L. H., 1972. Late Cenozoic planktonic diatom zones from the eastern Pacific. *Nova Hedwigia*, 39:217-246.

———, 1977. Pliocene and Pleistocene diatom datum levels for the equatorial Pacific. *Quat. Geol.*, 7:330-340.

Cowan, D. S., 1982. Origin of "vein structure" in slope sediments on the inner slope of the Middle America Trench off Guatemala. *In* Aubouin, J., von Huene, R., et al., *Init. Repts. DSDP*, 67: Washington (U.S. Govt. Printing Office), 645-650.

Espitalié, J., Laporte, J. L., Madec, M. F., Marquis, F., Laplat, P., Paulet, J., and Boutefeu, A., 1979. Méthode rapide de charactérisation des roches mères, de leur potentiel pétrolier et de leur degré d'évolution. *Rev. Inst. Fr. Pet.*, 32:23-42.

Fitch, T. J., and Scholz, C. H., 1971. Mechanism of underthrusting in southwest Japan: a model of convergent plate interactions. *J. Geophys. Res.*, 76:7260-7292.

Hays, J. D., 1970. The stratigraphy and evolutionary trends of Radiolaria in North Pacific deep-sea sediments. *Geol. Soc. Am. Mem.*, 126:185-218.

Hinz, K., Winterer, E. L., and Shipboard Scientific Party, 1983. Site 544. *In* Hinz, K., Winterer, E. L., et al., *Init. Repts. DSDP*, 79: Washington (U.S. Govt. Printing Office), 25-80.

Hunt, J. M., 1979. *Petroleum Geochemistry and Geology:* San Francisco (W. H. Freeman and Company).

Ingle, J. C., Jr., Karig, D. E., and Shipboard Scientific Party, 1975a. Site 297. *In* Karig, D. E., Ingle, J. C., Jr., et al., *Init. Repts. DSDP*, 31: Washington (U.S. Govt. Printing Office), 275-316.

———, 1975b. Site 298. *In* Karig, D. E., Ingle, J. C., Jr., et al., *Init. Repts. DSDP*, 31: Washington (U.S. Govt. Printing Office), 317-350.

Inoue, E. (Ed.), 1978. *Investigations of the Continental Margin of Southwest Japan (GH 75-4 Cruise):* Tokyo (Geological Survey of Japan).

Karig, D. E., Ingle, J. C., Jr., et al., 1975. *Init. Repts. DSDP*, 31: Washington (U.S. Govt. Printing Office).

Koizumi, I., 1973. The late Cenozoic diatoms of Sites 183-193, Leg 19, Deep Sea Drilling Project. *In* Creager, J. S., Scholl, D. W., et al., *Init. Repts. DSDP*, 19: Washington (U.S. Govt. Printing Office), 805-856.

Lundberg, N., and Moore, J. C., 1982. Structural features of the Middle America Trench slope off southern Mexico, Deep Sea Drilling Project Leg 66. *In* Watkins, J. W., Moore, J. C., et al., *Init. Repts. DSDP*, 66: Washington (U.S. Govt. Printing Office), 793-814.

Martini, E., and Worsely, T., 1970. Standard Neogene calcareous nannoplankton. *Nature*, 225:289.

Matsuda, T., 1977. Tertiary and Quaternary tectonism of Japan in relation to plate motion. *Assoc. Geolog. Collobor. Japan,* Monograph 20:213-225.

Molnar P., Freedman, D., and Shih, J. S. F., 1979. Lengths of intermediate and deep seismic zones and temperatures in downgoing slabs of lithosphere. *Geophys. J. R. Astron. Soc.*, 56:41-54.

Moore, G. F., Curray, J. R., Moore, D. G., and Karig, D. E., 1980. Variation in geologic structure along the Sunda forearc, northeastern Indian Ocean. *In* Hayes, D. E. (Ed.), *The Tectonic and Geologic Evolution of Southeast Asian Seas and Islands:* Washington (Am. Geophys. Union Mem.), 23:145-160.

Moore, J. C., and Karig, D. E., 1976. Sedimentology, structural geology, and tectonics of the Shikoku and subduction zone, southwest Japan. *Geol. Soc. Am. Bull.*, 87:1259-1268.

Nasu, N., Tomoda, Y., Kobayashi, K., Kagami, H., et al., 1982. *Multichannel Seismic Reflection Data Across Nankai Trough:* Tokyo (Ocean Research Institute, University of Tokyo), IPOD-Japan Basic Data Series, No. 4.

Nigrini, C. A., 1971. Radiolarian zones in the Quaternary of the equatorial Pacific Ocean. *In* Funnell, B. M., and Riedel, W. R. (Eds.), *The Micropalaeontology of Oceans:* New York (Cambridge Univ. Press), pp. 443-461.

Ogawa, Y., 1980. Beardlike veinlet structure as fracture cleavage in the Neogene siltstone in the Miura and Boso Peninsulas, central Japan. *Sci. Rep. Dep. Geol. Kyushu Univ.*, 13(2):321-327.

Saito, T., Thompson, P. R., and Breger, D., 1981. *Systematic Index of Recent and Pleistocene Planktonic Foraminifera:* Tokyo (Univ. of Tokyo Press).

Scientific Party, 1980. *Init. Repts. DSDP*, 56, 57: Washington (U.S. Govt. Printing Office).

Seno, T., 1977. The instantaneous rotation vector of the Philippine Sea plate relative to the Eurasian plate. *Tectonophysics*, 42:209–226.

Sheridan, R. E., Gradstein, F. M., and Shipboard Scientific Party, 1983. Site 533. *In* Sheridan, R. E., Gradstein, F. M., et al., *Init. Repts. DSDP*, 76: Washington (U.S. Govt. Printing Office), 35–140.

Tissot, B., and Welte, D. H., 1978. *Petroleum Formation and Occurrence:* New York (Springer-Verlag).

von Huene, R., Aubouin, J., and Shipboard Scientific Party, 1982a. Site 496. *In* Aubouin, J., von Huene, R., et al., *Init. Repts. DSDP*, 67: Washington (U.S. Govt. Printing Office), 143–192.

________, 1982b. Site 497. *In* Aubouin, J., von Huene, R., et al., *Init. Repts. DSDP*, 67: Washington (U.S. Govt. Printing Office), 193–244.

________, 1985. Site 565. *In* Aubouin, J., von Huene, R., et al., *Init. Repts. DSDP*, 84: Washington (U.S. Govt. Printing Office), 21–78.

Watkins, J. S., Moore, J. C., et al., 1982. *Init. Repts. DSDP*, 66: Washington (U.S. Govt. Printing Office).

SITE 582 HOLE CORE 1 CORED INTERVAL 0.0–9.7 m

TIME – ROCK UNIT	BIOSTRATIGRAPHIC ZONE	FOSSIL CHARACTER: FORAMINIFERS	NANNOFOSSILS	RADIOLARIANS	DIATOMS	SECTION	METERS	GRAPHIC LITHOLOGY	DRILLING DISTURBANCE	SEDIMENTARY STRUCTURES	SAMPLES	LITHOLOGIC DESCRIPTION
	Emiliania huxleyi–Gephyrocapsa oceanica zones (N) NN21–NN20	RG	CG	CP		1	0.5, 1.0	T2, V1			*	Muddy ash
								V1			*	Muddy ash
						2		T2			*	5Y 4/1
		FG	CG	FP		3		V1, T2			*	5Y 4/1; Ash, 5Y 4/2–4/3; 5Y 5/2; 5Y 4/1
												IW
	Buccinosphaera invaginata zone N22/23			CM		4		T2			*	5Y 4/1
				FP		5		T2			*	Dewatering feature, burrow? Color change 5Y 3/2
								OG				
				AM		6		T2			*	Mottles
						7		Void				
		CG	CG	CM		CC		T2				

HEMIPELAGIC MUD
Olive gray (5Y 3/2)

SMEAR SLIDE SUMMARY (%):

	1, 118 M	1, 145 M	1, 56 D	2, 75 M	3, 26 M
Texture:					
Sand	65	32	15	40	95
Silt	30	67	70	50	5
Clay	5	1	15	10	0
Composition:					
Quartz	Tr	2	45	50	3
Feldspar	Tr	Tr	5	Tr	2
Mica	Tr	–	–	Tr	–
Heavy minerals	–	Tr	2	–	Tr
Clay	–	–	15	12	–
Volcanic glass	83	90	3	35	95
Glauconite	1	1	2	–	–
Pyrite	2	1	5	Tr	Tr
Carbonate unspec.	–	4	–	–	–
Foraminifers	Tr	2	–	–	–
Calc. nannofossils	Tr	Tr	–	–	–
Diatoms	7	–	13	3	–
Radiolarians	Tr	Tr	5	Tr	Tr
Sponge spicules	7	Tr	5	–	–

	3, 45 D	4, 75 D	5, 74 D	6, 70 D
Texture:				
Sand	5	10	5	5
Silt	65	60	70	45
Clay	30	30	25	52
Composition:				
Quartz	43	60	10	35
Feldspar	3	–	55	Tr
Mica	–	Tr	–	2
Heavy minerals	3	Tr	Tr	Tr
Clay	30	30	20	37
Volcanic glass	2	5	8	–
Glauconite	–	–	–	5
Pyrite	5	1	Tr	1
Carbonate unspec.	–	–	1	–
Foraminifers	5	–	Tr	2
Calc. nannofossils	–	–	Tr	7
Diatoms	5	4	1	4
Radiolarians	2	–	1	2
Sponge spicules	2	Tr	1	Tr
Silicoflagellates	–	–	–	Tr
Plant debris	Tr	–	–	–
Volcanic lithic fragments	–	–	3	5

Core 2, 9.7–19.4 m: no recovery.

SITE 582 HOLE CORE 3 CORED INTERVAL 19.4–29.0 m

TIME – ROCK UNIT	BIOSTRATIGRAPHIC ZONE	FOSSIL CHARACTER: FORAMINIFERS	NANNOFOSSILS	RADIOLARIANS	DIATOMS	SECTION	METERS	GRAPHIC LITHOLOGY	DRILLING DISTURBANCE	SEDIMENTARY STRUCTURES	SAMPLES	LITHOLOGIC DESCRIPTION
	Emiliania huxleyi–Gephyrocapsa oceanica zones (N) NN21–NN20	RG	CG	CM		1	0.5, 1.0	Void, T2			*	Very dark gray (5Y 3/1); Black (5Y 2.5/1), deformed bed; Dark gray (5Y 4/1)
		RG	CG					T2			*	Void
						2		Void, T2				5Y 3/1
	Collosphaera tuberosa zone N22/23					3		Void, T2			* *	
						4					*	Mottles
		RG	CG			5		Void, T2				5Y 3/1; Mottle
								IW, Void				
		FG	CG	CM		6		T2			*	Void; 5Y 3/1; 5Y 2.5/1; Black (5Y 2.5/1) deformed bed
		CG	B	B		7, CC		Void, T2				5Y 3/1

HEMIPELAGIC MUD

Core-Catcher: thin section impregnation.

SMEAR SLIDE SUMMARY (%):

	3, 120 M	1, 75 D	2, 40 D	3, 120 M	4, 71 D	6, 87 D	CC D
Texture:							
Sand	80	10	10	80	10	10	70
Silt	15	60	50	15	60	70	20
Clay	5	30	40	5	30	20	10
Composition:							
Quartz	40	40	5	40	50	54	15
Feldspar	5	5	–	5	2	2	3
Mica	12	Tr	3	10	1	1	15
Heavy minerals	5	Tr	3	5	1	1	5
Clay	5	30	71	5	30	20	12
Volcanic glass	Tr	5	10	Tr	8	3	40
Pyrite	–	2	Tr	–	1	2	5
Foraminifers	3	–	Tr	3	–	–	–
Calc. nannofossils	–	–	–	–	–	10	Tr
Diatoms	–	10	3	–	5	5	–
Radiolarians	–	5	5	Tr	Tr	1	Tr
Sponge spicules	Tr	3	–	–	2	1	–
Silicoflagellates	–	Tr	–	–	–	–	–
Fish remains	–	–	–	–	Tr	–	–
Lithic fragments	30	–	–	27	–	–	5

Core 4, 29.1–38.8 m: no recovery.

Information on core description sheets, for ALL sites, represents field notes taken aboard ship under time pressure. Some of this information has been refined in accord with post-cruise findings, but production schedules prohibit definitive correlation of these sheets with subsequent findings. Thus the reader should be alerted to the occasional ambiguity or discrepancy.

SITE 582 HOLE A CORE 1 CORED INTERVAL 29.1–38.8 m

TIME-ROCK UNIT | BIOSTRATIGRAPHIC ZONE | FOSSIL CHARACTER (FORAMINIFERS, NANNOFOSSILS, RADIOLARIANS, DIATOMS) | SECTION | METERS | GRAPHIC LITHOLOGY | DRILLING DISTURBANCE | SEDIMENTARY STRUCTURES | SAMPLES | LITHOLOGIC DESCRIPTION

Biostratigraphic zone: N22/23, NN21–NN20

Fossil character: CG CM RM

Sections: 1, 2, 3, 4, 5, CC

Meters: 0.5, 1.0

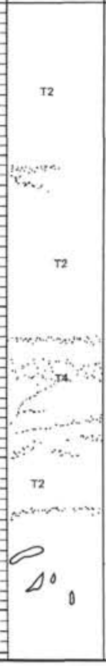

5Y 3/1

5Y 4/1

5Y 3/1

Sandy mud

5Y 3/1

T4

Zircon grain

Clay lenses

T1

5Y 3/1

HEMIPELAGIC MUD, SAND, AND MUDDY SAND

H_2S odor. Very dark gray (5Y 3/1). First extremely soupy.

SMEAR SLIDE SUMMARY (%):

	3, 70 D	4, 68 M	4, 88 M	CC D
Texture:				
Sand	60	65	5	30
Silt	30	10	65	45
Clay	10	25	30	25
Composition:				
Quartz	60	50	33	54
Feldspar	5	Tr	–	2
Mica	3	2	5	2
Heavy minerals	5	1	Tr	2
Clay	10	22	20	25
Volcanic glass	–	5	5	Tr
Pyrite	5	Tr	Tr	2
Carbonate unspec.	–	–	10	–
Foraminifers	2	Tr	–	2
Calc. nannofossils	5	–	10	5
Diatoms	Tr	Tr	10	1
Radiolarians	Tr	–	2	Tr
Sponge spicules	Tr	–	3	Tr
Silicoflagellates	–	–	2	Tr
Lithic fragments	5	–	–	5

Smear slide 4, 68: inc. glaucophane.

SITE 582 HOLE A CORE 2 CORED INTERVAL 38.8–48.5 m

TIME-ROCK UNIT | BIOSTRATIGRAPHIC ZONE | FOSSIL CHARACTER (FORAMINIFERS, NANNOFOSSILS, RADIOLARIANS, DIATOMS) | SECTION | METERS | GRAPHIC LITHOLOGY | DRILLING DISTURBANCE | SEDIMENTARY STRUCTURES | SAMPLES | LITHOLOGIC DESCRIPTION

Biostratigraphic zone: N22/23; N22/23, NN21–NN20

Fossil character: CG; FM CG FM

Sections: 1, 2, 3, 4, 5, 6, 7, CC

Meters: 0.5, 1.0

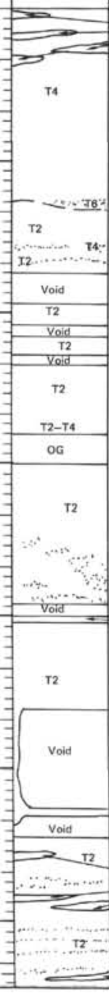

Void

5Y 3/1

5Y 3/2

5Y 3/1

IW

5Y 3/1

Void

5Y 3/1

Void

HEMIPELAGIC MUD AND SANDY MUD

Sandy mud, very dark gray (5Y 3/1).

Sand beds between Section 7, 15 and 20 cm are weakly graded.

SMEAR SLIDE SUMMARY (%):

	1, 70 D	3, 34 D	5, 42 M
Texture:			
Sand	60	5	45
Silt	30	50	45
Clay	10	45	10
Composition:			
Quartz	28	45	40
Feldspar	5	1	2
Mica	5	3	10
Heavy minerals	15	1	5
Clay	7	40	–
Volcanic glass	–	Tr	10
Pyrite	Tr	3	1
Carbonate unspec.	3	Tr	–
Foraminifers	Tr	1	5
Calc. nannofossils	3	3	Tr
Diatoms	2	3	–
Radiolarians	–	Tr	Tr
Sponge spicules	2	Tr	Tr
Silicoflagellates	Tr	Tr	–
Lithic fragments	30	–	27

SITE 582 HOLE B CORE 1 CORED INTERVAL 48.5–58.2 m

TIME – ROCK UNIT: Quaternary

BIOSTRATIGRAPHIC ZONE: (NN20–NN19) G. oceanica–P. lacunosa zone

FOSSIL CHARACTER: NANNOFOSSILS CM, RADIOLARIANS FM

SECTION: 1

T5

LITHOLOGIC DESCRIPTION

HEMIPELAGIC MUD
5Y 4/1
Total length of Core Catcher 7 cm.

SMEAR SLIDE SUMMARY (%):

	1, 3 D
Texture:	
Sand	10
Silt	45
Clay	45
Composition:	
Quartz	40
Feldspar	1
Mica	2
Clay	50
Pyrite	1
Foraminifers	Tr
Calc. nannofossils	Tr
Diatoms	1
Sponge spicules	Tr
Lithic fragments	5

SITE 582 HOLE B CORE 2 CORED INTERVAL 58.2–67.9 m

TIME – ROCK UNIT: Quaternary

BIOSTRATIGRAPHIC ZONE: NN20–NN19 G. oceanica–P. lacunosa zone

FOSSIL CHARACTER: FORAMINIFERS FM (top); RM, NANNOFOSSILS CM, RADIOLARIANS FM (base)

SECTIONS: 1, 2, 3, 4, 5, CC

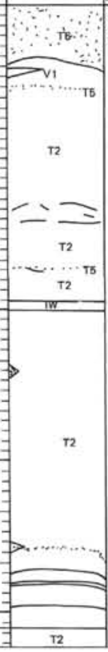

Thin section
Volcanic ash
Silt bed
Sand lamination
Ash lamination
Dark lamination
Silt bed
Silt
Silt
Dark layers and mottles

LITHOLOGIC DESCRIPTION

HEMIPELAGIC MUD AND SAND
Dark olive gray (5Y 3/2).

Gaps: open gaps (<10 cm each) in Sections 2, 3, and 4. Approximately 20–30% of affected sections.

Sub-horizontal gas expansion cracks throughout wafer-like separations which cross-cut drilling-deformed bedding featured.

SMEAR SLIDE SUMMARY (%):

	1, 62 M	1, 76 M	1, 102 D
Texture:			
Sand	70	85	5
Silt	25	10	60
Clay	5	5	35
Composition:			
Quartz	20	45	62
Feldspar	–	–	2
Mica	–	–	Tr
Heavy minerals	Tr	Tr	Tr
Clay	5	5	30
Volcanic glass	23	–	Tr
Pyrite	Tr	–	–
Foraminifers	–	Tr	Tr
Calc. nannofossils	Tr	–	Tr
Diatoms	Tr	Tr	Tr
Sponge spicules	–	Tr	Tr
Lithic fragments	2	50	5

Smear slide 1, 102: foram/nanno/diatom/sp = 1%.

ORGANIC CARBON AND CARBONATE (%):

	1, 50–52	2, 50	3, 50	4, 50
Carbonate	3.8	0	3.3	1.9

SITE 582 HOLE B CORE 3 CORED INTERVAL 67.9–77.6 m

TIME – ROCK UNIT: Quaternary

BIOSTRATIGRAPHIC ZONE: N22/23 NN20–NN19 A. ypsilon/C. tuberosa zone

FOSSIL CHARACTER: FORAMINIFERS FG, NANNOFOSSILS CM, RADIOLARIANS AM

SECTIONS: 1, 2, 3, CC

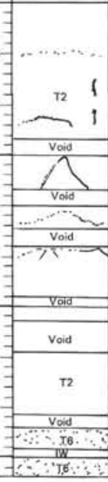

LITHOLOGIC DESCRIPTION

HEMIPELAGIC MUD
Mud cavings(?) top 40 cm.

Hemipelagic mud, dark gray (5Y 4/1), vertically streaked mottling 5Y 2/1.

Black (5Y 2/1) streaks.

Deformed lens, T5, 5Y 2/1.

Hemipelagic mud – 5Y 4/1.

Hemipelagic mud, 5Y 4/1. Some black (5Y 2/1) streaks.

Sand – 5Y 4/1.

SMEAR SLIDE SUMMARY (%):

	1, 76 D	3, 127 M
Texture:		
Sand	2	30
Silt	68	68
Clay	30	2
Composition:		
Quartz	40	50
Feldspar	5	20
Mica	3	4
Heavy minerals	4	5
Clay	30	2
Volcanic glass	4	2
Pyrite	Tr	1
Foraminifers	Tr	–
Calc. nannofossils	Tr	–
Diatoms	2	
Radiolarians	Tr	–
Sponge spicules	2	1
Silicoflagellates	Tr	–
Lithics	10	15

ORGANIC CARBON AND CARBONATE (%):

	1, 50	2, 50	3, 50
Carbonate	1.4	1.4	4.8

Core 4, 77.6–87.3 m: no recovery.

SITE 582 HOLE B CORE 5 CORED INTERVAL 87.3–96.9 m

TIME–ROCK UNIT	BIOSTRATIGRAPHIC ZONE	FORAMINIFERS	NANNOFOSSILS	RADIOLARIANS	DIATOMS	SECTION	METERS
Quaternary	N22/23 (NN19) A. ypsilon/C. tuberosa zone			RP		1	0.5, 1.0
				CM		2	
			CG				
			CM			3	
		RM	CM	CM		CC	

GRAPHIC LITHOLOGY / DRILLING DISTURBANCE / SEDIMENTARY STRUCTURES / SAMPLES

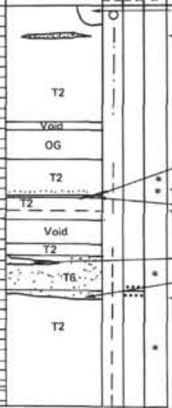

LITHOLOGIC DESCRIPTION

Void
Silty lens

HEMIPELAGIC MUD
Very dark gray (5Y 3/1).

T2
Silt
Light colored (5Y 3/2) siliceous mud
SB3
Black layer

Void }
T6 } Sand bed (black [5Y 2.5/2] top; black [5Y 2.5/1] base): graded turbidite bed, medium to very fine

Sand bed: fine sand, sharp base and gradational top

SMEAR SLIDE SUMMARY (%):

	2, 36 D	2, 118 M	3, 40 D
Texture:			
Sand	–	50	Tr
Silt	25	45	20
Clay	75	5	80
Composition:			
Quartz	20	45	20
Feldspar	2	20	10
Mica	2	13	–
Heavy minerals	–	2	–
Clay	58	5	50
Volcanic glass	–	5	–
Pyrite	–	Tr	Tr
Carbonate unspec.	–	–	Tr
Foraminifers	–	Tr	–
Calc. nannofossils	Tr	–	2
Diatoms	8	–	2
Radiolarians	2	–	1
Sponge spicules	4	Tr	2
Silicoflagellates	2	Tr	Tr
Lithics	2	10	13

ORGANIC CARBON AND CARBONATE (%):

	1, 50	2, 50	3, 50
Carbonate	1.0	1.4	1.9

Core 6, 96.9–106.5 m: no recovery.

SITE 582 HOLE B CORE 7 CORED INTERVAL 106.5–116.5 m

TIME–ROCK UNIT	BIOSTRATIGRAPHIC ZONE	FORAMINIFERS	NANNOFOSSILS	RADIOLARIANS	DIATOMS	SECTION	METERS
Quaternary						1	0.5, 1.0
						2	
						3	
						4	
						5	
						6	
						7	
Quaternary	N22/23	CG	CM	RM		CC	

GRAPHIC LITHOLOGY / DRILLING DISTURBANCE / SEDIMENTARY STRUCTURES / SAMPLES

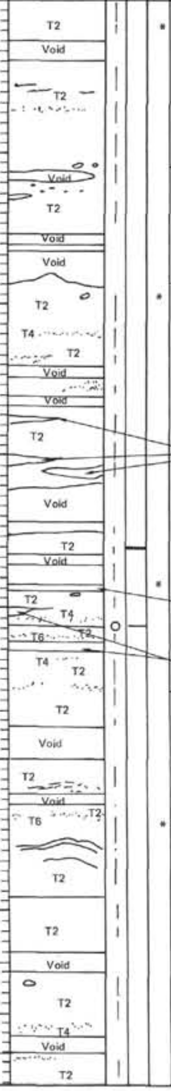

LITHOLOGIC DESCRIPTION

HEMIPELAGIC MUD
Very dark gray (5Y 3/1)

Black seams
Fine grain sand, dark olive gray (5Y 3/2)

Plant fragments (wood)
Black mottles
Dark olive gray (5Y 3/2) with black seams

Plant debris
~100% sponge spicules, 5Y 3/1
(small white spot)

5Y 3/2
5Y 3/1 with black seams
Void

Crack (gap)
Darker laminations
Black pyrite rich layer
135 cm pebble
Void

Void
Black, very fine sand

5Y 3/1 deformed beds

5Y 3/2

5Y 3/2

White sponge spicule aggregate

5Y 3/2

SMEAR SLIDE SUMMARY (%):

	1, 30 D	2, 140 M	4, 127 M	6, 67 M
Texture:				
Sand	–	–	65	30
Silt	40	–	30	65
Clay	60	–	5	5
Composition:				
Quartz	20	5	41	30
Feldspar	–	–	5	10
Mica	2	–	3	5
Heavy minerals	1	–	1	5
Clay	54	20	5	5
Volcanic glass	10	–	3	–
Pyrite	3	2	20	3
Carbonate unspec.	2	–	1	2
Calc. nannofossils	Tr	–	2	–
Diatoms	5	3	Tr	Tr
Radiolarians	1	Tr	–	–
Sponge spicules	2	70	–	–
Lithic fragments	–	–	18	40

SITE 582 HOLE B CORE 8 CORED INTERVAL 116.5–125.7 m

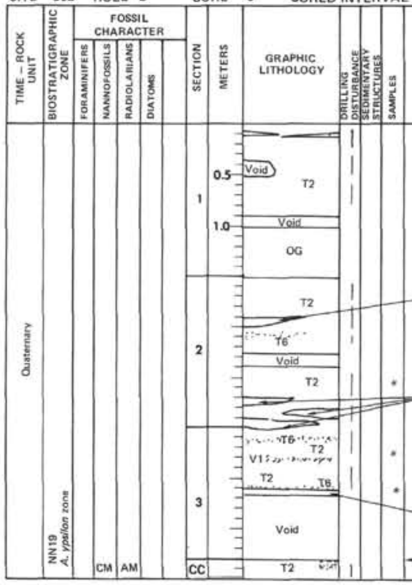

LITHOLOGIC DESCRIPTION

Cracks

Void

5Y 3/1

Gap

Thin ash layer
Mud 5Y 3/1

T2

Fine black (5Y 2.5/1) sand

SILICEOUS HEMIPELAGIC MUD
Very dark gray (5Y 3/1).

SMEAR SLIDE SUMMARY (%):

	2, 106	3, 28	3, 61
	D	M	M
Texture:			
Sand	–	75	70
Silt	40	20	25
Clay	60	5	5
Composition:			
Quartz	5	15	30
Feldspar	–	4	3
Mica	2	1	5
Clay	71	5	5
Volcanic glass	2	75	–
Pyrite	4	–	3
Foraminifers	1	–	2
Calc. nannofossils	3	–	–
Diatoms	7	–	–
Sponge spicules	5	–	–
Fecal pellet	Tr	–	–
Lithic fragments	–	–	52

Smear slide 3, 28: volcanic glass includes 10% pumice.

SITE 582 HOLE B CORE 9 CORED INTERVAL 125.7–135.3 m

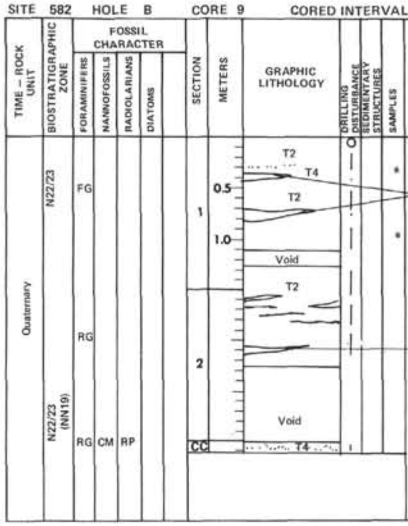

LITHOLOGIC DESCRIPTION

Gap

Very dark gray (5Y 3/1)

Cracks

Gap

Very dark gray (5Y 3/1)

HEMIPELAGIC MUD

SMEAR SLIDE SUMMARY (%):

	1, 34	1, 98
	D	D
Texture:		
Sand	–	5
Silt	20	45
Clay	80	50
Composition:		
Quartz	30	25
Feldspar	1	2
Mica	1	3
Heavy minerals	–	Tr
Clay	30	50
Volcanic glass	2	5
Pyrite	2	–
Carbonate unspec.	–	5
Foraminifers	1	–
Calc. nannofossils	2	5
Diatoms	30	3
Radiolarians	1	–
Sponge spicules	–	2

SITE 582 HOLE B CORE 10 CORED INTERVAL 135.3–144.9 m

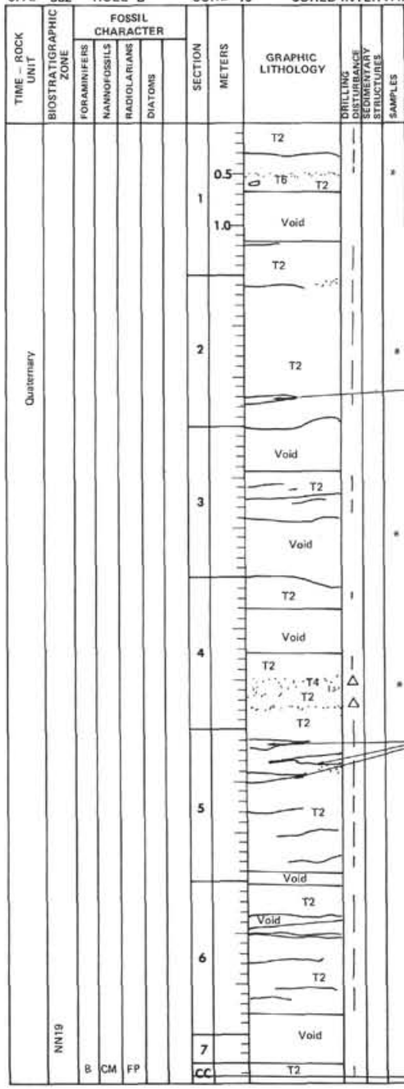

LITHOLOGIC DESCRIPTION

5Y 3/1

White spot: sponge spicules

Mica flakes and pyrite
5Y 3/1–5Y 3/2

Crack

5Y 3/1

Gap

Cracks
5Y 3/1

5Y 2.5/1

Very dark gray (5Y 3/1)

Gap

Cracks

5Y 3/1

Cracks

HEMIPELAGIC MUD

SMEAR SLIDE SUMMARY (%):

	1, 50	3, 107	4, 108	2, 76
	D	M	D	D
Texture:				
Sand	2	65	20	Tr
Silt	38	30	75	60
Clay	60	5	5	40
Composition:				
Quartz	20	32	33	20
Feldspar	1	5	1	2
Mica	2	5	5	2
Heavy minerals	–	10	10	–
Clay	57	5	30	30
Volcanic glass	5	Tr	–	5
Glauconite	1	–	–	–
Pyrite	2	3	1	5
Foraminifers	Tr	–	Tr	–
Calc. nannofossils	2	–	–	10
Diatoms	6	–	–	8
Radiolarians	2	–	–	–
Sponge spicules	2	Tr	–	3
Lithic fragments	–	40	–	5
Opaque veins	–	–	20	–

Smear slide 3, 107: heavy minerals: zircon, pyroxene, apatite. Chert and shale.

ORGANIC CARBON AND CARBONATE (%):

	1, 127	2, 69	3, 73	4, 145
Carbonate	0.4	1.3	0.4	1.7

	5, 76	6, 70
Carbonate	2.3	5.0

SITE 582 HOLE B CORE 11 CORED INTERVAL 144.9–154.6 m

TIME – ROCK UNIT	BIOSTRATIGRAPHIC ZONE	FORAMINIFERS	NANNOFOSSILS	RADIOLARIANS	DIATOMS	SECTION	METERS	GRAPHIC LITHOLOGY	DRILLING DISTURBANCE	SEDIMENTARY STRUCTURES	SAMPLES	LITHOLOGIC DESCRIPTION
Quaternary	NN19	B	CM	RP		CC		T2	|		*	←Clay layer

HEMIPELAGIC MUD
Dark gray (5Y 4/1).
Core Catcher only.

SMEAR SLIDE SUMMARY (%):

	CC, 8 (Tr apatite)
Texture:	
Sand	60
Silt	40
Composition:	
Quartz	33
Feldspar	2
Mica	Tr
Heavy minerals	1
Clay	40
Volcanic glass	5
Pyrite	1
Diatoms	5
Radiolarians	Tr
Sponge spicules	3
Silicoflagellates	Tr
Lithic fragments	10

ORGANIC CARBON AND CARBONATE (%):

	CC
Carbonate	2.7

SITE 582 HOLE B CORE 12 CORED INTERVAL 154.8–164.4 m

TIME – ROCK UNIT	BIOSTRATIGRAPHIC ZONE	FORAMINIFERS	NANNOFOSSILS	RADIOLARIANS	DIATOMS	SECTION	METERS	GRAPHIC LITHOLOGY	DRILLING DISTURBANCE	SEDIMENTARY STRUCTURES	SAMPLES	LITHOLOGIC DESCRIPTION
Quaternary	N22/23 NN19	RG	CM	RP		1	0.5, 1.0	T2, T2	|		*	Void; ←Dark gray (5Y 4/1); ←Dark patches: dark gray (5Y 4/1)

HEMIPELAGIC MUD
Very dark gray (5Y 3/1).
Horizontal cracks above 80 cm.

SMEAR SLIDE SUMMARY (%):

	1, 33 D	1, 91 D
Texture:		
Sand	5	–
Silt	60	70
Clay	35	30
Composition:		
Quartz	30	45
Feldspar	8	5
Mica	5	1
Heavy minerals	2	1
Clay	31	30
Volcanic glass	5	3
Pyrite	1	1
Foraminifers	1	–
Calc. nannofossils	1	Tr
Diatoms	1	2
Radiolarians	–	Tr
Sponge spicules	–	2
Lithics	15	10

ORGANIC CARBON AND CARBONATE (%):

	1, 50
Carbonate	1.8

SITE 582 HOLE B CORE 13 CORED INTERVAL 164.4–174.0 m

TIME – ROCK UNIT	BIOSTRATIGRAPHIC ZONE	FORAMINIFERS	NANNOFOSSILS	RADIOLARIANS	DIATOMS	SECTION	METERS	GRAPHIC LITHOLOGY	DRILLING DISTURBANCE	SEDIMENTARY STRUCTURES	SAMPLES	LITHOLOGIC DESCRIPTION
Quaternary		B	RM	RP		1, CC	0.5	T2, T2			*	Void

HEMIPELAGIC MUD
Dark gray (5Y 4/1).

SMEAR SLIDE SUMMARY (%):

	1, 2.5 D
Texture:	
Silt	75
Clay	25
Composition:	
Quartz	50
Feldspar	2
Mica	2
Heavy minerals	1
Clay	25
Volcanic glass	5
Pyrite	Tr
Calc. nannofossils	Tr
Diatoms	3
Radiolarians	Tr
Sponge spicules	2
Lithic fragments	10

ORGANIC CARBON AND CARBONATE (%):

	1, 10
Carbonate	1.4

SITE 582 HOLE B CORE 14 CORED INTERVAL 174.0–183.6 m

TIME – ROCK UNIT: Quaternary

BIOSTRATIGRAPHIC ZONE: NN19

FOSSIL CHARACTER (FORAMINIFERS, NANNOFOSSILS, RADIOLARIANS, DIATOMS): B; RM; B; RM CM RP

SECTION: 1, 2, 3, 4, 5, 6, 7, CC

METERS: 0.5, 1.0

GRAPHIC LITHOLOGY

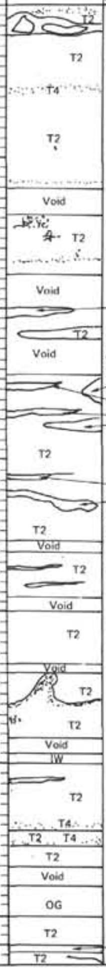

DRILLING DISTURBANCE / SEDIMENTARY STRUCTURES / SAMPLES

LITHOLOGIC DESCRIPTION

5Y 3/1

Faint layering in more cohesive intervals

T4 Very dark gray (5Y 3/1) silty sand

5Y 4/1

T2

Void

Gap

Gap

5Y 4/1

T4, deformed sandy layers

5Y 3/1

Graded sandy mud

1–2 mm horizontal cracks

PP

HEMIPELAGIC MUD AND SAND

Dark gray (5Y 4/1), numerous sub-horizontal cracks

SMEAR SLIDE SUMMARY (%):

	1, 88	1, 117	2, 95	6, 66
	M	D	D	M
Texture:				
Sand	5	–	–	50
Silt	90	45	50	45
Clay	5	55	50	5
Composition:				
Quartz	50	40	40	45
Feldspar	10	4	10	10
Mica	2	1	1	2
Heavy minerals	3	2	3	3
Clay	5	40	40	5
Volcanic glass	–	–	–	Tr
Pyrite	–	1	Tr	Tr
Calc. nannofossils	–	Tr	–	Tr
Diatoms	–	1	Tr	Tr
Radiolarians	–	Tr	Tr	Tr
Sponge spicules	–	1	1	Tr
Silicoflagellates	–	Tr	–	–
Fish remains	Tr	Tr	–	–
Lithic fragments	30	10	5	35

ORGANIC CARBON AND CARBONATE (%):

	1, 50	2, 60	3, 50	4, 70
Carbonate	3.2	1.0	1.0	1.4
	5, 50	6, 50	7, 20	
	1.4	1.8	1.4	

SITE 582 HOLE B CORE 15 CORED INTERVAL 183.6–193.2 m

TIME – ROCK UNIT: Quaternary

BIOSTRATIGRAPHIC ZONE: NN19

FOSSIL CHARACTER: B; B CM FP

SECTION: 1, 2, 3, CC

METERS: 0.5, 1.0

GRAPHIC LITHOLOGY

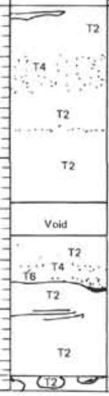

LITHOLOGIC DESCRIPTION

5Y 3/1

Dark gray (5Y 4/1)

5Y 3/1

5Y 3/1

5Y 2.5/1

5Y 4/1

5Y 2.5/1

5Y 4/1

Void

5Y 4/1

HEMIPELAGIC MUD AND SANDY MUD

Muddy portions show new horizontal cracks. Spacing related to grain size: finer muds ~1.0 mm; coarser muds 1.5–2.0 mm.

SMEAR SLIDE SUMMARY (%):

	1, 117	3, 12
	M	D
Texture:		
Sand	50	Tr
Silt	45	40
Clay	5	60
Composition:		
Quartz	60	30
Feldspar	10	5
Mica	3	3
Heavy minerals	6	–
Clay	5	40
Volcanic glass	Tr	5
Glauconite	Tr	–
Pyrite	1	–
Carbonate unspec.	Tr	–
Calc. nannofossils	–	Tr
Diatoms	Tr	1
Radiolarians	–	Tr
Sponge spicules	Tr	1
Lithic fragments	15	15

ORGANIC CARBON AND CARBONATE (%):

	1, 50	2, 43	3, 50
Carbonate	1.4	2.3	2.3

SITE 582 HOLE B CORE 16 CORED INTERVAL 193.2–202.8 m

TIME – ROCK UNIT: Quaternary

BIOSTRATIGRAPHIC ZONE: NN19

FOSSIL CHARACTER: B CM RP

SECTION: 1, 2, 3, CC

METERS: 0.5, 1.0

GRAPHIC LITHOLOGY

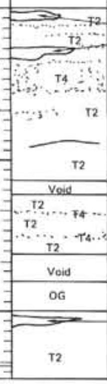

LITHOLOGIC DESCRIPTION

Void

Black (5Y 2.5/1) with dark gray blebs

5Y 3/1

Void

Sub-horizontal cracks of intervals of 1–2 mm

Dark gray (5Y 4/1) mud

HEMIPELAGIC MUD AND SANDY MUD

T4 layers generally 5Y 3/1.

No strong evidence of grading.

SMEAR SLIDE SUMMARY (%):

	3, 34	1, 70	2, 52
	D	M	M
Texture:			
Sand	–	50	20
Silt	50	45	60
Clay	50	5	20
Composition:			
Quartz	40	45	30
Feldspar	5	10	3
Mica	Tr	2	1
Heavy minerals	Tr	6	1
Clay	40	5	20
Volcanic glass	Tr	Tr	–
Pyrite	Tr	1	30
Carbonate unspec.	–	Tr	–
Foraminifers	–	Tr	–
Calc. nannofossils	Tr	–	Tr
Diatoms	4	1	–
Radiolarians	Tr	Tr	–
Sponge spicules	1	Tr	–
Silicoflagellates	Tr	–	–
Lithic fragments	10	30	20

Smear slide 1, 70: includes plagioclase with biotite inclusions.

ORGANIC CARBON AND CARBONATE (%):

	1, 50	2, 50	3, 50
Carbonate	1.0	2.3	6.4

SITE 582 HOLE B CORE 17 CORED INTERVAL 202.8–212.5 m

TIME – ROCK UNIT	BIOSTRATIGRAPHIC ZONE	FORAMINIFERS	NANNOFOSSILS	RADIOLARIANS	DIATOMS	SECTION	METERS	GRAPHIC LITHOLOGY	DRILLING DISTURBANCE	SEDIMENTARY STRUCTURES	SAMPLES	LITHOLOGIC DESCRIPTION
Quaternary	NN19	B	CM	FM		1		T2			*	Very dark gray (5Y 3/1)
						CC	0.5	Void				

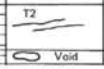

HEMIPELAGIC MUD

SMEAR SLIDE SUMMARY (%):

	1, 33
	D
Texture:	
Sand	5
Silt	45
Clay	50
Composition:	
Quartz	32
Feldspar	8
Mica	3
Heavy minerals	2
Clay	37
Volcanic glass	5
Pyrite	2
Foraminifers	Tr
Calc. nannofossils	1
Diatoms	5
Silicoflagellates	Tr
Lithic fragments	5

SITE 582 HOLE B CORE 18 CORED INTERVAL 212.5–222.2 m

TIME – ROCK UNIT	BIOSTRATIGRAPHIC ZONE	FORAMINIFERS	NANNOFOSSILS	RADIOLARIANS	DIATOMS	SECTION	METERS	GRAPHIC LITHOLOGY	DRILLING DISTURBANCE	SEDIMENTARY STRUCTURES	SAMPLES	LITHOLOGIC DESCRIPTION
Quaternary	NN19	B	CM	FM		1, 2, 3, 4, 5, 6, CC	0.5, 1.0	T2, T6, T4, Void, T4, T2, Void, T2, T2, T5, T2, IW, T2, Void, T2, Void, T2, Void, T4, T2, T4, T2, T4, T2			*	

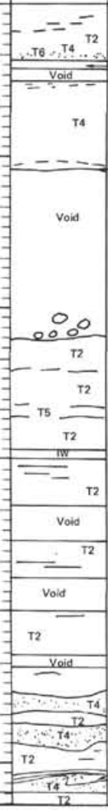

Sub-horizontal cracks

T2

5Y 2.5/2 fine sand

T2

5GY 4/1
Seam

5Y 2.5/1 silt

Sub-horizontal cracks

5Y 3/2

V1

Mixed layer (5Y 5/3)

Ash 5Y 8/1

5Y 3/2

HEMIPELAGIC MUD, SILT AND SANDY MUD

SMEAR SLIDE SUMMARY (%):

	1, 110	3, 50	6, 20	3, 108
	D	D	M	M
Texture:				
Sand	40	0	50	15
Silt	50	25	45	82
Clay	10	75	5	3
Composition:				
Quartz	57	12	5	35
Feldspar	5	2	Tr	–
Mica	3	2	–	4
Heavy minerals	2	1	–	5
Clay	10	65	–	9
Volcanic glass	2	3	95	3
Glauconite	–	–	–	5
Pyrite	5	2	–	4
Carbonate unspec.	1	1	Tr	–
Foraminifers	Tr	–	–	2
Calc. nannofossils	Tr	10	–	–
Diatoms	Tr	2	–	–
Radiolarians	–	Tr	–	–
Sponge spicules	Tr	1	–	–
Lithic fragments	15	–	–	–
Altered glass or clay aggregates	–	–	–	35

ORGANIC CARBON AND CARBONATE (%):

	1, 50	3, 50	4, 50	5, 50
Carbonate	3.2	4.6	2.3	1.8

SITE 582 HOLE B CORE 19 CORED INTERVAL 222.2–231.9 m

TIME – ROCK UNIT: Quaternary

BIOSTRATIGRAPHIC ZONE: N22/23, NN19

FOSSIL CHARACTER: FORAMINIFERS RG; NANNOFOSSILS CM; RADIOLARIANS FM; DIATOMS

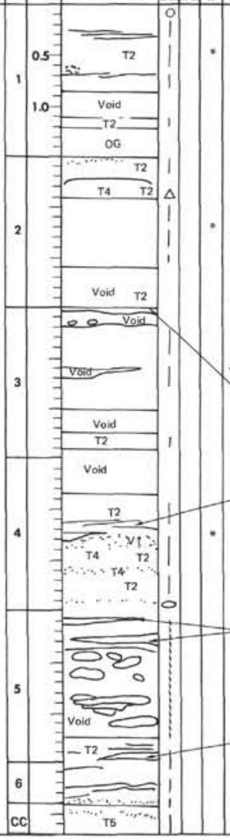

LITHOLOGIC DESCRIPTION

5Y 3/1
Cracks
(especially evident in silty layers)

Color change
Olive (5Y 4/3) – ash rich

T2

Void
5Y 3/1

5Y 8/1

5Y 3/1

Void

Void
5Y 3/1

Cracks

Silty layers
5Y 3/1

ASHY HEMIPELAGIC MUD AND SILICEOUS MUD

SMEAR SLIDE SUMMARY (%):

	1, 47	2, 70	4, 77
	D	M	M
Texture:			
Sand	3	10	5
Silt	57	60	90
Clay	40	30	5
Composition:			
Quartz	17	6	5
Feldspar	3	3	5
Mica	3	Tr	Tr
Heavy minerals	2	3	5
Clay	35	23	5
Volcanic glass	Tr	55	70
Pyrite	5	–	2
Calc. nannofossils	5	7	–
Diatoms	20	Tr	5
Radiolarians	–	Tr	Tr
Sponge spicules	10	3	3

ORGANIC CARBON AND CARBONATE (%):

	1, 50	2, 50	3, 50	4, 50	5, 50
Carbonate	2.3	1.4	4.6	1.4	1.4

SITE 582 HOLE B CORE 20 CORED INTERVAL 231.9–241.5 m

TIME – ROCK UNIT: Quaternary

FOSSIL CHARACTER: FORAMINIFERS B; NANNOFOSSILS B; RADIOLARIANS CM; DIATOMS

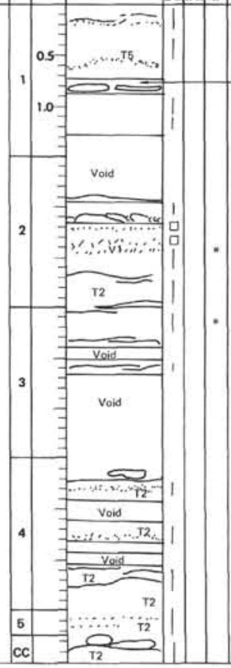

LITHOLOGIC DESCRIPTION

Crack
T5

T5 – silt

Void

Very dark gray
(5Y 3/1)

Void

T5

T5

5Y 3/1

5Y 3/1

HEMIPELAGIC MUD

SMEAR SLIDE SUMMARY (%):

	2, 91	3, 18
	M	D
Texture:		
Sand	60	–
Silt	30	50
Clay	10	50
Composition:		
Quartz	30	25
Feldspar	15	5
Mica	5	5
Heavy minerals	5	2
Clay	10	40
Volcanic glass	2	3
Pyrite	3	3
Carbonate unspec.	–	Tr
Foraminifers	Tr	Tr
Calc. nannofossils	–	Tr
Diatoms	–	1
Radiolarians	Tr	–
Sponge spicules	–	2
Lithic fragments plus zircon and pyroxene	30	14

SITE 582 HOLE B CORE 21 CORED INTERVAL 241.5–251.1 m

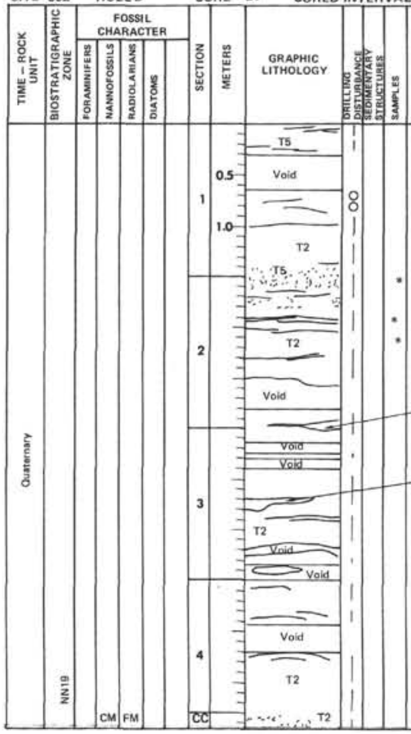

LITHOLOGIC DESCRIPTION

Very dark gray (5Y 3/1)

5Y 2.5/1

Sub-horizontal crack

Crack

Crack

Void
5Y 3/1

Void

Very dark gray
(5Y 3/1)

5Y 3/1
silty mud

Silt and muddy silt

HEMIPELAGIC MUD, SILT

SMEAR SLIDE SUMMARY (%):

	2, 5	2, 41	2, 60
	M	M	D
Texture:			
Sand	20	10	5
Silt	60	45	40
Clay	20	45	55
Composition:			
Quartz	28	25	20
Feldspar	2	8	3
Mica	2	2	2
Heavy minerals	2	1	2
Clay	–	40	42
Volcanic glass	10	–	2
Pyrite	8	1	2
Carbonate unspec.	2	–	Tr
Foraminifers	–	–	Tr
Calc. nannofossils	–	Tr	2
Diatoms	4	–	15
Radiolarians	1	–	–
Sponge spicules	1	1	5
Silicoflagellates	–	Tr	Tr
Lithic fragments	–	22	5
Clay aggregates	20	–	–
Altered glass	20	–	–

SITE 582 HOLE B CORE 22 CORED INTERVAL 251.1–260.7 m

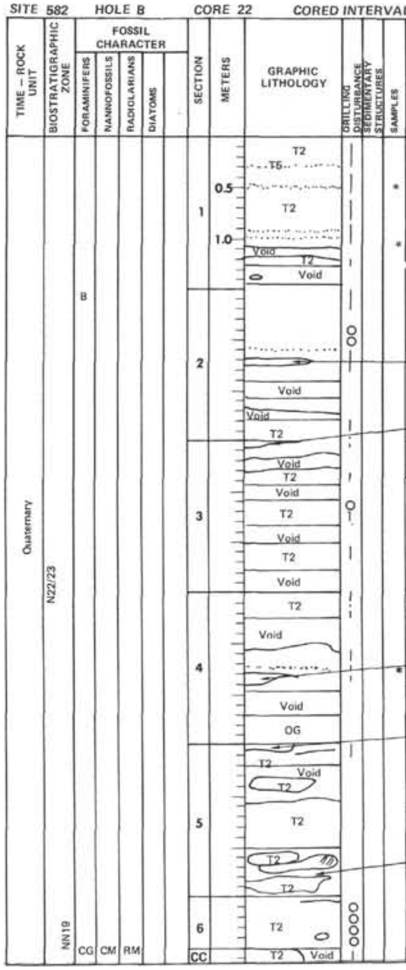

LITHOLOGIC DESCRIPTION

Numerous sub-horizontal cracks

5Y 4/1
5G 4/1

T2

Silty
Void

Dark olive gray (5Y 3/2)
Void

Begin cutting
with super saw

Soupy!
5GY 4/1

5GY 4/1

Void
Chondrites
(5Y 3/1)

Void

Void

Wood

FIRM HEMIPELAGIC MUD

SMEAR SLIDE SUMMARY (%):

	1, 50	1, 108	4, 73
	M	D	M
Texture:			
Sand	1	5	–
Silt	75	55	40
Clay	24	40	60
Composition:			
Quartz	50	20	20
Feldspar	2	Tr	3
Mica	–	3	1
Heavy minerals	2	2	1
Clay	10	40	60
Volcanic glass	25	–	–
Pyrite and opaques	5	5	2
Carbonate	–	Tr	–
Foraminifers	2	–	–
Calc. nannofossils	Tr	–	–
Diatoms	2	15	8
Radiolarians	2	–	–
Sponge spicules	1	5	–
Silicoflagellates	–	–	5
Lithic fragments	–	10	–

Smear slide 1, 50: includes glaucophane

SITE 582 HOLE B CORE 23 CORED INTERVAL 260.7–270.3 m

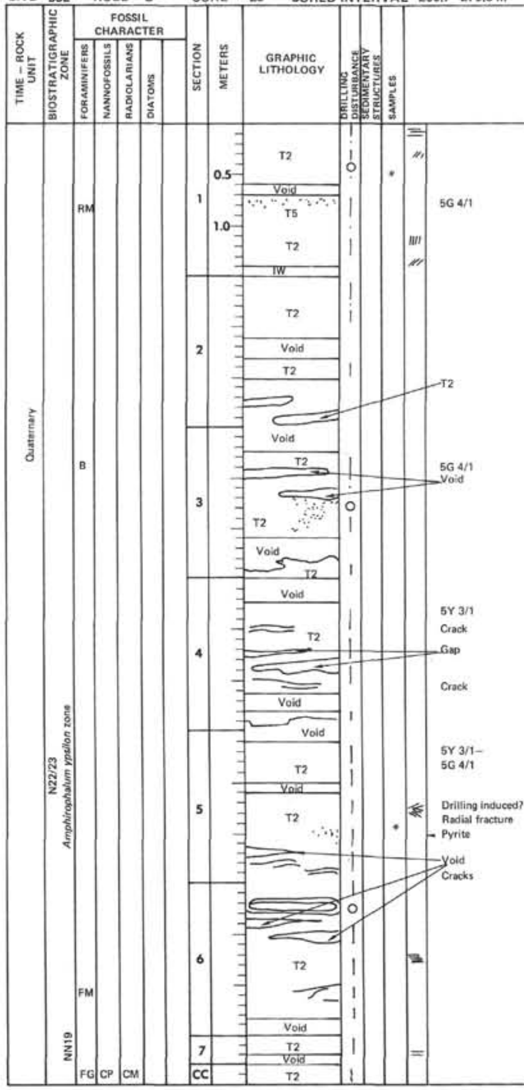

LITHOLOGIC DESCRIPTION

HEMIPELAGIC MUD

SMEAR SLIDE SUMMARY (%):

	1, 50	5, 97
	D	M
Texture:		
Sand	Tr	Tr
Silt	60	40
Clay	40	60
Composition:		
Quartz	40	20
Feldspar	5	2
Mica	3	2
Heavy minerals	2	3
Clay	40	57
Pyrite	3	10
Calc. nannofossils	2	3
Diatoms	3	5
Sponge spicules	2	3

ORGANIC CARBON AND CARBONATE (%):

	2, 97	4, 97
Carbonate	1.4	1.4

SITE 582 HOLE B CORE 24 CORED INTERVAL 270.3–279.9 m

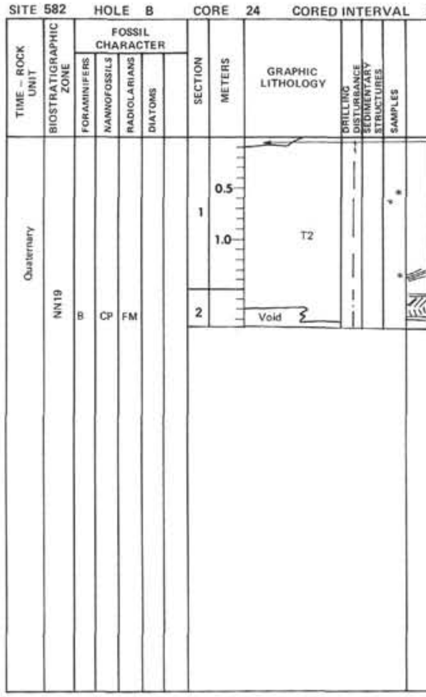

LITHOLOGIC DESCRIPTION

Gap
5Y 3/1

DIATOMACEOUS HEMIPELAGIC MUD
Drilling laminations throughout

Dark (5Y 3/1) layer: contains grains >2 mm diameter; these are mainly pyrite binding biogenic and detrital matter

Incipient fissility = parting surfaces sub-parallel to bedding

SMEAR SLIDE SUMMARY (%):

	1, 58	1, 63	1, 136
	M	D	M
Sand	5	–	10
Silt	60	60	50
Clay	35	40	40
Composition:			
Quartz	50	30	15
Feldspar	–	3	3
Mica	1	Tr	2
Heavy minerals	1	Tr	–
Clay	20	19	42
Pyrite	1	1	25
Foraminifers	Tr	Tr	–
Calc. nannofossils	5	2	–
Diatoms	20	35	5
Radiolarians	Tr	–	–
Sponge spicules	2	1	Tr
Silicoflagellates	–	1	–
Lithic fragments	–	8	8

ORGANIC CARBON AND CARBONATE (%):

	1, 46
Carbonate	1.4

SITE 582 HOLE B CORE 25 CORED INTERVAL 279.9–289.5 m

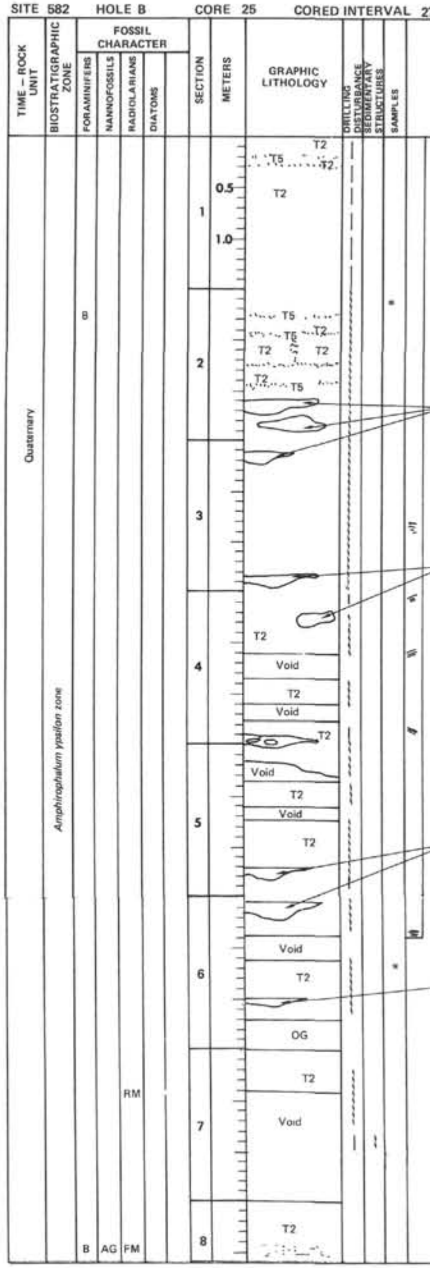

LITHOLOGIC DESCRIPTION

Dark olive gray (5Y 3/2) with black (5Y 2/2) layers in planar, horizontal laminations

Gap

Incipient fissility

Gap

5Y 3/1 and 5Y 3/2
Darker blebs probably burrows

Sub-vertical flows

Gap
5Y 3/1

Gap

Very dark gray (5Y 3/1)

Sub-vertical flow
5Y 3/1

HEMIPELAGIC MUD

SMEAR SLIDE SUMMARY (%):

	2, 12	6, 70
	D	D
Texture:		
Sand	Tr	Tr
Silt	70	60
Clay	30	40
Composition:		
Quartz	40	45
Feldspar	5	5
Mica	4	2
Heavy minerals	3	2
Clay	30	30
Volcanic glass	Tr	–
Pyrite	1	–
Foraminifers	Tr	1
Calc. nannofossils	Tr	Tr
Diatoms	1	Tr
Radiolarians	Tr	–
Sponge spicules	1	Tr
Silicoflagellates	Tr	–
Lithic fragments	15	15

ORGANIC CARBON AND CARBONATE (%):

	1, 50	3, 50	5, 50	7, 30
Carbonate	1.4	2.3	2.3	2.3

SITE 582 HOLE B CORE 26 CORED INTERVAL 289.5–299.1 m

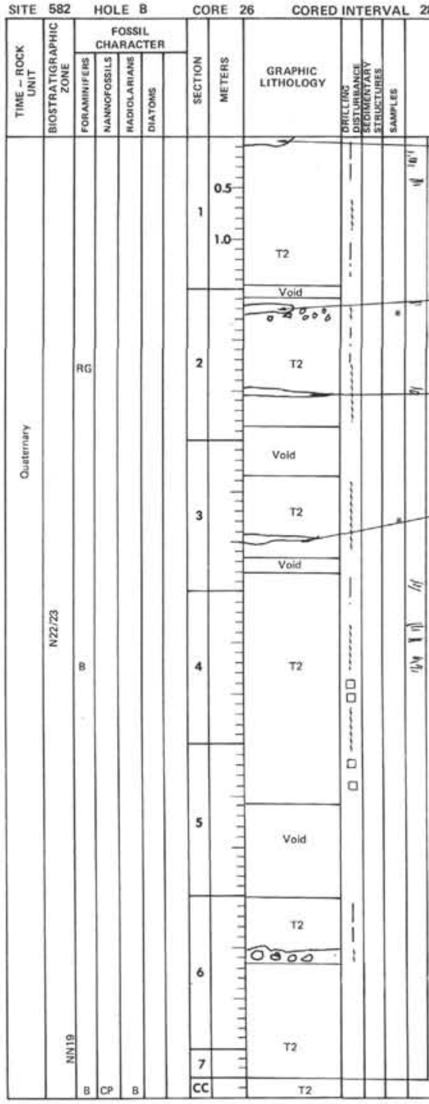

LITHOLOGIC DESCRIPTION

Gap
Horizontal cracks

Drilling laminations

Very dark gray (5Y 3/1)

Gap
Frothy drilling deformed mud

5Y 3/1
Inclined breaks
Gap

Gap

Fissility

Biscuits darker than surrounding groundmass
5Y 3/1–5Y 4/1

HEMIPELAGIC MUD

SMEAR SLIDE SUMMARY (%):

	2, 27	3, 80
	M	D
Texture:		
Sand	10	–
Silt	85	80
Clay	5	20
Composition:		
Quartz	35	50
Feldspar	10	4
Mica	2	1
Heavy minerals	4	–
Clay	5	20
Volcanic glass	3	2
Pyrite	1	1
Carbonate unspec.	Tr	Tr
Foraminifers	Tr	Tr
Calc. nannofossils	–	Tr
Diatoms	Tr	1
Sponge spicules	Tr	1
Lithic fragments includes: pumice, shale, argillite	40	20

ORGANIC CARBON AND CARBONATE (%):

	1, 50	3, 50	5, 50
Carbonate	1.8	1.8	4.6

Core 27, 299.1–308.7 m: no recovery.
Core 28, 308.7–318.3 m: no recovery.

SITE 582 HOLE B CORE 29 CORED INTERVAL 299.1–308.7 m

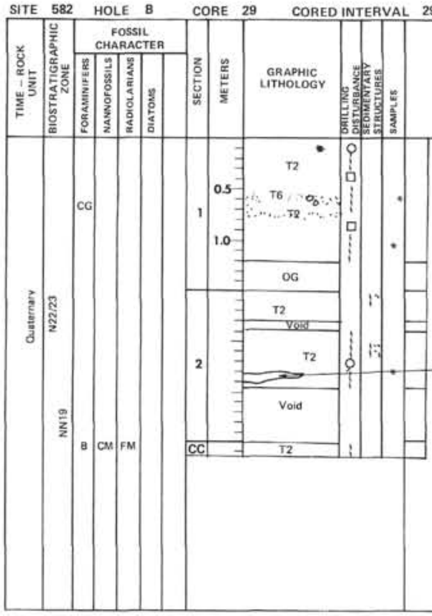

LITHOLOGIC DESCRIPTION

HEMIPELAGIC MUD
Sandy layer with pumice fragments
Incipient fissility in fine intervals.

Dark halos around horizontal and elliptical burrows.

SMEAR SLIDE SUMMARY (%):

	1, 60	2, 80	1, 105
	M	D	M
Texture:			
Sand	25	–	15
Silt	65	40	50
Clay	10	60	35
Composition:			
Quartz	30	35	25
Feldspar	8	5	5
Mica	3	4	2
Heavy minerals	6	1	2
Clay	15	30	30
Volcanic glass	—	2	—
Pyrite	3	2	5
Calc. nannofossils	–	5	5
Diatoms	12	10	1
Lithic fragments	23	8	25

ORGANIC CARBON AND CARBONATE (%):

	2, 50
Carbonate	1.0

SITE 582 HOLE B CORE 30 CORED INTERVAL 327.9–337.5 m

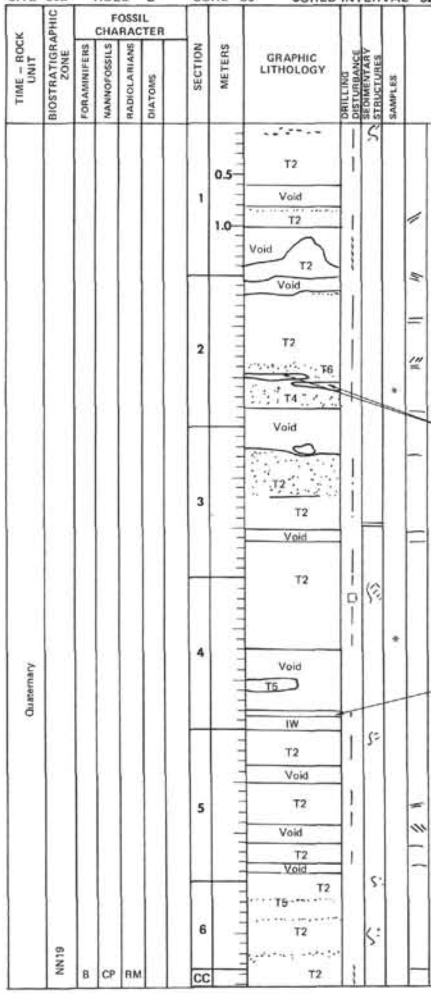

LITHOLOGIC DESCRIPTION

Chondrites
5Y 3/1

5Y 3/1

Plant debris
5Y 3/1–5GY 4/1

Structureless
coarse-grained sand layer
with larger pumice fragments
and plant debris

Void

Crack

Black laminations and mottles

5Y 3/2–3/1

5Y 4/1

5Y 4/1
T2

5Y 4/1

5Y 4/1
drilling
laminations
throughout

HEMIPELAGIC MUD

SMEAR SLIDE SUMMARY (%):

	2, 113	4, 60
	M	D
Texture:		
Sand	50	10
Silt	30	30
Clay	20	60
Composition:		
Quartz	30	25
Feldspar	5	3
Mica	–	2
Heavy minerals	2	3
Clay	26	50
Volcanic glass	–	5
Pyrite	2	13
Carbonate unspec.	Tr	1
Foraminifers	Tr	–
Calc. nannofossils	–	5
Diatoms	–	Tr
Radiolarians	–	Tr
Silicoflagellates	–	Tr
Lithic fragments	35	5

ORGANIC CARBON AND CARBONATE (%):

	1, 50	3, 50	5, 20
Carbonate	2.7	1.0	2.3

SITE 582 HOLE B CORE 31 CORED INTERVAL 337.5–347.1 m

TIME – ROCK UNIT: Quaternary; BIOSTRATIGRAPHIC ZONE: NN19; FOSSIL CHARACTER: FORAMINIFERS B, NANNOFOSSILS CP, RADIOLARIANS B; SECTIONS 1, 2, CC; GRAPHIC LITHOLOGY: T4, T2

LITHOLOGIC DESCRIPTION

FIRM HEMIPELAGIC SILT AND MUD
(Sandy mud)
5Y 3/2 sand and mud (probably homogenized by drilling).
Laminations from drilling.

SMEAR SLIDE SUMMARY (%):

	1, 62	1, 58
	D	M
Texture:		
Sand	15	–
Silt	65	40
Clay	20	60
Composition:		
Quartz	50	30
Feldspar	2	3
Mica	1	1
Heavy minerals	2	1
Clay	20	50
Volcanic glass	6	Tr
Pyrite	1	1
Carbonate unspec.	Tr	–
Foraminifers	Tr	Tr
Calc. nannofossils	Tr	Tr
Diatoms	1	Tr
Radiolarians	1	–
Sponge spicules	1	4
Plant debris	Tr	–
Lithic fragments	15	10

ORGANIC CARBON AND CARBONATE (%):

	1, 50
Carbonate	3.2

SITE 582 HOLE B CORE 32 CORED INTERVAL 347.1–356.5 m

TIME – ROCK UNIT: Quaternary; BIOSTRATIGRAPHIC ZONE: N22/23 *Amphirophalum ypsilon zone*, NN19; FOSSIL CHARACTER: AM, RG, RM, RM CM RP; SECTIONS 1, 2, 3, 4, CC; GRAPHIC LITHOLOGY: T2, T4, Void, T4, T6, T2, Void, T2

LITHOLOGIC DESCRIPTION

Void
Chondrites
(First clear example of grading cycle from sand to silt to clays with chondrites capped by barren clays)

5Y 4/1–5Y 3/1
Chondrites

Gap

Drilling laminations

Pumice

5Y 3/2

SMEAR SLIDE SUMMARY (%):

	3, 75
	D
Texture:	
Sand	Tr
Silt	40
Clay	60
Composition:	
Quartz	18
Feldspar	3
Mica	2
Heavy minerals	2
Clay	55
Volcanic glass	3
Pyrite	2
Carbonate unspec.	5
Calc. nannofossils	5
Diatoms	3
Sponge spicules	2

SITE 582 HOLE B CORE 33 CORED INTERVAL 356.5–365.9 m

TIME – ROCK UNIT: Quaternary; BIOSTRATIGRAPHIC ZONE: N22/23 NN19; FOSSIL CHARACTER: FP, B, B, FM, FM B, FM RP B; SECTIONS 1, 2, 3, 4; GRAPHIC LITHOLOGY: T2, T5, T2, Void, Void, T2, T5, Void, T2, T5, T2, T5, T6, PP, IW

Mottles

Black laminations and mottles

LITHOLOGIC DESCRIPTION

FIRM, HEMIPELAGIC MUD AND GRADED SEQUENCES
5Y 4/1–5Y 3/2
5Y 3/1 drilling laminations throughout Section 2

SMEAR SLIDE SUMMARY (%):

	2, 74	4, 77	4, 88	4, 100	4, 114
	D	–	–	–	–
Texture:					
Sand	Tr	Tr	5	20	40
Silt	50	50	65	60	20
Clay	50	50	30	20	40
Composition:					
Quartz	20	37	20	20	30
Feldspar	5	3	2	–	2
Mica	2	2	–	2	2
Heavy minerals	2	2	20	15	2
Clay	50	48	43	38	49
Volcanic glass	2	–	10	15	10
Pyrite	5	–	5	5	2
Carbonate unspec.	3	3	–	2	1
Foraminifers	–	–	–	–	1
Calc. nannofossils	3	2	–	–	1
Diatoms	5	2	–	–	–
Sponge spicules	3	1	–	–	–
Fecal pellets	–	–	–	3	–

ORGANIC CARBON AND CARBONATE (%):

	1, 50	3, 50	4, 63	4, 72
Carbonate	2.7	1.4	3.2	2.3

	4, 81	4, 90	4, 99
Carbonate	1.8	–	1.4

SITE 582 HOLE B CORE 34 CORED INTERVAL 365.9–375.3 m

TIME – ROCK UNIT: Quaternary
BIOSTRATIGRAPHIC ZONE: *Amphirophalum ypsilon*
FOSSIL CHARACTER: Radiolarians CM, B

SECTION 1, 2; Graphic lithology: T2, T4, T2, Void, T4

Very dark gray (5Y 3/1)

Frothy

LITHOLOGIC DESCRIPTION

FIRM HEMIPELAGIC MUD

SMEAR SLIDE SUMMARY (%):

	1, 80	2, 56
	D	D
Texture:		
Sand	5	25
Silt	40	50
Clay	55	25
Composition:		
Quartz	20	45
Feldspar	5	5
Mica	2	2
Heavy minerals	3	4
Clay	50	25
Volcanic glass	1	–
Pyrite	3	1
Carbonate unspec.	2	–
Foraminifers	1	–
Calc. nannofossils	5	Tr
Diatoms	2	2
Radiolarians	Tr	–
Sponge spicules	1	1
Silicoflagellates	Tr	–
Lithic fragments	5	15

ORGANIC CARBON AND CARBONATE (%):

	1, 95	1, 104	1, 115
Carbonate	1.8	3.2	1.8

Core 35, 375.3–384.8 m: no recovery.

SITE 582 HOLE B CORE 36 CORED INTERVAL 384.8–394.3 m

TIME – ROCK UNIT: Quaternary
BIOSTRATIGRAPHIC ZONE: NN19
FOSSIL CHARACTER: Radiolarians B, FM; CC: Nannofossils CM, Radiolarians FM

SECTION 1, CC; Graphic lithology: Void, T2, T2, T2

T5 (not T6) silt

T5 (not T6) 5Y 3/2

LITHOLOGIC DESCRIPTION

FIRM, GRADED SILT AND HEMIPELAGIC MUD
Dark olive gray (5Y 3/2) with black mottles and laminations

SMEAR SLIDE SUMMARY (%):

	1, 69
	D
Texture:	
Sand	5
Silt	30
Clay	65
Composition:	
Quartz	20
Feldspar	2
Mica	2
Heavy minerals	2
Clay	65
Volcanic glass	Tr
Pyrite	3
Carbonate unspec.	1
Foraminifers	1
Calc. nannofossils	Tr
Diatoms	1
Radiolarians	Tr
Lithic fragments	3

ORGANIC CARBON AND CARBONATE (%):

	1, 90
Carbonate	1.8

SITE 582 HOLE B CORE 37 CORED INTERVAL 399.3–403.8 m

TIME – ROCK UNIT: Quaternary
BIOSTRATIGRAPHIC ZONE: NN19
FOSSIL CHARACTER: Radiolarians B; CC: Foraminifers B, Nannofossils FM, Radiolarians RM

SECTION 1, 2, CC; Graphic lithology: T2, T2, T2, T8, T2, T2, T2, Void

Void

Black mottles

5Y 3/1

LITHOLOGIC DESCRIPTION

FIRM HEMIPELAGIC MUD AND GRADED SILT
Dark olive gray (5Y 3/2)

SMEAR SLIDE SUMMARY (%):

	1, 60
	D
Texture:	
Silt	50
Clay	50
Composition:	
Quartz	32
Mica	2
Heavy minerals	2
Clay	52
Volcanic glass	10
Pyrite	2
Foraminifers	Tr
Sponge spicules	Tr

ORGANIC CARBON AND CARBONATE (%):

	2, 87
Carbonate	2.3

SITE 582 HOLE B CORE 38 CORED INTERVAL 403.8–413.2 m

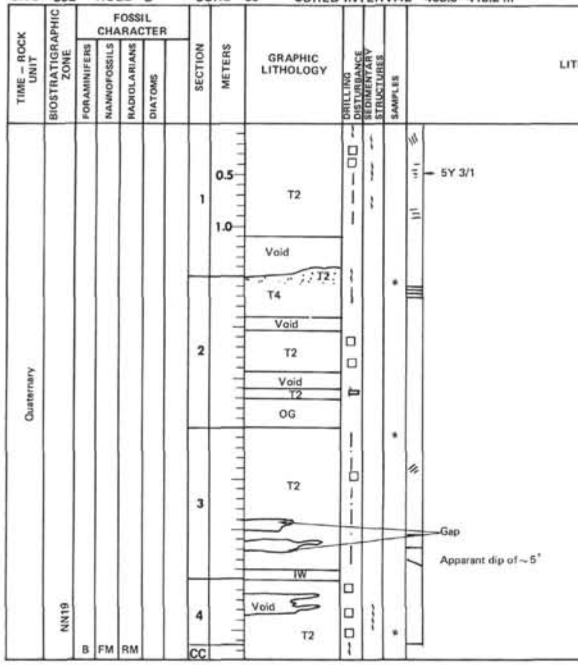

LITHOLOGIC DESCRIPTION

FIRM HEMIPELAGIC MUD
5Y 4/1

Remarks: Lithics include felsitic volcanic and vitric volcanic grains, shale, and chert plagioclases are zoned with albite twinning zircon and apatite inclusions.

SMEAR SLIDE SUMMARY (%):

	2, 3	3, 9	4, 51
	M	M	D
Texture:			
Sand	50	15	–
Silt	45	65	70
Clay	5	20	30
Composition:			
Quartz	40	35	30
Feldspar	10	5	3
Mica	3	Tr	2
Heavy minerals	10	4	5
Clay	5	21	30
Volcanic glass	2	10	1
Pyrite	–	–	1
Foraminifers	–	–	Tr
Calc. nannofossils	–	Tr	Tr
Diatoms	–	–	2
Radiolarians	–	–	Tr
Sponge spicules	Tr	–	1
Fish remains	–	–	Tr
Lithic fragments	30	25	25

ORGANIC CARBON AND CARBONATE (%):

	2, 50	4, 50
Carbonate	2.7	2.3

SITE 582 HOLE B CORE 39 CORED INTERVAL 413.2–422.6 m

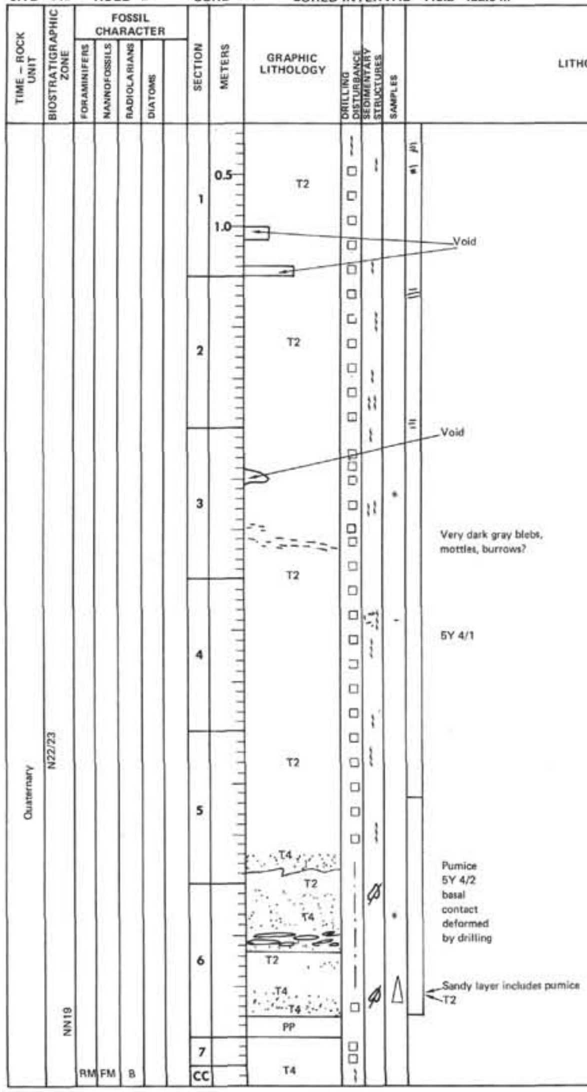

LITHOLOGIC DESCRIPTION

FIRM HEMIPELAGIC MUD
Dark gray (5Y 4/1) with black (5Y 2.5/1) layers.

Section 6, 60 cm: alternating sandy mud and mud, possibly due to drilling deformation.

SMEAR SLIDE SUMMARY (%):

	3, 70	6, 30
	D	M
Texture:		
Sand	0	50
Silt	60	45
Clay	40	5
Composition:		
Quartz	30	50
Feldspar	3	10
Mica	1	3
Heavy minerals	2	5
Clay	30	5
Volcanic glass	2	–
Glauconite	Tr	–
Pyrite	1	1
Carbonate unspec.	Tr	–
Foraminifers	Tr	–
Calc. nannofossils	Tr	Tr
Diatoms	1	1
Radiolarians	Tr	Tr
Sponge spicules	Tr	Tr
Fish remains	Tr	–
Lithic fragments	30	25

ORGANIC CARBON AND CARBONATE (%):

	1, 50	3, 50	5, 50	7, 20
Carbonate	2.3	1.4	3.2	3.2

SITE 582 HOLE B CORE 40 CORED INTERVAL 422.6–432.0 m

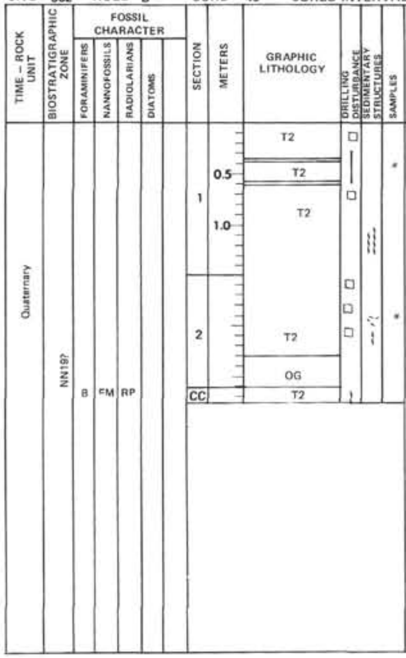

LITHOLOGIC DESCRIPTION

FIRM HEMIPELAGIC MUD

Very dark gray/black (5Y 3/1–2.5/1) layers.
Bioturbation obvious where color contrast occurs, perhaps more general in extent

Remarks: Euhedral plagioclase laths disseminated in mud.

SMEAR SLIDE SUMMARY (%):

	1, 40	2,48
	D	D
Texture:		
Sand	10	–
Silt	30	50
Clay	60	50
Composition:		
Quartz	12	30
Feldspar	8	10
Mica	Tr	2
Heavy minerals	3	2
Clay	53	40
Volcanic glass	4	2
Pyrite	1	1
Carbonate unspec.	Tr	Tr
Foraminifers	Tr	Tr
Calc. nannofossils	1	Tr
Diatoms	8	1
Radiolarians	–	Tr
Sponge spicules	2	2
Silicoflagellates	Tr	–
Fish remains	–	Tr
Lithic fragments	8	10

SITE 582 HOLE B CORE 41 CORED INTERVAL 432.0–441.5 m

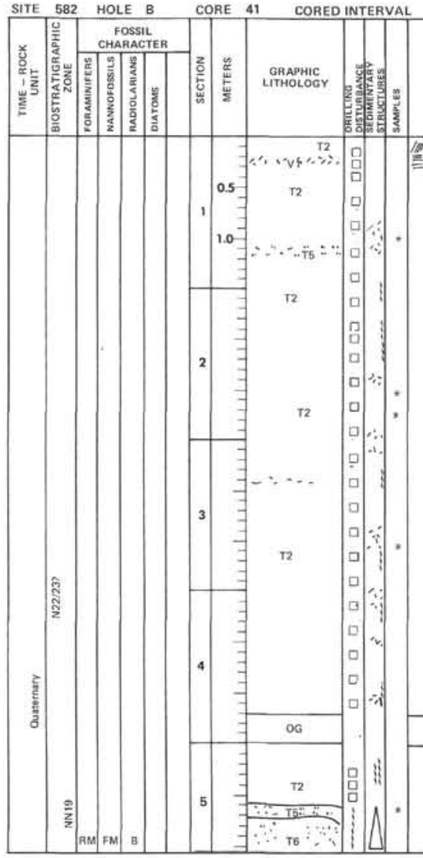

LITHOLOGIC DESCRIPTION

FIRM, HEMIPELAGIC MUD

5Y 4/1

Very dark gray (5Y 3/1) blebs

5Y 4/1

5Y 3/1

Collapsed spheres or tubes

3 mm

SMEAR SLIDE SUMMARY (%):

	3, 108	1, 102	2, 107	2, 127	5, 69
	D	M	D	M	M
Texture:					
Sand	–	–	–	10	20
Silt	20	50	40	85	50
Clay	80	50	60	5	30
Composition:					
Quartz	10	30	30	45	30
Feldspar	4	4	5	6	6
Mica	Tr	2	2	4	2
Heavy minerals	Tr	3	3	8	2
Clay	80	40	50	5	26
Volcanic glass	Tr	4	Tr	4	3
Pyrite	1	1	Tr	3	1
Carbonate unspec.	–	–	–	Tr	–
Foraminifers	–	–	Tr	–	Tr
Calc. nannofossils	Tr	–	–	Tr	2
Diatoms	Tr	Tr	–	Tr	2
Radiolarians	–	Tr	–	–	Tr
Sponge spicules	1	1	Tr	Tr	2
Silicoflagellates	–	–	–	–	Tr
Lithic fragments	4	15	10	25	25

ORGANIC CARBON AND CARBONATE (%):

	1, 50	3, 50
Carbonate	3.8	2.3

SITE 582 HOLE B CORE 42 CORED INTERVAL 441.5–451.0 m

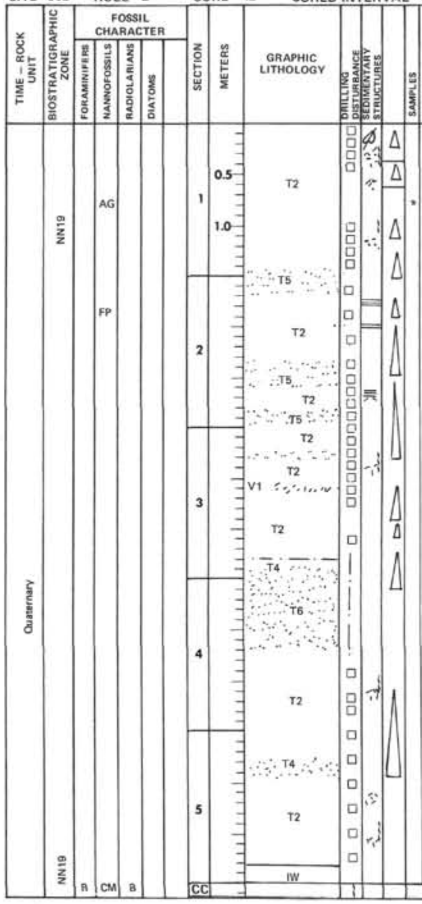

LITHOLOGIC DESCRIPTION

FIRM HEMIPELAGIC MUD AND GRADED SANDS
Nanno-rich mud
5Y 3/2 to 4/1

Grading shown from here to top is extremely faint... not to be confused with previous clear examples

Fine laminations

Muddy silt, 5Y 3/1

SMEAR SLIDE SUMMARY (%):

	1, 80
	D
Texture:	
Sand	Tr
Silt	10
Clay	90
Composition:	
Quartz	4
Feldspar	Tr
Mica	1
Heavy minerals	1
Clay	60
Volcanic glass	Tr
Pyrite	1
Foraminifers	Tr
Calc. nannofossils	30
Diatoms	Tr
Radiolarians	Tr
Sponge spicules	1
Silicoflagellates	Tr
Lithic fragments	2

5Y 3/2

ORGANIC CARBON AND CARBONATE (%):

	1, 50	2, 32	3, 50	5, 50
Carbonate	2.7	12.7	1.3	5.5

5Y 3/1

SITE 582 HOLE B CORE 43 CORED INTERVAL 451.0–460.5 m

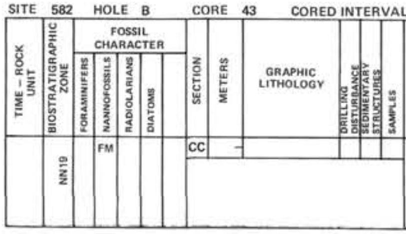

LITHOLOGIC DESCRIPTION

Trace recovery.

SITE 582 HOLE B CORE 44 CORED INTERVAL 460.5–470.0 m

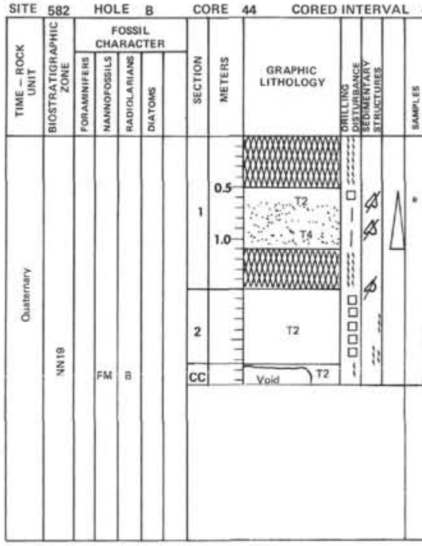

LITHOLOGIC DESCRIPTION

5Y 3/1
Sandy mud with wood fragments, grading questionable

5Y 3/1

FIRM HEMIPELAGIC MUD AND SANDY MUD AND DRILL BRECCIA

SMEAR SLIDE SUMMARY (%):

	1, 69
	M
Texture:	
Sand	40
Silt	40
Clay	20
Composition:	
Quartz	50
Feldspar	10
Mica	3
Heavy minerals	5
Clay	19
Pyrite	3
Carbonate unspec.	2
Foraminifers	Tr
Calc. nannofossils	1
Diatoms	Tr
Sponge spicules	Tr
Plant debris	2
Lithic fragments	5

SITE 582 HOLE B CORE 45 CORED INTERVAL 470.0–479.5 m

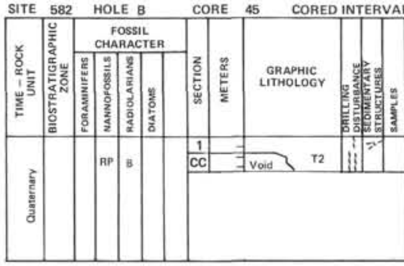

LITHOLOGIC DESCRIPTION

FIRM HEMIPELAGIC MUD
Dark olive gray (5Y 3/2)

SITE 582 HOLE B CORE 46 CORED INTERVAL 479.5–489.0 m

TIME – ROCK UNIT	BIOSTRATIGRAPHIC ZONE	FORAMINIFERS	NANNOFOSSILS	RADIOLARIANS	DIATOMS	SECTION	METERS
Quaternary	NN19	B	FM	RM		1	0.5, 1.0
						CC	

GRAPHIC LITHOLOGY / DRILLING DISTURBANCE / SEDIMENTARY STRUCTURES / SAMPLES

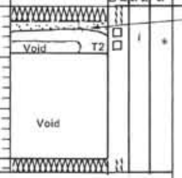

LITHOLOGIC DESCRIPTION

HEMIPELAGIC MUD AND DRILL BRECCIA
5Y 3/2–3/1

SMEAR SLIDE SUMMARY (%):

	1, 32
	D
Texture:	
Sand	5
Silt	35
Clay	60
Composition:	
Quartz	24
Feldspar	1
Mica	2
Heavy mineals	2
Clay	65
Volcanic glass	1
Pyrite	3
Carbonate unspec.	Tr
Calc. nannofossils	Tr
Sponge spicules	1
Lithic fragments	1

SITE 582 HOLE B CORE X1 CORED INTERVAL 489.0 m

TIME – ROCK UNIT	BIOSTRATIGRAPHIC ZONE	FORAMINIFERS	NANNOFOSSILS	RADIOLARIANS	DIATOMS	SECTION	METERS
						1	

GRAPHIC LITHOLOGY / DRILLING DISTURBANCE / SEDIMENTARY STRUCTURES / SAMPLES

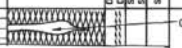

LITHOLOGIC DESCRIPTION

X-core taken in process of clearing of bit attempt
5Y 4/1 sand size drill hash

SITE 582 HOLE B CORE 47 CORED INTERVAL 489.0–498.6 m

TIME – ROCK UNIT	BIOSTRATIGRAPHIC ZONE	FORAMINIFERS	NANNOFOSSILS	RADIOLARIANS	DIATOMS	SECTION	METERS
Quaternary	NN19	B	FM	B		1	0.5
						CC	

GRAPHIC LITHOLOGY / DRILLING DISTURBANCE / SEDIMENTARY STRUCTURES / SAMPLES

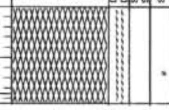

LITHOLOGIC DESCRIPTION

DRILL BRECCIA
Olive gray (5Y 3/2) drill chips

SMEAR SLIDE SUMMARY (%):

	1, 65
	D
Texture:	
Sand	15
Silt	70
Clay	15
Composition:	
Quartz	47
Feldspar	5
Mica	5
Heavy minerals	10
Clay	15
Volcanic glass	3
Pyrite	5
Carbonate unspec.	3
Calc. nannofossils	Tr
Radiolarians	Tr
Sponge spicules	Tr
Lithic fragments	7

SITE 582 HOLE B CORE 48 CORED INTERVAL 498.6–508.2 m

TIME – ROCK UNIT	BIOSTRATIGRAPHIC ZONE	FORAMINIFERS	NANNOFOSSILS	RADIOLARIANS	DIATOMS	SECTION	METERS
Quaternary	NN19	B	FP	B		1	0.5, 1.0
						CC	

GRAPHIC LITHOLOGY / DRILLING DISTURBANCE / SEDIMENTARY STRUCTURES / SAMPLES

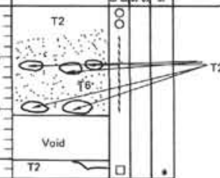

LITHOLOGIC DESCRIPTION

SAND AND SAND WITH MUD CLASTS
Some of the sand is quite coarse and grains rounded ...grains include quartz, quartzite, and dark lithic fragments.

SMEAR SLIDE SUMMARY (%):

	CC, 18
	D
Texture:	
Sand	2
Silt	48
Clay	50
Composition:	
Quartz	40
Feldspar	5
Mica	2
Heavy minerals	Tr
Clay	49
Volcanic glass	Tr
Pyrite	Tr
Calc. nannofossils	Tr
Diatoms	Tr
Sponge spicules	2
Lithic fragments	2

Core 49, 508.2–517.8 m: no recovery.

SITE 582 HOLE B CORE 50 CORED INTERVAL 517.8–527.5 m

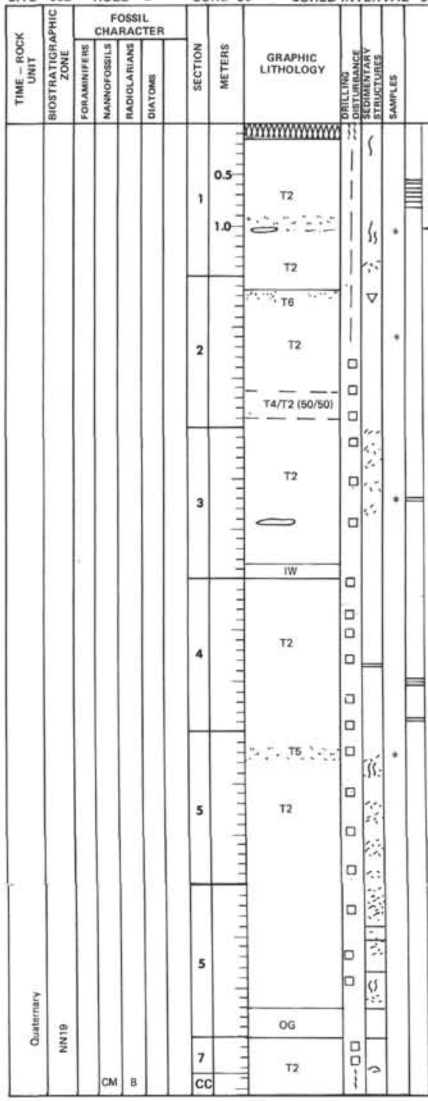

LITHOLOGIC DESCRIPTION

5Y 3/1

HARD HEMIPELAGIC MUD AND MUDSTONE

T5–T4

Flattened, inclined blebs – probably burrows

Reverse graded bed

5Y 3/1

Slightly paler patch (5Y 4/1)

Very dark gray (5Y 3/1)

SMEAR SLIDE SUMMARY (%):

	2, 62 M	1, 105 D	5, 21 M	3, 79 M
Texture:				
Sand	5	Tr	–	–
Silt	40	30	90	60
Clay	55	70	10	40
Composition:				
Quartz	20	15	40	25
Feldspar	5	5	8	9
Mica	2	1	3	1
Heavy minerals	2	2	5	5
Clay	54	62	5	30
Volcanic glass	1	1	–	4
Pyrite	1	2	1	1
Micronodules	–	–	–	Tr
Carbonate unspec.	–	5	5	–
Foraminifers	–	Tr	–	Tr
Calc. nannofossils	Tr	3	Tr	–
Diatoms	–	Tr	Tr	Tr
Radiolarians	–	–	Tr	–
Sponge spicules	Tr	2	Tr	Tr
Lithic fragments	15	2	30	25

SITE 582 HOLE B CORE 51 CORED INTERVAL 527.5–537.2 m

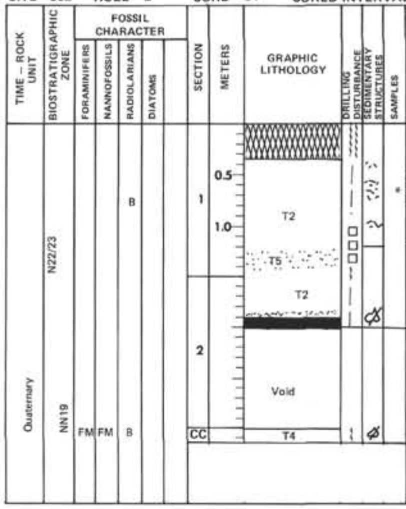

LITHOLOGIC DESCRIPTION

HARD HEMIPELAGIC MUD AND MUDSTONE
Very dark gray (5Y 3/1) (shale)

The whole forest! large (~ 10 cm diameter) twigs

SMEAR SLIDE SUMMARY (%):

	1, 62 D
Texture:	
Sand	–
Silt	50
Clay	50
Composition:	
Quartz	25
Feldspar	5
Mica	1
Heavy minerals	3
Clay	40
Volcanic glass	5
Pyrite	1
Micronodules	Tr
Carbonate unspec.	Tr
Sponge spicules	Tr
Lithic fragments	20

SITE 582 HOLE B CORE 52 CORED INTERVAL 537.2–546.9 m

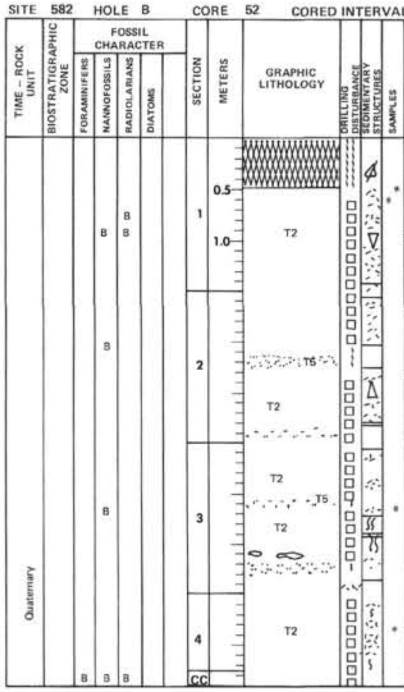

LITHOLOGIC DESCRIPTION

HARD HEMIPELAGIC MUD AND MUDSTONE
Dark olive gray (5Y 3/2)

Flattened ellipses, white periphery, black center

SMEAR SLIDE SUMMARY (%):

	1, 50 D	1, 62 D	4, 35 M	3, 63 M
Texture:				
Sand	–	–	–	5
Silt	40	50	15	60
Clay	60	50	85	35
Composition:				
Quartz	15	25	15	49
Feldspar	3	5	–	3
Mica	2	1	2	2
Heavy minerals	4	3	–	3
Clay	50	40	71	34
Volcanic glass	3	5	8	2
Palagonite	–	–	3	–
Pyrite	1	1	–	2
Micronodules	–	Tr	–	–
Carbonate unspec.	2	Tr	1	2
Calc. nannofossils	–	–	Tr	1
Diatoms	–	–	–	Tr
Sponge spicules	Tr	Tr	Tr	1
Lithic fragments	20	20	–	–

SITE 582 HOLE B CORE 53 CORED INTERVAL 546.9–556.5 m

TIME – ROCK UNIT: Quaternary?

Fossil character: Foraminifers B, Nannofossils B, Radiolarians B

Section: CC

LITHOLOGIC DESCRIPTION

DRILL BRECCIA

SMEAR SLIDE SUMMARY (%):

	CC, 2
	D
Texture:	
Sand	–
Silt	50
Clay	50
Composition:	
Quartz	25
Feldspar	10
Mica	1
Heavy minerals	3
Clay	40
Volcanic glass	5
Carbonate unspec.	1
Foraminifers	Tr
Calc. nannofossils	Tr
Diatoms	Tr
Sponge spicules	Tr
Lithic fragments	15

SITE 582 HOLE B CORE 54 CORED INTERVAL 556.5–566.1 m

TIME – ROCK UNIT: Quaternary

Sections: 1, 2, CC

T2

T5 muddy silt

5Y 4/1–5Y 4/2

5Y 3/2
Lots of drill deformation,
small biscuits and
inter-biscuit flow

LITHOLOGIC DESCRIPTION

HARD HEMIPELAGIC MUD/MUDSTONE
AND FINE GRAINED TURBIDITES

SMEAR SLIDE SUMMARY (%):

	1, 142	1, 142	1, 84	1, 84	1, 62
	M	M	M	M	D
Texture:					
Sand	Tr	–	10	45	–
Silt	45	70	60	50	50
Clay	55	30	30	5	50
Composition:					
Quartz	26	15	33	30	25
Feldspar	3	10	5	10	6
Mica	2	1	3	3	2
Heavy minerals	2	3	3	5	–
Clay	55	25	30	5	40
Volcanic glass	3	25	2	5	5
Pyrite	2	1	2	2	1
Carbonate unspec.	2	Tr	2	Tr	–
Foraminifers	Tr	–	Tr	Tr	–
Calc. nannofossils	1	Tr	1	–	–
Radiolarians	Tr	–	–	–	Tr
Sponge spicules	–	–	1	Tr	1
Fish remains	–	Tr	–	–	Tr
Lithic fragments	5	20	10	40	20

ORGANIC CARBON AND CARBONATE (%):

	1, 61
Carbonate	0.8

SITE 582 HOLE B CORE 55 CORED INTERVAL 566.0–575.7 m

TIME – ROCK UNIT: Quaternary

BIOSTRATIGRAPHIC ZONE: NN19

Sections: 1, 2, 3, 4, CC

T2, IW, T2, OG, T2

Ash filling
burrow (V1)
is light colored
7.5YR 5/4

Zoophycus
~1 cm thick
burrow

LITHOLOGIC DESCRIPTION

HEMIPELAGIC MUDSTONE
Dark olive gray (5Y 3/1–5Y 3/2)

SMEAR SLIDE SUMMARY (%):

	1, 86	1, 86	3, 73	1, 126
	M	M	M	D
Texture:				
Sand	2	3	10	Tr
Silt	58	55	30	60
Clay	40	42	60	40
Composition:				
Quartz	20	30	10	32
Feldspar	2	3	2	5
Mica	2	Tr	1	3
Heavy minerals	1	2	2	3
Clay	32	56	55	40
Volcanic glass	40	5	25	–
Pyrite	1	2	Tr	5
Carbonate unspec.	–	–	–	2
Calc. nannofossils	–	Tr	Tr	–
Sponge spicules	2	4	2	Tr
Silicoflagellates	–	–	Tr	–
Chert	Tr	–	–	–
Lithic fragments	–	–	3	5

SITE 582 HOLE B CORE 56 CORED INTERVAL 575.7–585.3 m

TIME – ROCK UNIT	BIOSTRATIGRAPHIC ZONE	FORAMINIFERS	NANNOFOSSILS	RADIOLARIANS	DIATOMS	SECTION	METERS	GRAPHIC LITHOLOGY	DRILLING DISTURBANCE	SEDIMENTARY STRUCTURES	SAMPLES	LITHOLOGIC DESCRIPTION
Quaternary	NN19	B	CM	B		1	0.5, 1.0					
						CC					*	1 biscuit is in good shape

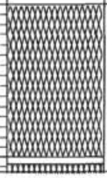

DRILL BRECCIA

SMEAR SLIDE SUMMARY (%):

	CC, 4
	D
Texture:	
Sand	3
Silt	55
Clay	42
Composition:	
Quartz	35
Feldspar	5
Mica	2
Heavy minerals	4
Clay	40
Volcanic glass	10
Pyrite	1
Carbonate unspec.	Tr
Calc. nannofossils	Tr
Diatoms	Tr
Sponge spicules	Tr
Lithic fragments	3

SITE 582 HOLE B CORE 57 CORED INTERVAL 585.3–594.9 m

TIME – ROCK UNIT	BIOSTRATIGRAPHIC ZONE	FORAMINIFERS	NANNOFOSSILS	RADIOLARIANS	DIATOMS	SECTION	METERS	GRAPHIC LITHOLOGY	DRILLING DISTURBANCE	SEDIMENTARY STRUCTURES	SAMPLES	FABRIC	LITHOLOGIC DESCRIPTION
Quaternary						1	0.5, 1.0				*		Sample is from groundmass lith; Olive gray (5Y 5/2) lighter layer; Cylindrichnus; Zoophycus; Ashy burrow-fill, olive (5Y 4/3)
						2							Thin silt layers; Olive gray (5Y 3/2) matrix; (V1) ash layer with pumice grains; (T5) muddy siltstone, 5Y 3/1
			CM			3					*		Thin, light colored (5Y 4/3) layer; (V1) olive (5Y 4/3); Brown laminations (ashy?)
			AG			4							Light (5GY 4/1) spots; Nanno-rich horizon
						5							Sandy mud, 5Y 4/1
	NN19	B	FP	B		CC							5Y 3/2

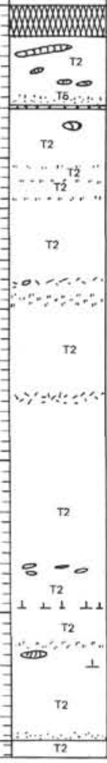

HEMIPELAGIC MUDSTONE

SMEAR SLIDE SUMMARY (%):

	1, 50	3, 40
	D	M
Texture:		
Sand	–	3
Silt	50	40
Clay	50	57
Composition:		
Quartz	20	24
Feldspar	5	4
Mica	2	3
Heavy minerals	–	2
Clay	70	53
Volcanic glass	5	–
Pyrite	2	3
Carbonate unspec.	–	5
Foraminifers	–	Tr
Calc. nannofossils	–	4
Sponge spicules	1	Tr
Lithic fragments (chert)	–	2

ORGANIC CARBON AND CARBONATE (%):

	1, 50
Carbonate	0.4

SITE 582 HOLE B CORE 58 CORED INTERVAL 594.9–604.5 m

TIME – ROCK UNIT | BIOSTRATIGRAPHIC ZONE | FOSSIL CHARACTER (FORAMINIFERS, NANNOFOSSILS, RADIOLARIANS, DIATOMS) | SECTION | METERS | GRAPHIC LITHOLOGY | DRILLING DISTURBANCE | SEDIMENTARY STRUCTURES | SAMPLES | LITHOLOGIC DESCRIPTION

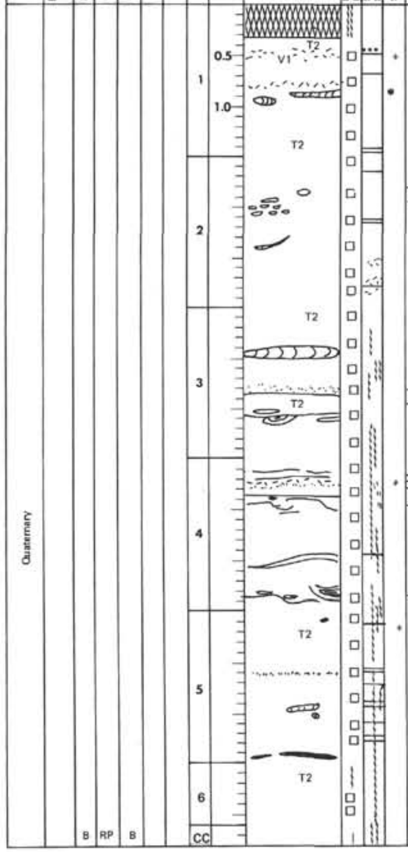

5Y 5/1 ash layer
Cylindrichnus

Pumice
Cylindrichnus

Olive (5Y 4/3)
Dark lamination

Diffuse green halo
(dusky green – 5G 3/2) underlain by sandy lens
V1
Black layer (sharp basal contact, diffuse upward)
Pumice grain (and at 5–9)

Burrow

Load cast of lighter color (5Y 5/2)

(nanno-rich?)
mud

Mud, 5Y 4/1

5GY 4/1

HEMIPELAGIC MUDSTONE
Dark gray (5Y 3/2–4/1)

SMEAR SLIDE SUMMARY (%):

	1, 50	1, 84	4, 25	5, 18
	D	M	M	–
Texture:				
Sand	Tr	–	–	–
Silt	40	90	40	20
Clay	60	10	60	80
Composition:				
Quartz	20	13	10	57
Feldspar	5	10	2	15
Mica	1	2	2	–
Heavy minerals	1	3	1	3
Clay	55	10	60	15
Volcanic glass	5	60	20	4
Pyrite	3	2	2	–
Carbonate unspec.	3	–	–	–
Calc. nannofossils	5	–	–	–
Sponge spicules	2	–	3	1
Fish remains	–	–	–	1
Lithic fragments	–	–	–	4

ORGANIC CARBON AND CARBONATE (%):

	1, 87	4, 96
Carbonate	1.3	0.0

SITE 582 HOLE B CORE 59 CORED INTERVAL 604.5–614.1 m

TIME – ROCK UNIT | BIOSTRATIGRAPHIC ZONE | FOSSIL CHARACTER (FORAMINIFERS, NANNOFOSSILS, RADIOLARIANS, DIATOMS) | SECTION | METERS | GRAPHIC LITHOLOGY | DRILLING DISTURBANCE | SEDIMENTARY STRUCTURES | SAMPLES | LITHOLOGIC DESCRIPTION

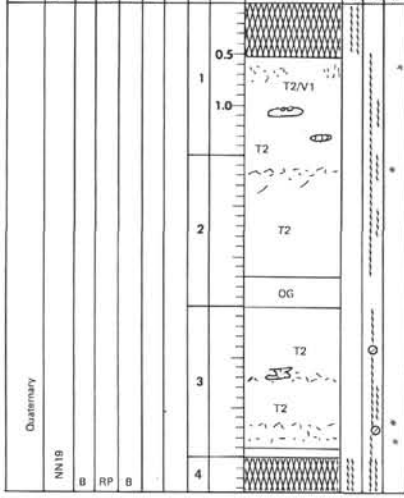

5Y 3/1 = matrix color

Dewatering lines

5Y 4/1–4/2

5Y 5/2

HEMIPELAGIC MUDSTONE

Ash patches throughout 5Y 4/1 and nannos.

SMEAR SLIDE SUMMARY (%):

	3, 120	3, 132	2, 17	1, 66
	M	M		D
Texture:				
Sand	65	–	15	2
Silt	32	15	75	40
Clay	3	85	10	58
Composition:				
Quartz	Tr	20	25	10
Feldspar	–	5	10	6
Mica	–	–	–	1
Heavy minerals	–	–	5	3
Clay	2	68	45	45
Volcanic glass	98	1	5	5
Pyrite	–	3	–	–
Carbonate unspec.	–	–	3	15
Calc. nannofossils	Tr	–	–	10
Sponge spicules	–	–	1	–
Fish remains	–	1	1	–
Lithic fragments	–	2	5	5

ORGANIC CARBON AND CARBONATE (%):

	1, 50	3, 50
Carbonate	1.7	3.3

SITE 582 HOLE B CORE 60 CORED INTERVAL 614.1–623.7 m

TIME – ROCK UNIT | BIOSTRATIGRAPHIC ZONE | FOSSIL CHARACTER (FORAMINIFERS, NANNOFOSSILS, RADIOLARIANS, DIATOMS) | SECTION | METERS | GRAPHIC LITHOLOGY | DRILLING DISTURBANCE | SEDIMENTARY STRUCTURES | SAMPLES | LITHOLOGIC DESCRIPTION

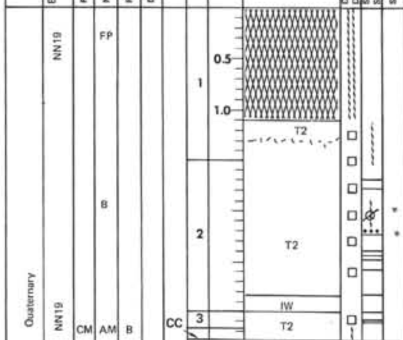

Dark gray (5Y 4/1)

Green laminations

HEMIPELAGIC MUDSTONE

Section 2, 73 cm: smear slide; black lamination ~1 cm thick and thin sequence of graded bedding.

SMEAR SLIDE SUMMARY (%):

	2, 44	2, 73
	D	M
Texture:		
Sand	2	Tr
Silt	50	70
Clay	48	30
Composition:		
Quartz	45	40
Feldspar	15	6
Mica	Tr	1
Heavy minerals	2	3
Clay	35	25
Volcanic glass	2	15
Pyrite	1	1
Carbonate unspec.	–	3
Calc. nannofossils	–	1
Sponge spicules	Tr	–
Fish remains	–	Tr
Lithic fragments	–	5

ORGANIC CARBON AND CARBONATE (%):

	2, 50
Carbonate	0.8

SITE 582 HOLE B CORE 61 CORED INTERVAL 623.7–633.3 m

TIME – ROCK UNIT	BIOSTRATIGRAPHIC ZONE	FORAMINIFERS	NANNOFOSSILS	RADIOLARIANS	DIATOMS	SECTION	METERS
Quaternary	NN19	B	B	B		1, 2, 3, 4, CC	0.5, 1.0
			B				
			RP				

GRAPHIC LITHOLOGY / DRILLING DISTURBANCE / SEDIMENTARY STRUCTURES / SAMPLES

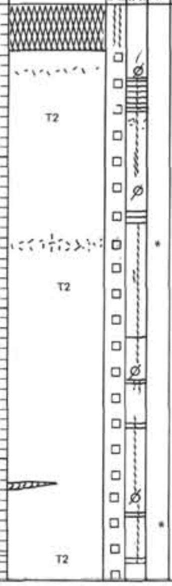

LITHOLOGIC DESCRIPTION

(V1) ash layer

Pumice

5Y 4/1

Green laminations throughout

5Y 4/1

HEMIPELAGIC MUDSTONE
5Y 4/2

Section 2, 86–89 cm: thick white ash layer.

SMEAR SLIDE SUMMARY (%):

	2, 88 M	4, 68
Texture:		
Sand	15	–
Silt	70	40
Clay	15	60
Composition:		
Quartz	10	35
Feldspar	3	3
Mica	Tr	1
Heavy minerals	Tr	1
Clay	15	59
Volcanic glass	70	–
Pyrite	Tr	Tr
Sponge spicules	–	1
Lithic fragments	2	–

ORGANIC CARBON AND CARBONATE (%):

	2, 50
Carbonate	2.5

SITE 582 HOLE B CORE 62 CORED INTERVAL 633.3–642.9 m

TIME – ROCK UNIT	BIOSTRATIGRAPHIC ZONE	FORAMINIFERS	NANNOFOSSILS	RADIOLARIANS	DIATOMS	SECTION	METERS
Quaternary		RM	B	B		1, 2, 3, 4, CC	0.5, 1.0

GRAPHIC LITHOLOGY / DRILLING DISTURBANCE / SEDIMENTARY STRUCTURES / SAMPLES

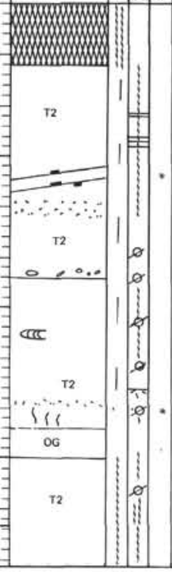

LITHOLOGIC DESCRIPTION

Black mottling

Green laminations

Normal faults

Sharp contact at 199 cm... contorted beds above many small pumice fragments

5BG 4/1

Subtle de-watering veins (not toally obvious)

HEMIPELAIGC MUDSTONE
5GY 4/1

SMEAR SLIDE SUMMARY (%):

	2, 21 M	3, 105 M
Texture:		
Sand	40	10
Silt	20	70
Clay	40	20
Composition:		
Quartz	45	40
Feldspar	5	10
Mica	Tr	1
Heavy minerals	Tr	2
Clay	40	20
Volcanic glass	10	25
Pyrite	Tr	Tr
Micronodules	Tr	–
Sponge spicules	Tr	–
Lithic fragments	–	2

ORGANIC CARBON AND CARBONATE (%):

	2, 90
Carbonate	7.8

SITE 582 HOLE B CORE 63 CORED INTERVAL 642.9–652.5 m

TIME – ROCK UNIT	BIOSTRATIGRAPHIC ZONE	FORAMINIFERS	NANNOFOSSILS	RADIOLARIANS	DIATOMS	SECTION	METERS
Quaternary		B	FP	B		1, 2, 3, CC	0.5, 1.0

GRAPHIC LITHOLOGY / DRILLING DISTURBANCE / SEDIMENTARY STRUCTURES / SAMPLES

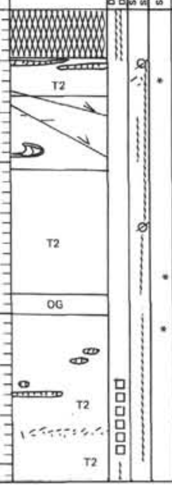

LITHOLOGIC DESCRIPTION

Normal faults

Black layer

Burrows (5Y 4/2) are frequent and in darker (5Y 2.5/1) groundmass

HEMIPELAGIC MUDSTONE
Olive gray (5Y 4/2).

SMEAR SLIDE SUMMARY (%):

	1, 70 D	2, 119 M	3, 20 D
Texture:			
Sand	2	5	2
Silt	30	65	40
Clay	68	30	58
Composition:			
Quartz	17	10	17
Feldspar	3	2	10
Mica	2	3	1
Heavy minerals	1	Tr	2
Clay	66	30	48
Volcanic glass	2	55	5
Pyrite	–	–	5
Carbonate unspec.	3	–	1
Foraminifers	–	–	Tr
Calc. nannofossils	5	–	10
Sponge spicules	1	–	1
Fish remains	–	–	Tr

ORGANIC CARBON AND CARBONATE (%):

	2, 98
Carbonate	0.8

SITE 582 HOLE B CORE 64 CORED INTERVAL 652.5–662.1 m

TIME – ROCK UNIT: Quaternary

FOSSIL CHARACTER (Foraminifers, Nannofossils, Radiolarians, Diatoms): FM B; B B B

SECTIONS: 1, 2, 3, 4, 5, 6, 7, CC

METERS: 0.5, 1.0

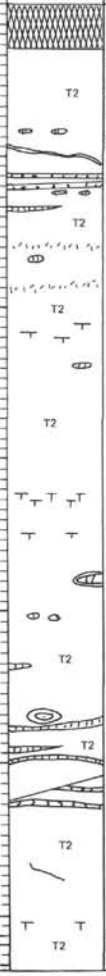

LITHOLOGIC DESCRIPTION

100 cm: dark layer

Dewatering vein, offset

Zoophycus

Ashy layer

5GY 5/1 lighter layer

Foram tests visible in mud matrix

5GY 4/1

Black mottles

To top

Alternating 2.5 cm cycle 5GY 4/1 – 5G 5/1 greenish layers

Zoophycus

Fault

Dewatering vein?

HEMIPELAGIC MUDSTONE
Alternating 5GY 4/1 bioturbated olive gray mud and 5G 4/1 chlorite-rich layers.

SMEAR SLIDE SUMMARY (%):

	2, 87	3, 94
	M	D
Texture:		
Sand	Tr	Tr
Silt	60	30
Clay	41	70
Composition:		
Quartz	11	15
Feldspar	2	2
Mica	Tr	1
Heavy minerals	Tr	1
Clay	38	70
Volcanic glass	40	–
Pyrite	1	5
Carbonate unspec.	5	5
Foraminifers	Tr	–
Calc. nannofossils	2	1
Sponge spicules	Tr	–

ORGANIC CARBON AND CARBONATE (%):

	4, 89
Carbonate	1.3

SITE 582 HOLE B CORE 65 CORED INTERVAL 662.1–671.8 m

TIME – ROCK UNIT: Quaternary

FOSSIL CHARACTER: RM B B

SECTION: 1

METERS: 0.5

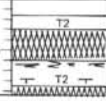

LITHOLOGIC DESCRIPTION

Zoophycus

Light patches

HEMIPELAGIC MUDSTONE
Olive gray (5GY 4/1)

SMEAR SLIDE SUMMARY (%):

	1, 70
	D
Texture:	
Sand	–
Silt	25
Clay	75
Composition:	
Quartz	11
Feldspar	5
Mica	Tr
Heavy minerals	1
Clay	70
Volcanic glass	3
Pyrite	4
Carbonate unspec.	1
Foraminifers	Tr
Calc. nannofossils	5

SITE 582 HOLE B CORE 66 CORED INTERVAL 671.8–681.5 m

TIME – ROCK UNIT: Quaternary

BIOSTRATIGRAPHIC ZONE: NN19

FOSSIL CHARACTER: B RP B

SECTIONS: 1, 2, 3, 4, CC

METERS: 0.5, 1.0

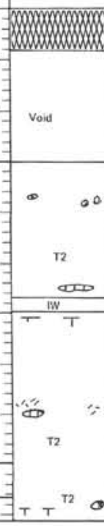

LITHOLOGIC DESCRIPTION

(CB8)

Ashy spots
Green laminations

Dark green gray
(5GY 4/1)

5GY 4/1

HEMIPELAGIC MUDSTONE
Dark olive gray (5Y 3/2)

SMEAR SLIDE SUMMARY (%):

	3, 50
	D
Texture:	
Sand	–
Silt	30
Clay	70
Composition:	
Quartz	18
Feldspar	2
Mica	2
Heavy minerals	Tr
Clay	70
Volcanic glass	5
Pyrite	2
Silicoflagellates	1

ORGANIC CARBON AND CARBONATE (%):

	3, 43
Carbonate	0.4

SITE 582 HOLE B CORE 67 CORED INTERVAL 681.5–691.2 m

TIME – ROCK UNIT	BIOSTRATIGRAPHIC ZONE	FORAMINIFERS	NANNOFOSSILS	RADIOLARIANS	DIATOMS	SECTION	METERS	GRAPHIC LITHOLOGY	DRILLING DISTURBANCE / SEDIMENTARY STRUCTURES	SAMPLES	LITHOLOGIC DESCRIPTION
Quaternary	NN19	B	FP	B		1, 2, 3, 4, CC	0.5, 1.0	Void; T2; Void; Void		*	Olive gray (5GY 4/1) with dark gray-green (5G 4/1) shades

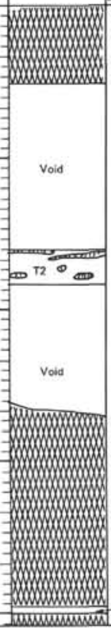

DRILL BRECCIA AND HEMIPELAGIC MUDSTONE

SMEAR SLIDE SUMMARY (%):

	2, 120
	D
Texture:	
Sand	Tr
Silt	35
Clay	65
Composition:	
Quartz	24
Feldspar	2
Mica	Tr
Heavy minerals	2
Clay	63
Volcanic glass	5
Pyrite	1
Carbonate unspec.	Tr
Calc. nannofossils	2
Sponge spicules	Tr
Silicoflagellates	Tr
Fish remains	Tr
Plant debris	1

ORGANIC CARBON AND CARBONATE (%):

	2, 24
Carbonate	1.3

SITE 582 HOLE B CORE 68 CORED INTERVAL 691.2–700.9 m

TIME – ROCK UNIT	BIOSTRATIGRAPHIC ZONE	FORAMINIFERS	NANNOFOSSILS	RADIOLARIANS	DIATOMS	SECTION	METERS	GRAPHIC LITHOLOGY	DRILLING DISTURBANCE / SEDIMENTARY STRUCTURES	SAMPLES	LITHOLOGIC DESCRIPTION
Quaternary	NN19	RM	FP	B		1, 2, CC	0.5, 1.0	T2; Void; T1 T2		*	Green laminations; Numerous black spots; Glaucophane present; Zoophycus

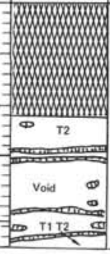

HEMIPELAGIC MUDSTONE
5GY 4/1

SMEAR SLIDE SUMMARY (%):

	2, 48
	D
Texture:	
Sand	–
Silt	30
Clay	70
Composition:	
Quartz	15
Heavy minerals	1
Clay	74
Volcanic glass	5
Pyrite	2
Carbonate unspec.	2
Calc. nannofossils	Tr
Sponge spicules	1

ORGANIC CARBON AND CARBONATE (%):

	1, 134
Carbonate	0.4

SITE 582 HOLE B CORE 69 CORED INTERVAL 700.9–710.6 m

TIME – ROCK UNIT	BIOSTRATIGRAPHIC ZONE	FORAMINIFERS	NANNOFOSSILS	RADIOLARIANS	DIATOMS	SECTION	METERS	GRAPHIC LITHOLOGY	DRILLING DISTURBANCE / SEDIMENTARY STRUCTURES	SAMPLES	LITHOLOGIC DESCRIPTION
Quaternary		RM	B	B		CC		T2		*	

HEMIPELAGIC MUDSTONE

SMEAR SLIDE SUMMARY (%):

	CC, 17
	D
Texture:	
Sand	5
Silt	75
Clay	20
Composition:	
Quartz	50
Feldspar	11
Mica	Tr
Heavy minerals	4
Clay	20
Volcanic glass	10
Pyrite	1
Carbonate unspec.	1
Sponge spicules	Tr
Lithic fragments	3

SITE 582 HOLE B CORE 70 CORED INTERVAL 710.6–720.3 m

TIME – ROCK UNIT	BIOSTRATIGRAPHIC ZONE	FORAMINIFERS	NANNOFOSSILS	RADIOLARIANS	DIATOMS	SECTION	METERS	GRAPHIC LITHOLOGY	SAMPLES
Quaternary / upper Pliocene	NN18		VR/P			1	0.5, 1.0	T2, T2, IW	* , *
			FC/M			2		T2, T2, T2, Void	
		B	RP	B		CC			

Ash layer, gray (5Y 6/1)

Flattened burrows

T2 5GY 4/1

LITHOLOGIC DESCRIPTION

HEMIPELAGIC MUDSTONE
Dark greenish gray (5GY 4/1)

Burrows are flattened

SMEAR SLIDE SUMMARY (%):

	1, 70	1, 113
	D	M
Texture:		
Sand	–	15
Silt	50	80
Clay	50	5
Composition:		
Quartz	40	3
Feldspar	10	2
Mica	Tr	–
Heavy minerals	Tr	Tr
Clay	40	5
Volcanic glass	8	90
Carbonate unspec.	Tr	–
Calc. nannofossils	Tr	–
Lithic fragments	2	Tr

SITE 582 HOLE B CORE 71 CORED INTERVAL 720.3–730.3 m

TIME – ROCK UNIT	BIOSTRATIGRAPHIC ZONE	FORAMINIFERS	NANNOFOSSILS	RADIOLARIANS	DIATOMS	SECTION	METERS	GRAPHIC LITHOLOGY	SAMPLES
upper Pliocene	NN18		CM			1	0.5		*
			CM				1.0	T2	
		FM	CM	B		CC			

T2

LITHOLOGIC DESCRIPTION

DRILL BRECCIA
Dark greenish gray (5GY 4/1)

SMEAR SLIDE SUMMARY (%):

	1, 85
Texture:	
Sand	–
Silt	60
Clay	40
Composition:	
Quartz	45
Feldspar	8
Mica	Tr
Heavy minerals	2
Clay	40
Volcanic glass	5
Pyrite	Tr
Foraminifers	Tr
Calc. nannofossils	Tr
Sponge spicules	Tr

SITE 582 HOLE B CORE 72 CORED INTERVAL 730.0–739.7 m

TIME – ROCK UNIT	BIOSTRATIGRAPHIC ZONE	FORAMINIFERS	NANNOFOSSILS	RADIOLARIANS	DIATOMS	SECTION	METERS	GRAPHIC LITHOLOGY	SAMPLES
upper Pliocene	NN18	B	CM	B		1, CC	0.5	T2	*

LITHOLOGIC DESCRIPTION

HEMIPELAGIC MUDSTONE
Dark greenish gray (5GY 4/1)

SMEAR SLIDE SUMMARY (%):

	1, 18
	D
Texture:	
Sand	2
Silt	58
Clay	40
Composition:	
Quartz	45
Feldspar	9
Mica	1
Heavy minerals	3
Clay	35
Micronodules	1
Carbonate unspec.	1
Calc. nannofossils	1
Sponge spicules	1
Lithic fragments	3

SITE 582 HOLE B CORE 73 CORED INTERVAL 739.7–749.4 m

TIME – ROCK UNIT	BIOSTRATIGRAPHIC ZONE	FORAMINIFERS	NANNOFOSSILS	RADIOLARIANS	DIATOMS	SECTION	METERS	GRAPHIC LITHOLOGY	SAMPLES
upper Pliocene	NN18					1	0.5, 1.0	T2, PP, T2, OG	*
						2		T2	
		FM	FP	B		CC			

Several light spots
Dark green laminations

LITHOLOGIC DESCRIPTION

HEMIPELAGIC MUDSTONE
5GY 4/1

SMEAR SLIDE SUMMARY (%):

	1, 90
	D
Texture:	
Sand	Tr
Silt	45
Clay	55
Composition:	
Quartz	28
Feldspar	5
Mica	1
Heavy minerals	2
Clay	50
Volcanic glass	5
Pyrite	2
Micronodules	Tr
Carbonate unspec.	1
Calc. nannofossils	5
Radiolarians	Tr
Sponge spicules	1
Fish remains	Tr
Plant debris	Tr

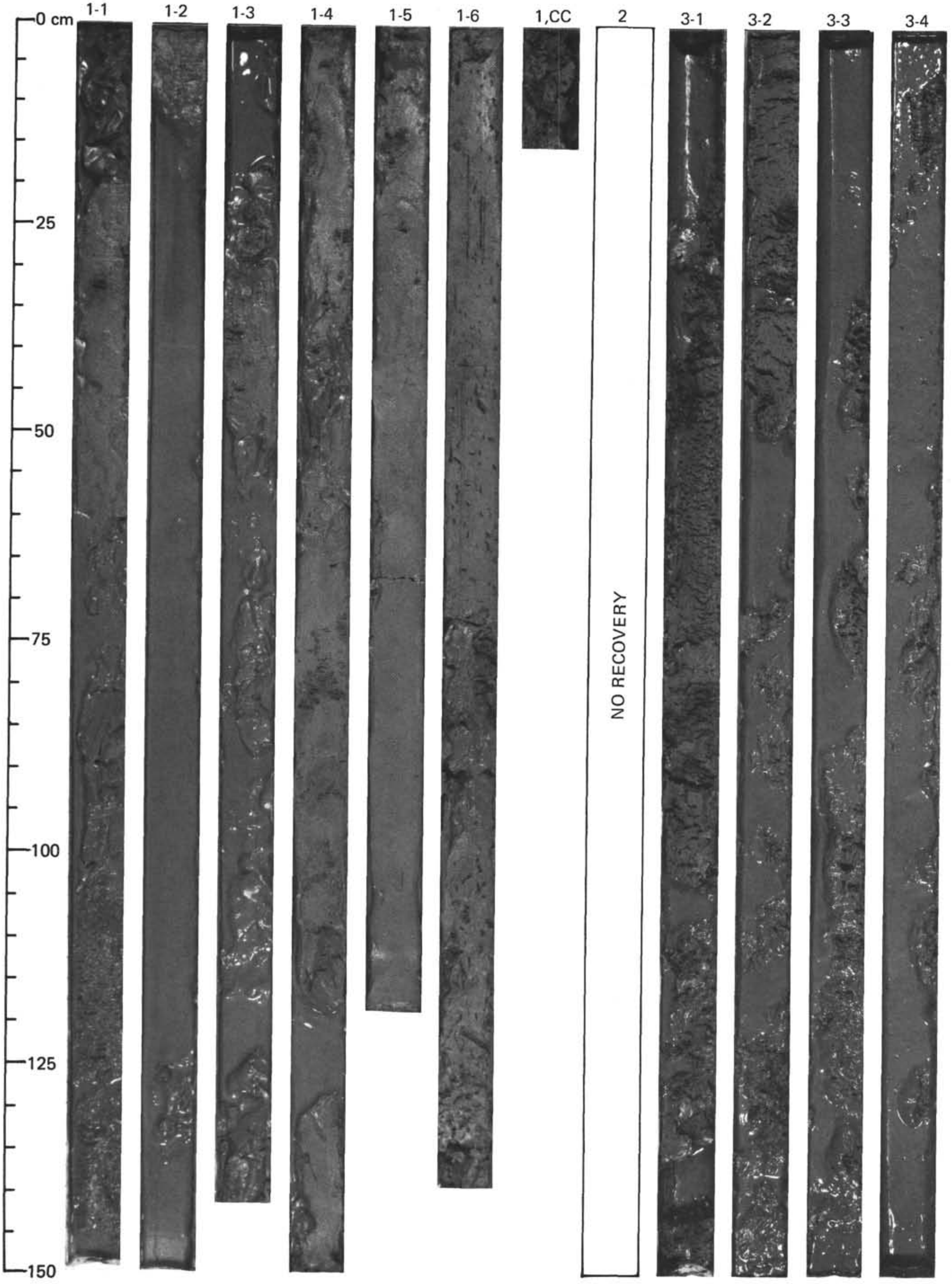
0 cm
25
50
75
100
125
150
1-1
1-2
1-3
1-4
1-5
1-6
1,CC
2
3-1
3-2
3-3
3-4
NO RECOVERY

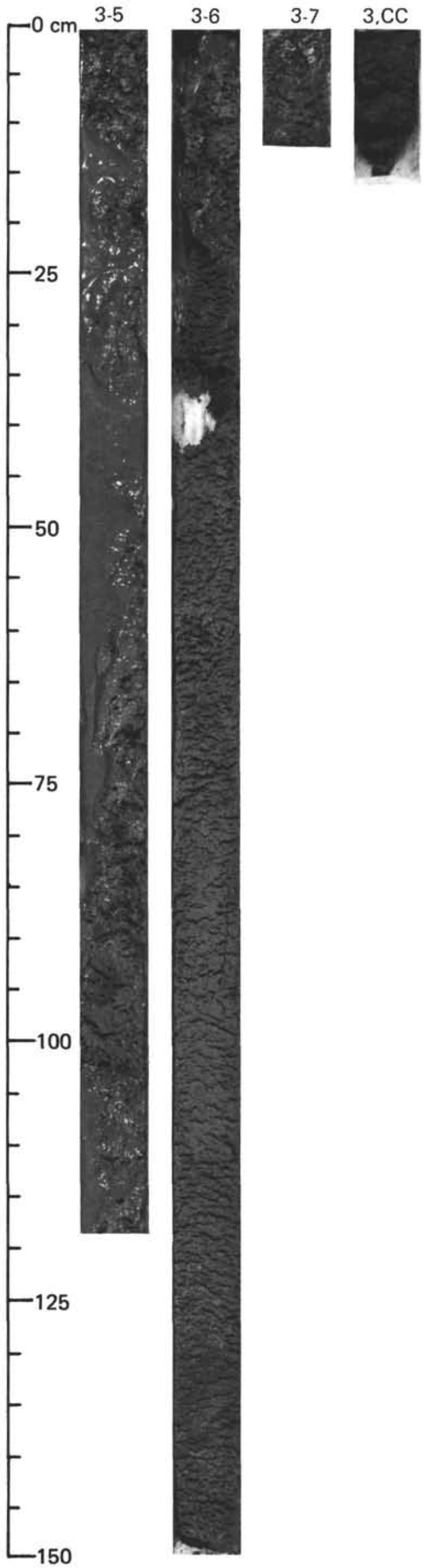
3-5
3-6
3-7
3,CC
0 cm
25
50
75
100
125
150

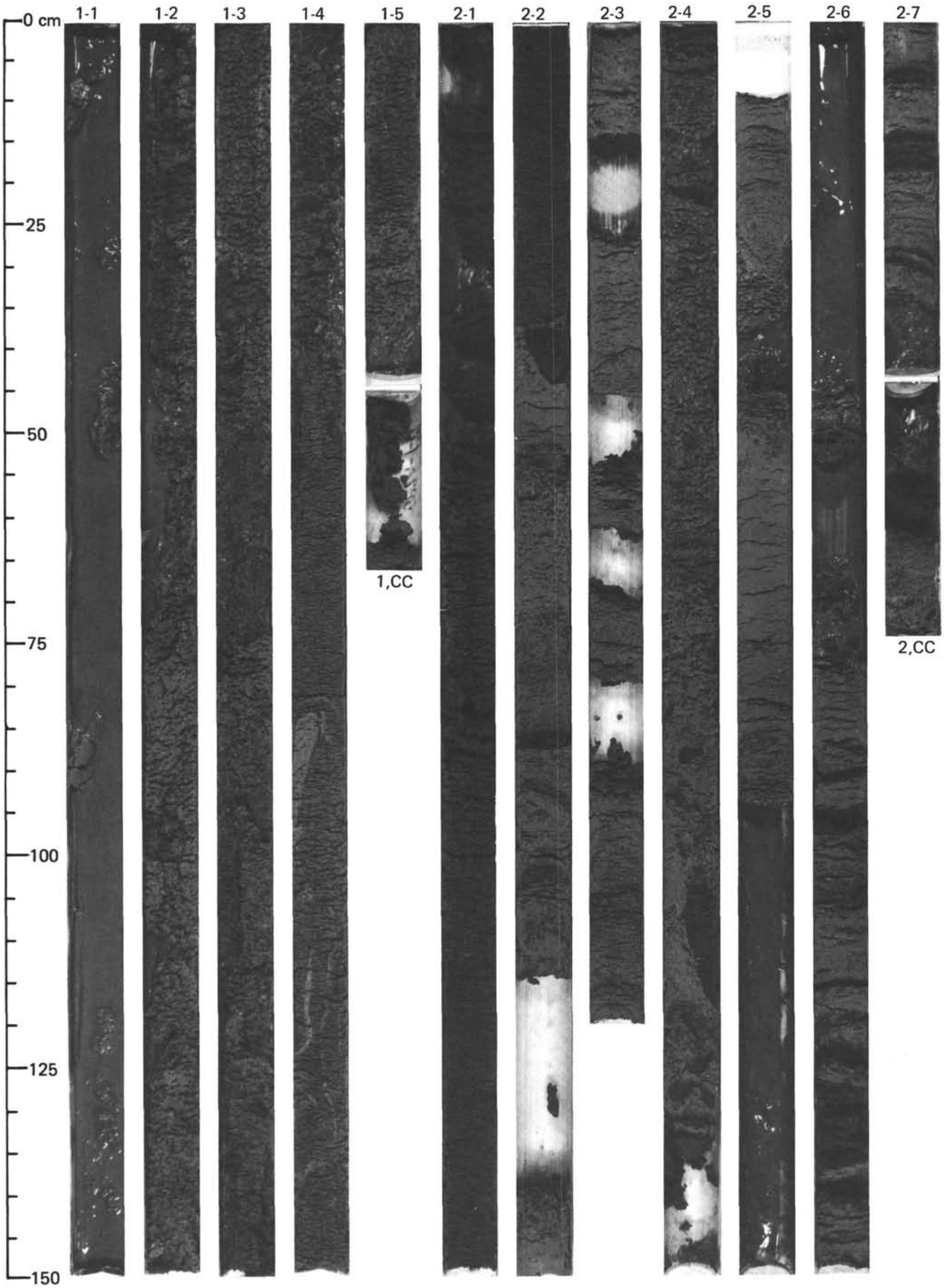
0 cm
25
50
75
100
125
150
1-1
1-2
1-3
1-4
1-5
1,CC
2-1
2-2
2-3
2-4
2-5
2-6
2-7
2,CC

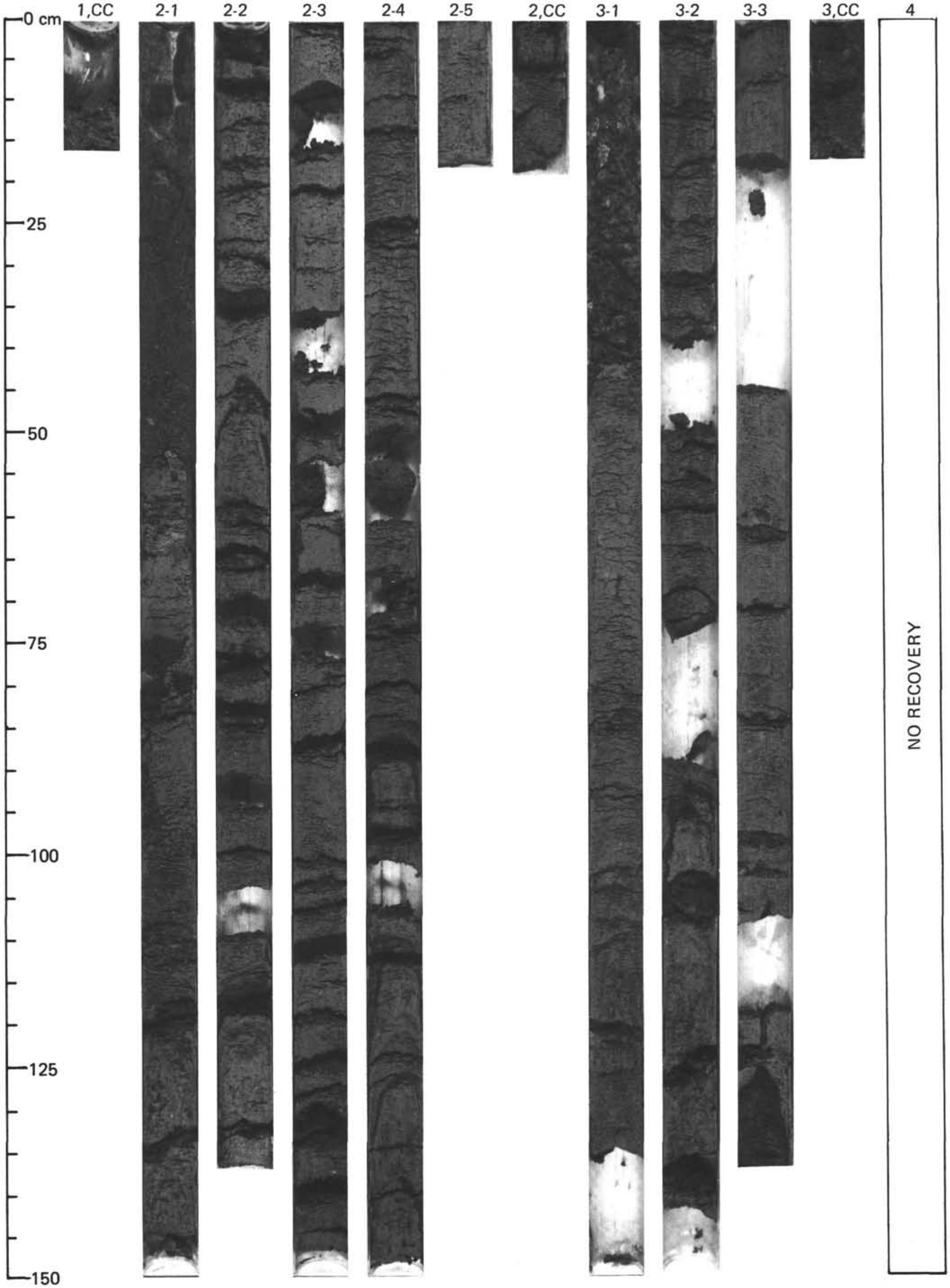
0 cm
25
50
75
100
125
150
1,CC
2-1
2-2
2-3
2-4
2-5
2,CC
3-1
3-2
3-3
3,CC
4
NO RECOVERY

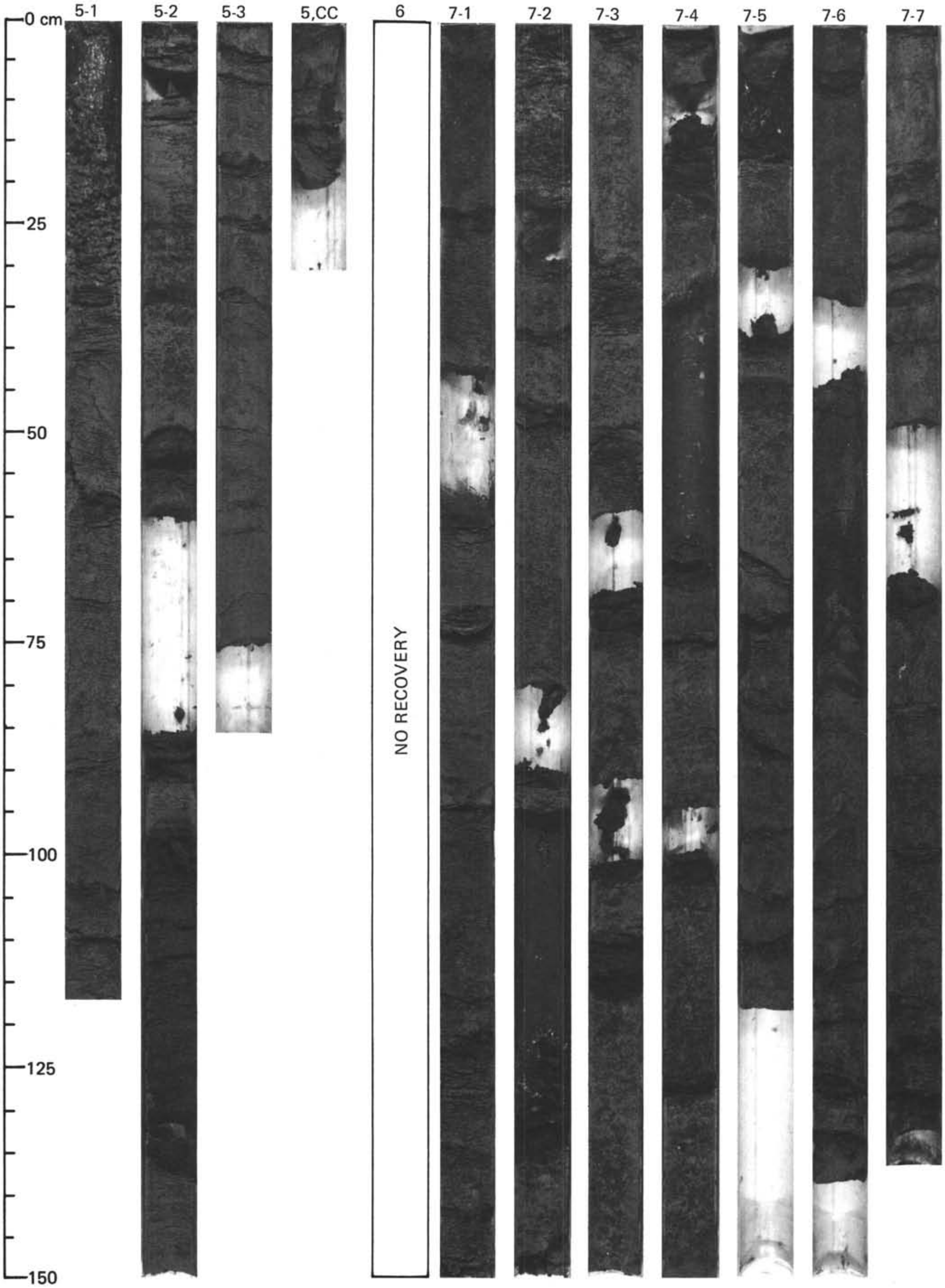
0 cm
25
50
75
100
125
150
5-1
5-2
5-3
5,CC
6
NO RECOVERY
7-1
7-2
7-3
7-4
7-5
7-6
7-7

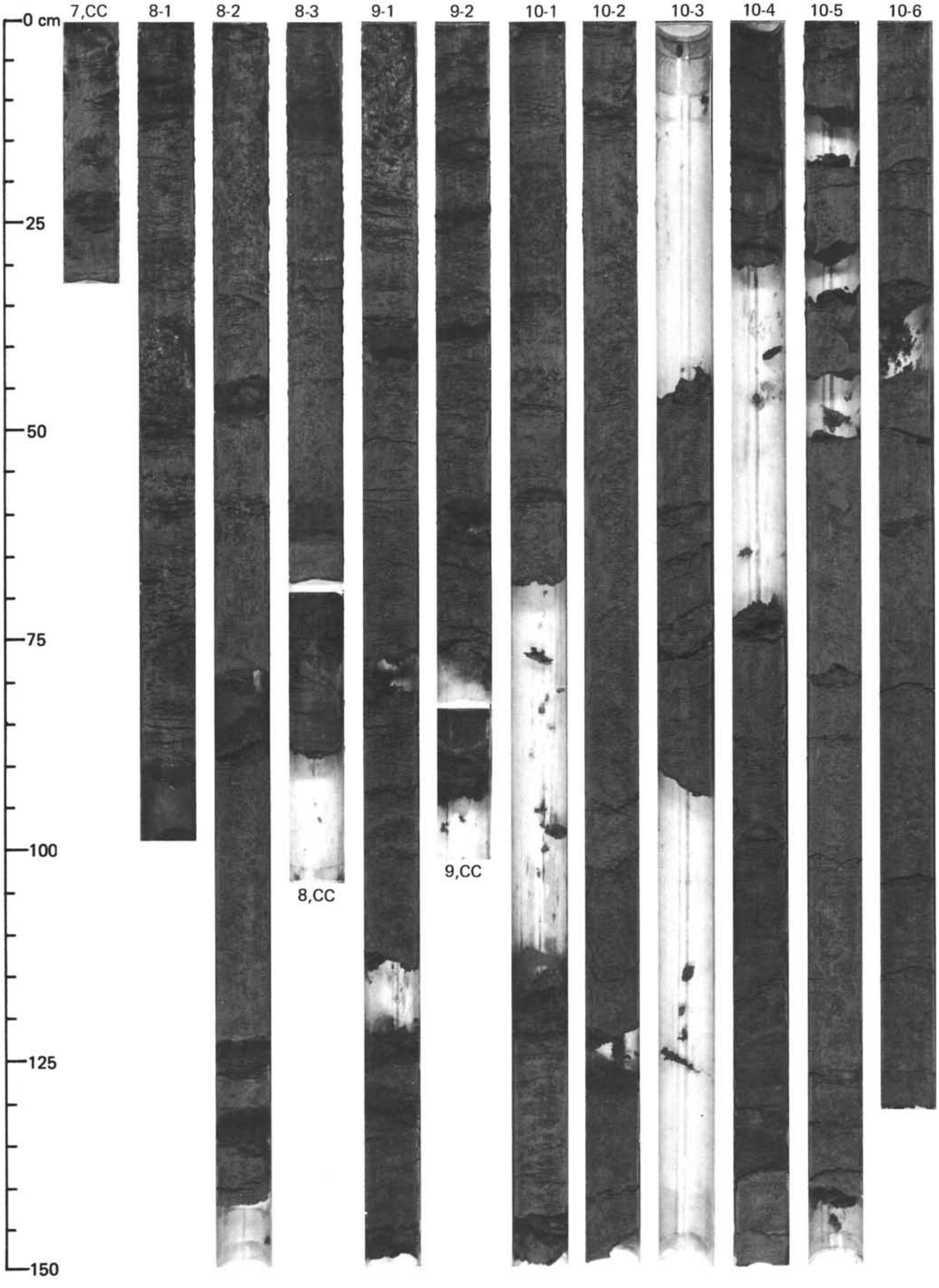
0 cm
25
50
75
100
125
150
7,CC
8-1
8-2
8-3
9-1
9-2
10-1
10-2
10-3
10-4
10-5
10-6
8,CC
9,CC

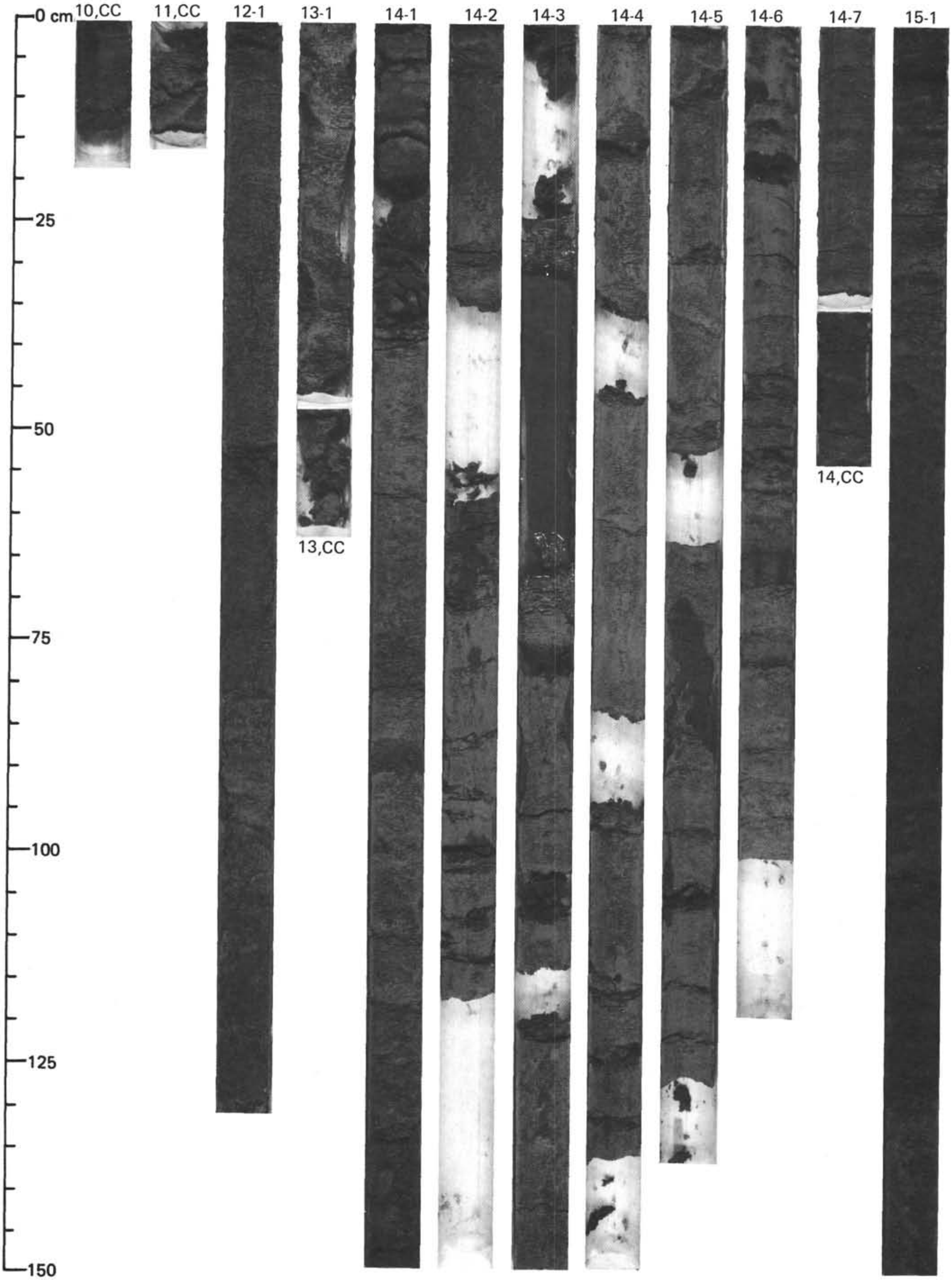
0 cm
25
50
75
100
125
150
10,CC
11,CC
12-1
13-1
13,CC
14-1
14-2
14-3
14-4
14-5
14-6
14-7
14,CC
15-1

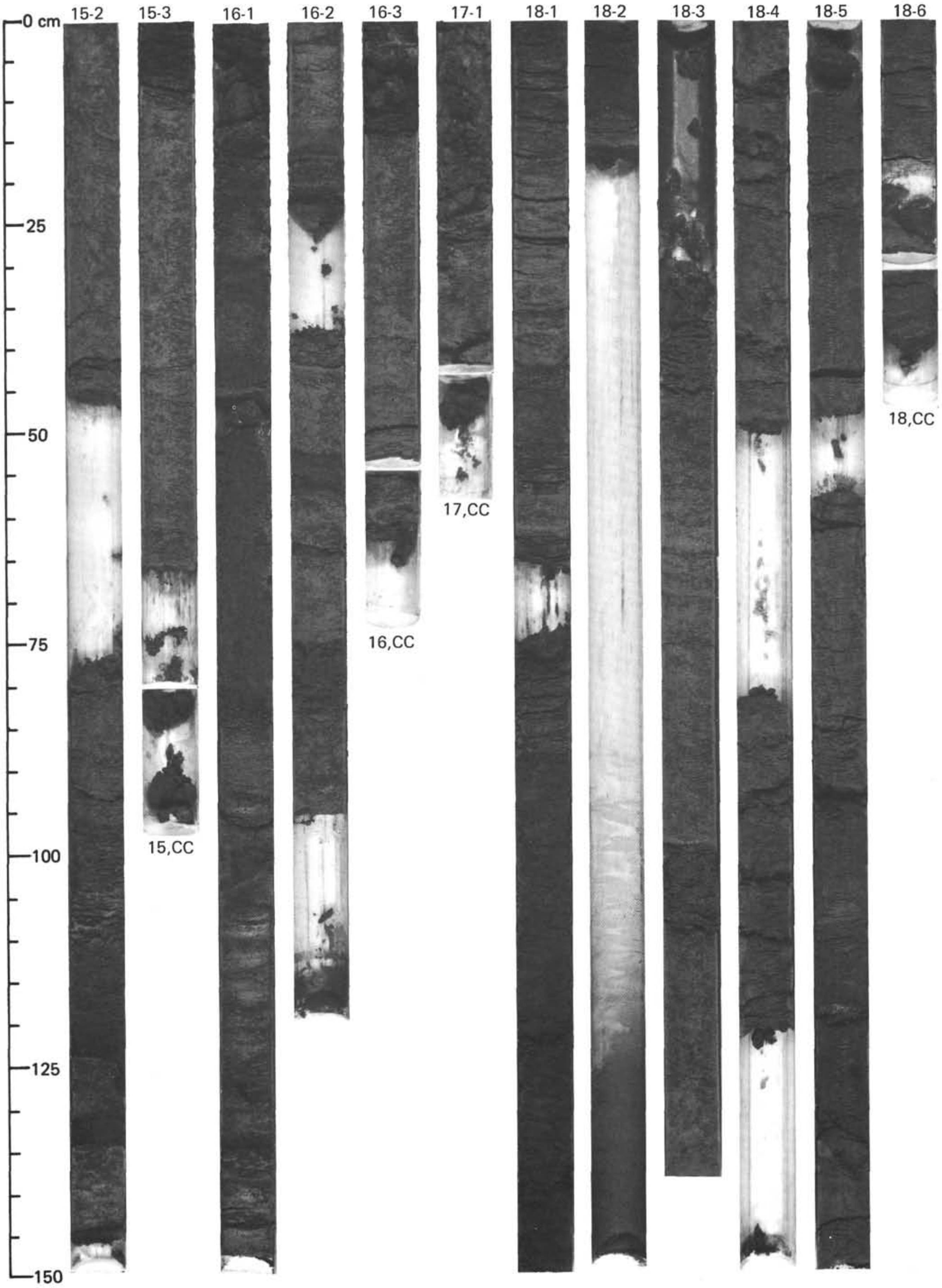

0 cm
25
50
75
100
125
150
15-2
15-3
16-1
16-2
16-3
17-1
18-1
18-2
18-3
18-4
18-5
18-6
15,CC
16,CC
17,CC
18,CC

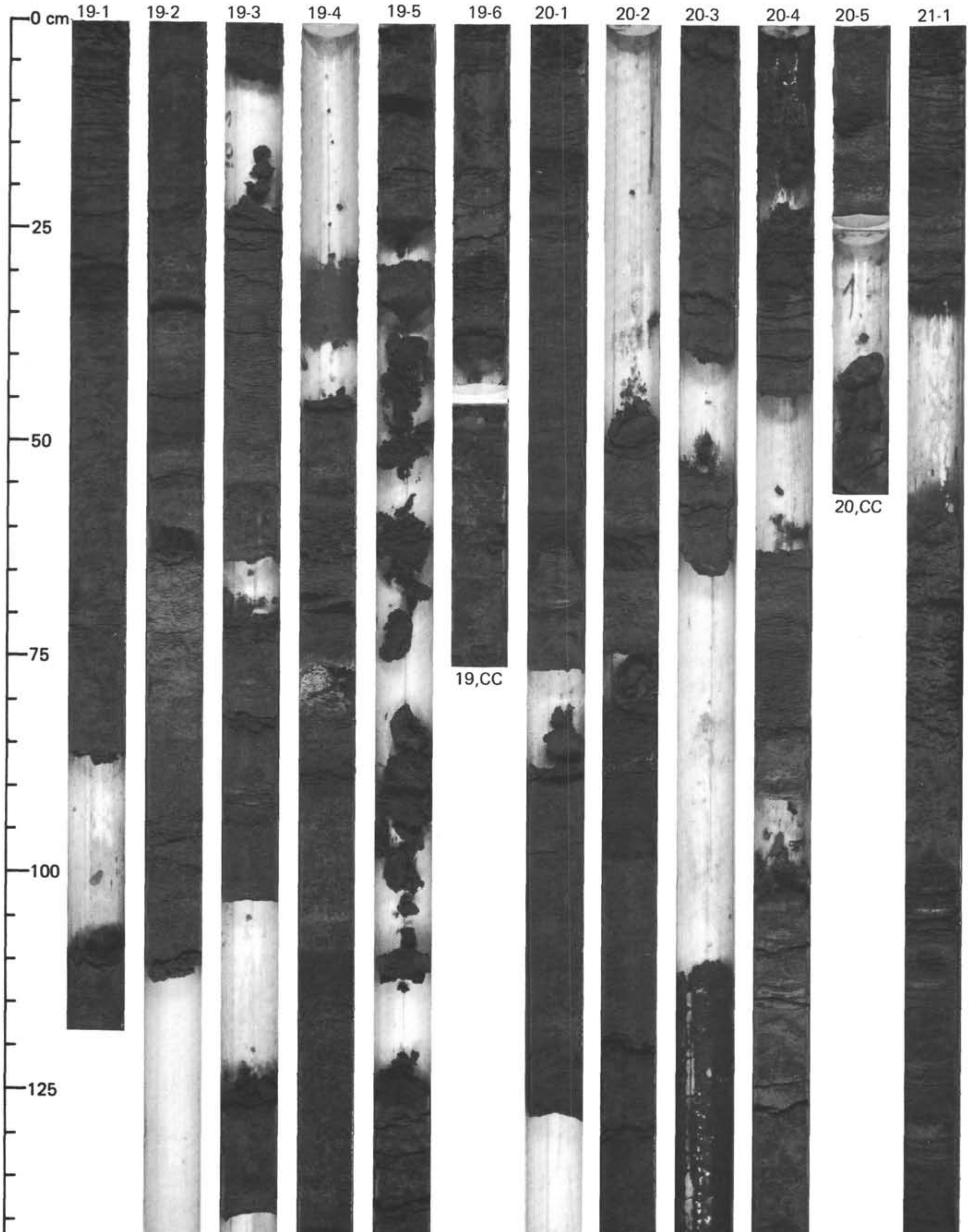
0 cm
25
50
75
100
125
150
19-1
19-2
19-3
19-4
19-5
19-6
19,CC
20-1
20-2
20-3
20-4
20-5
20,CC
21-1

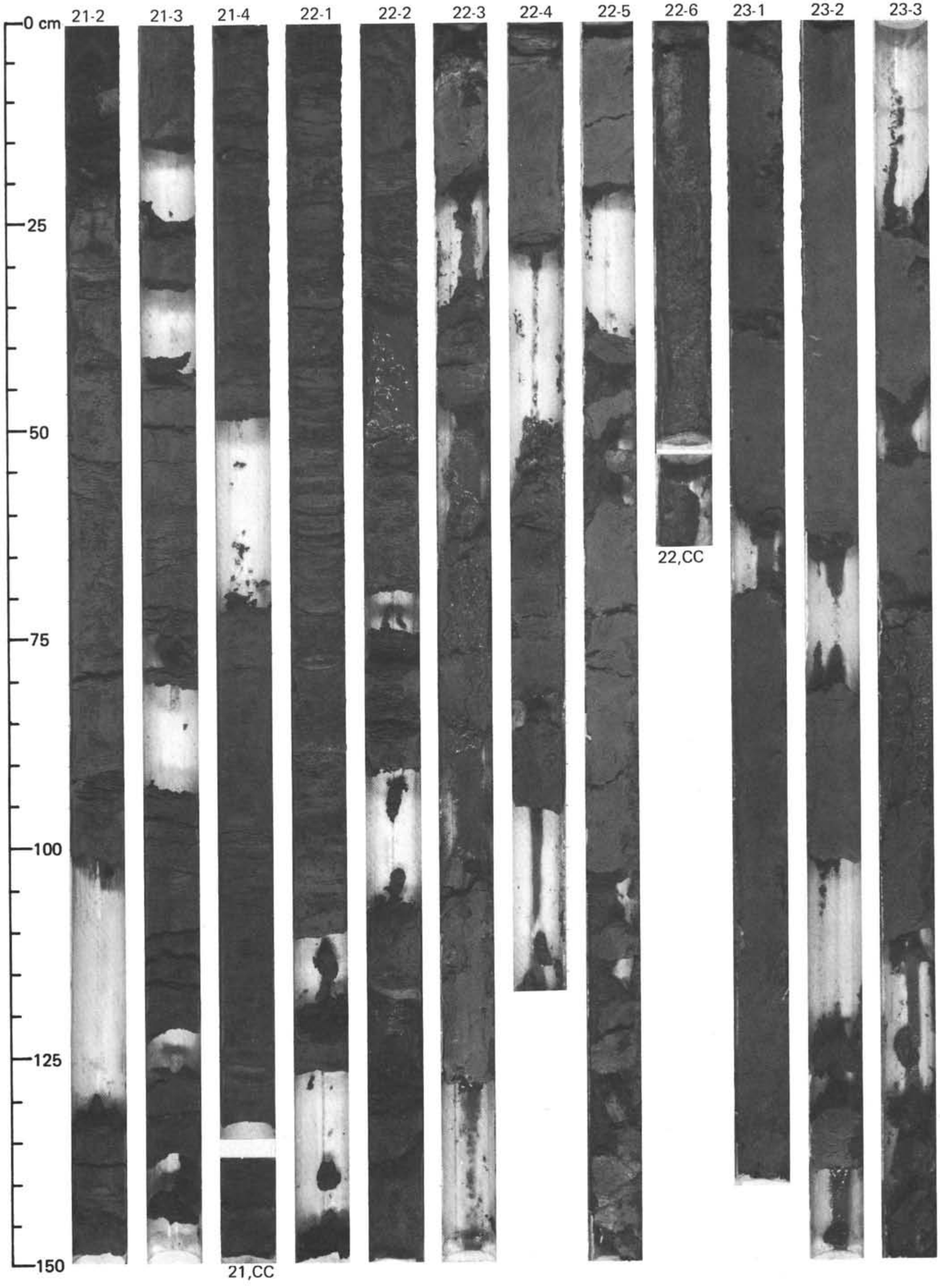
0 cm
25
50
75
100
125
150
21-2
21-3
21-4
21,CC
22-1
22-2
22-3
22-4
22-5
22-6
22,CC
23-1
23-2
23-3

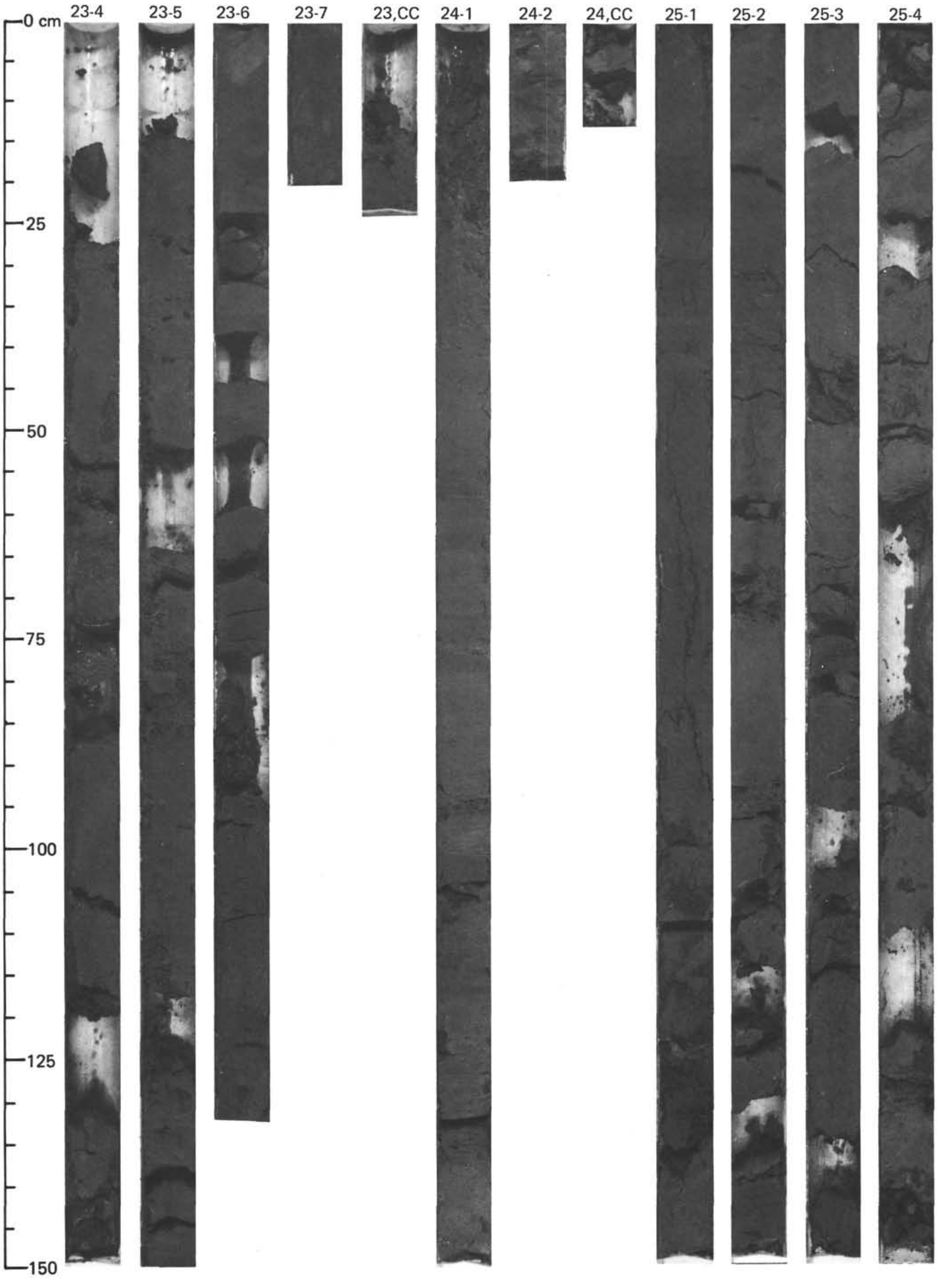
23-4
23-5
23-6
23-7
23,CC
24-1
24-2
24,CC
25-1
25-2
25-3
25-4
0 cm
25
50
75
100
125
150

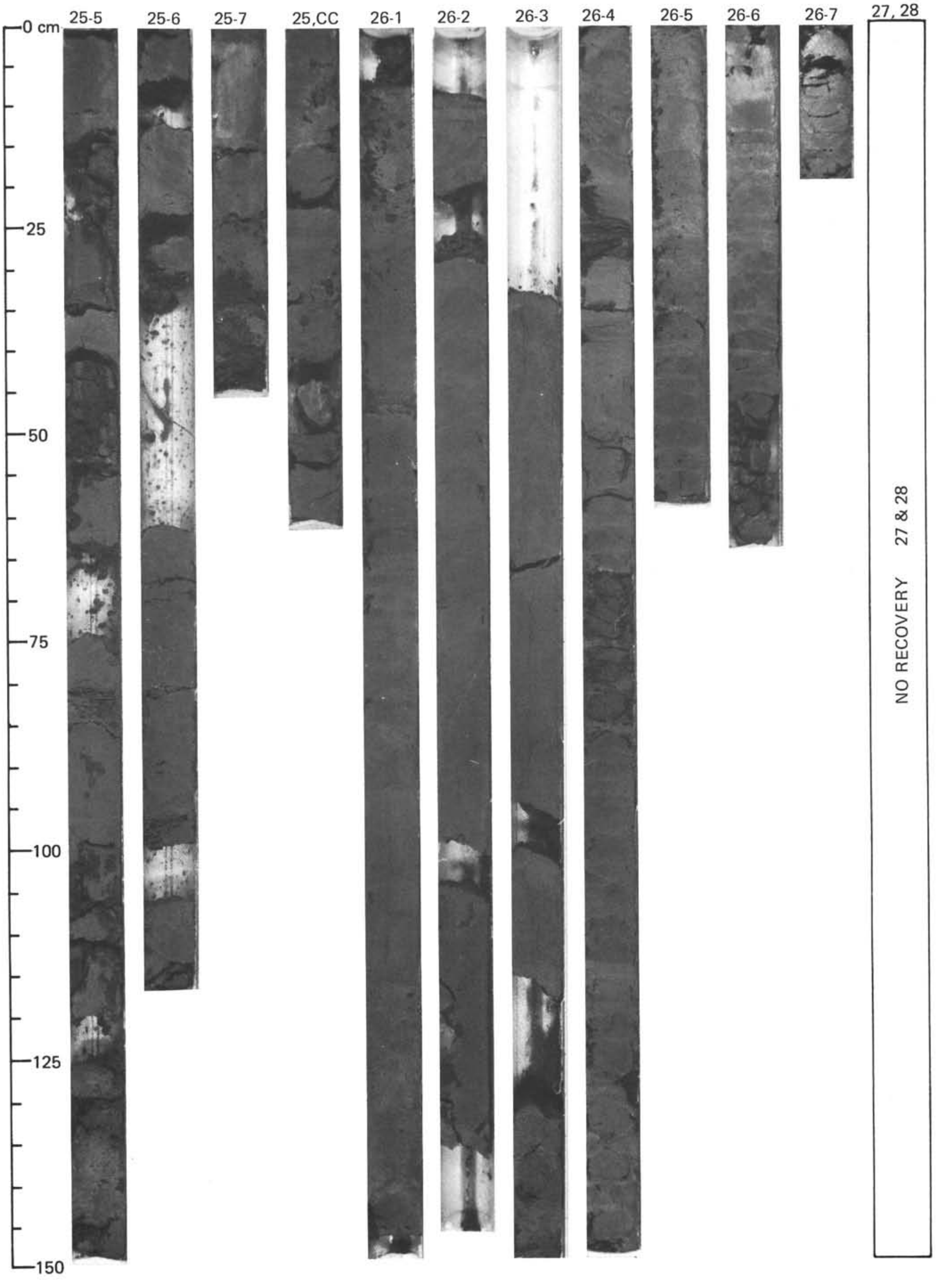
25-5
25-6
25-7
25,CC
26-1
26-2
26-3
26-4
26-5
26-6
26-7
27, 28
0 cm
25
50
75
100
125
150
NO RECOVERY 27 & 28

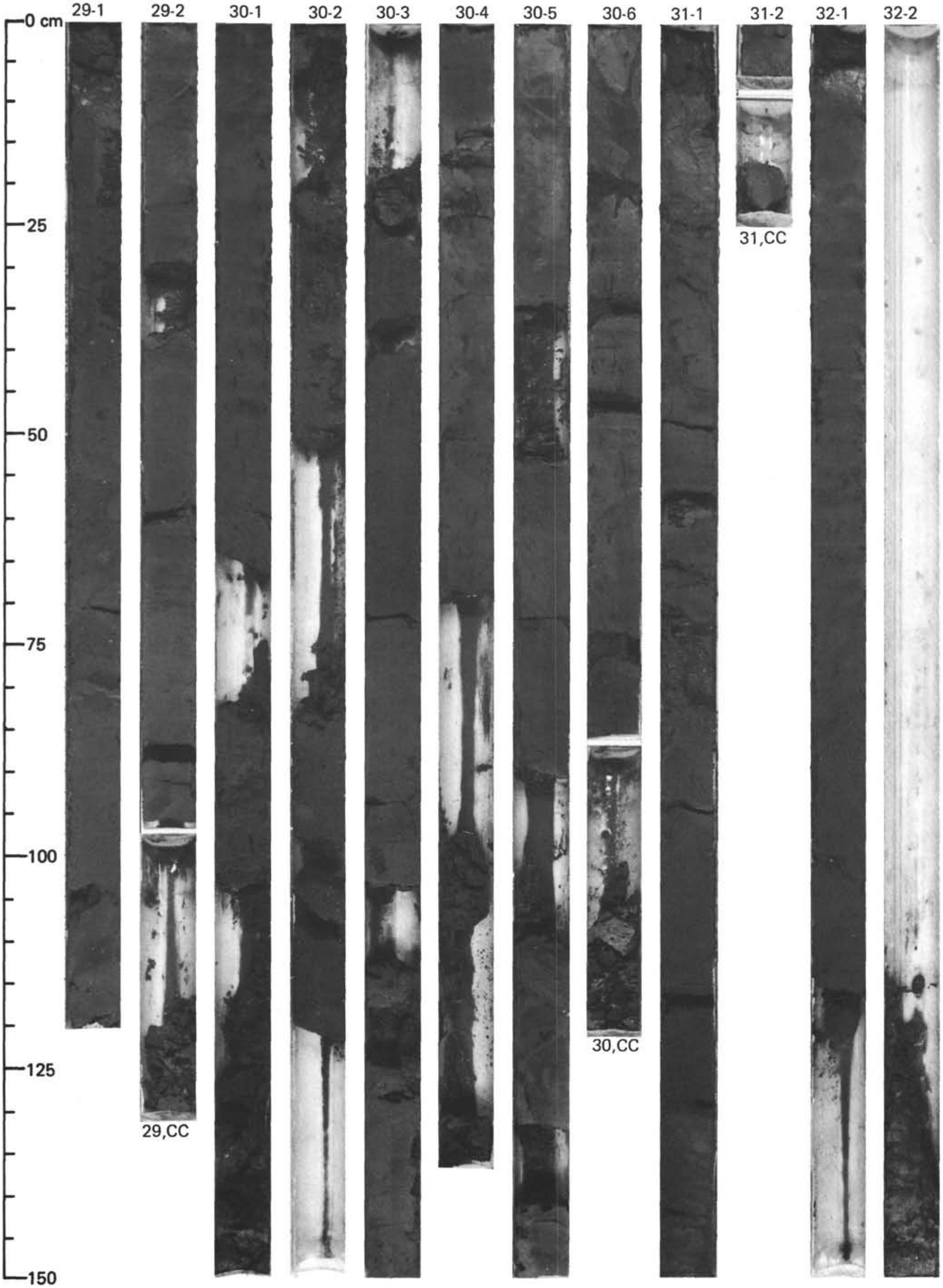
0 cm
25
50
75
100
125
150
29-1
29-2
30-1
30-2
30-3
30-4
30-5
30-6
31-1
31-2
32-1
32-2
31,CC
30,CC
29,CC

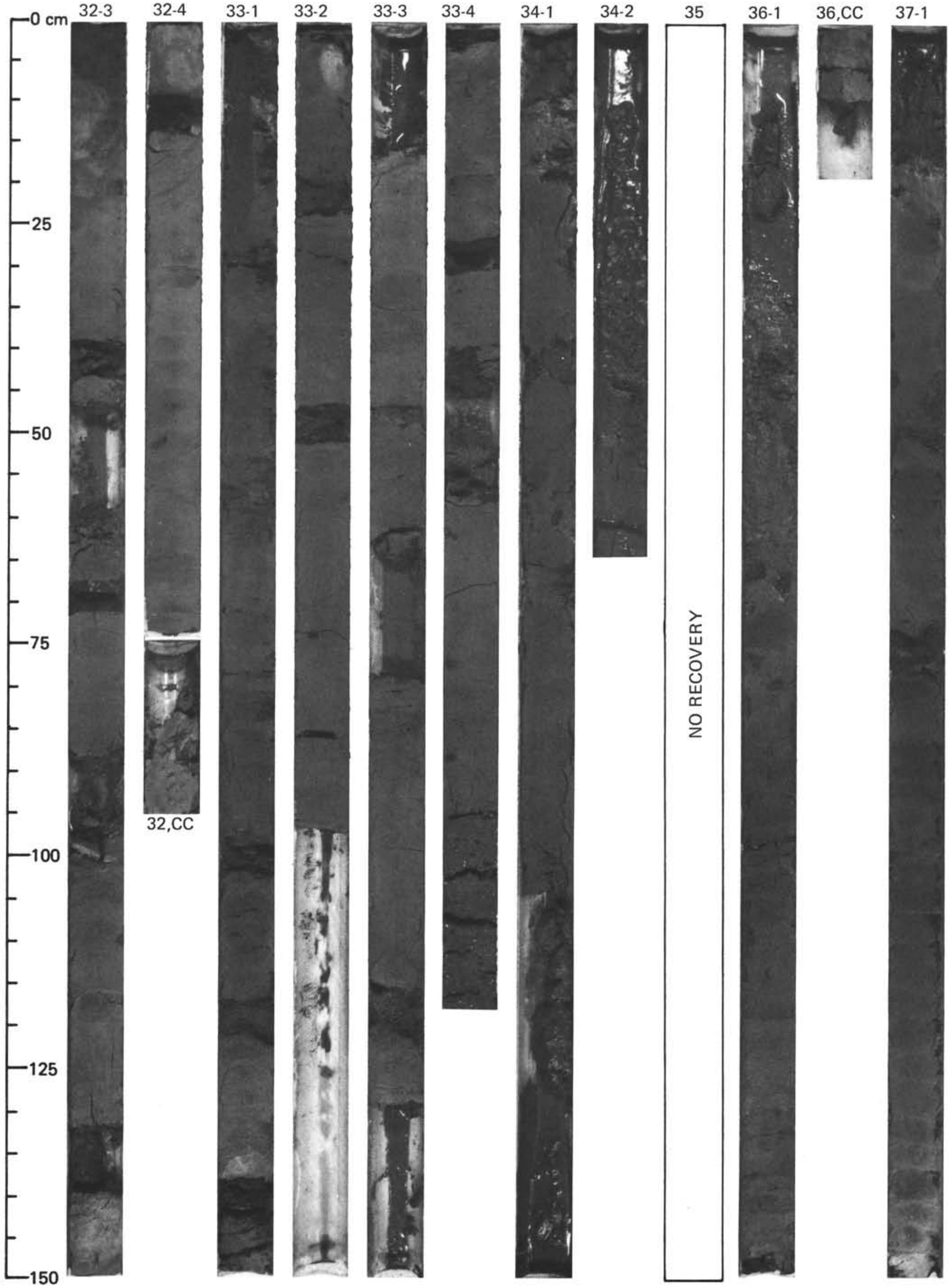
0 cm
25
50
75
100
125
150
32-3
32-4
32,CC
33-1
33-2
33-3
33-4
34-1
34-2
35
NO RECOVERY
36-1
36,CC
37-1

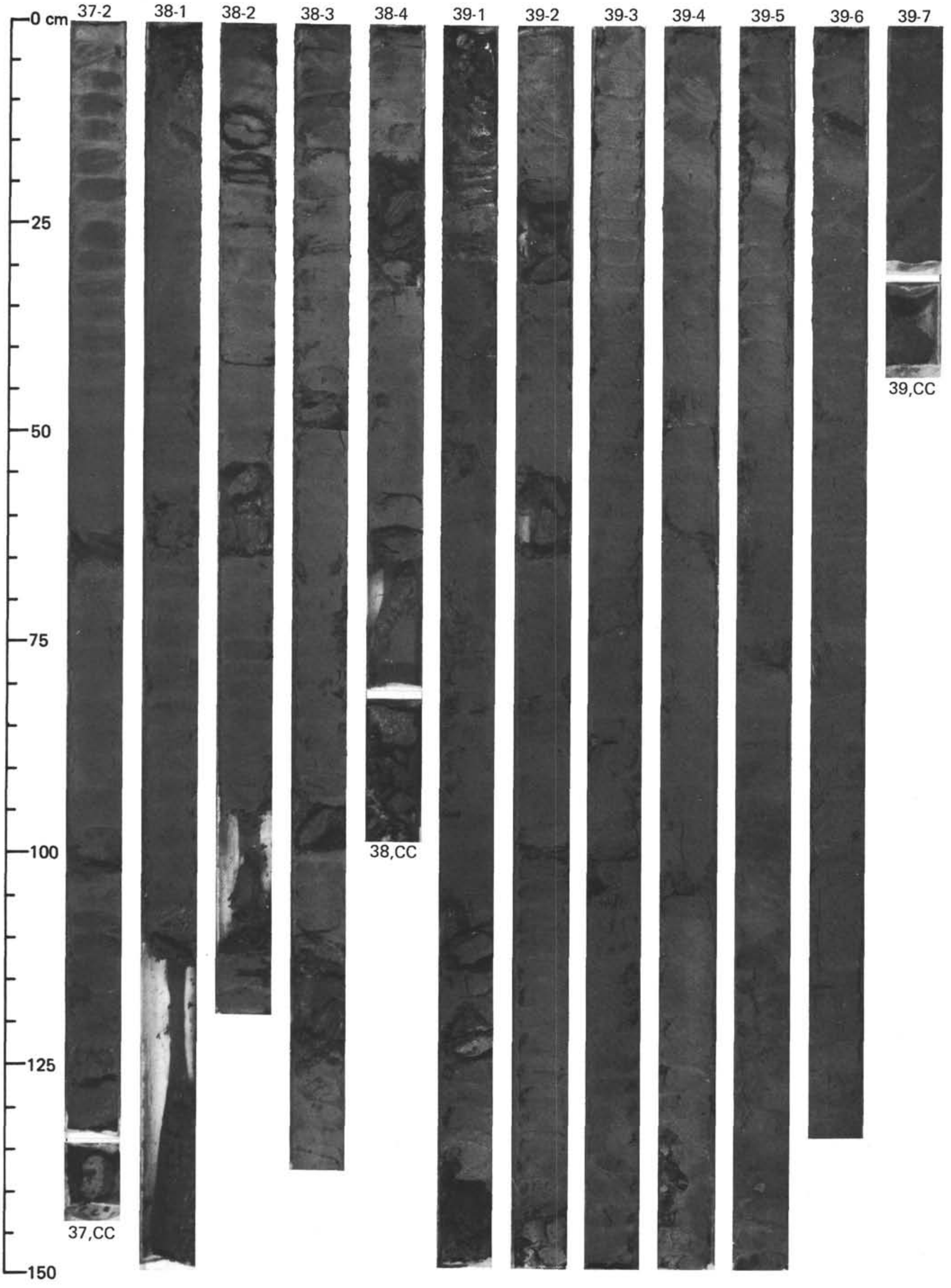
0 cm
25
50
75
100
125
150
37-2
38-1
38-2
38-3
38-4
39-1
39-2
39-3
39-4
39-5
39-6
39-7
37,CC
38,CC
39,CC

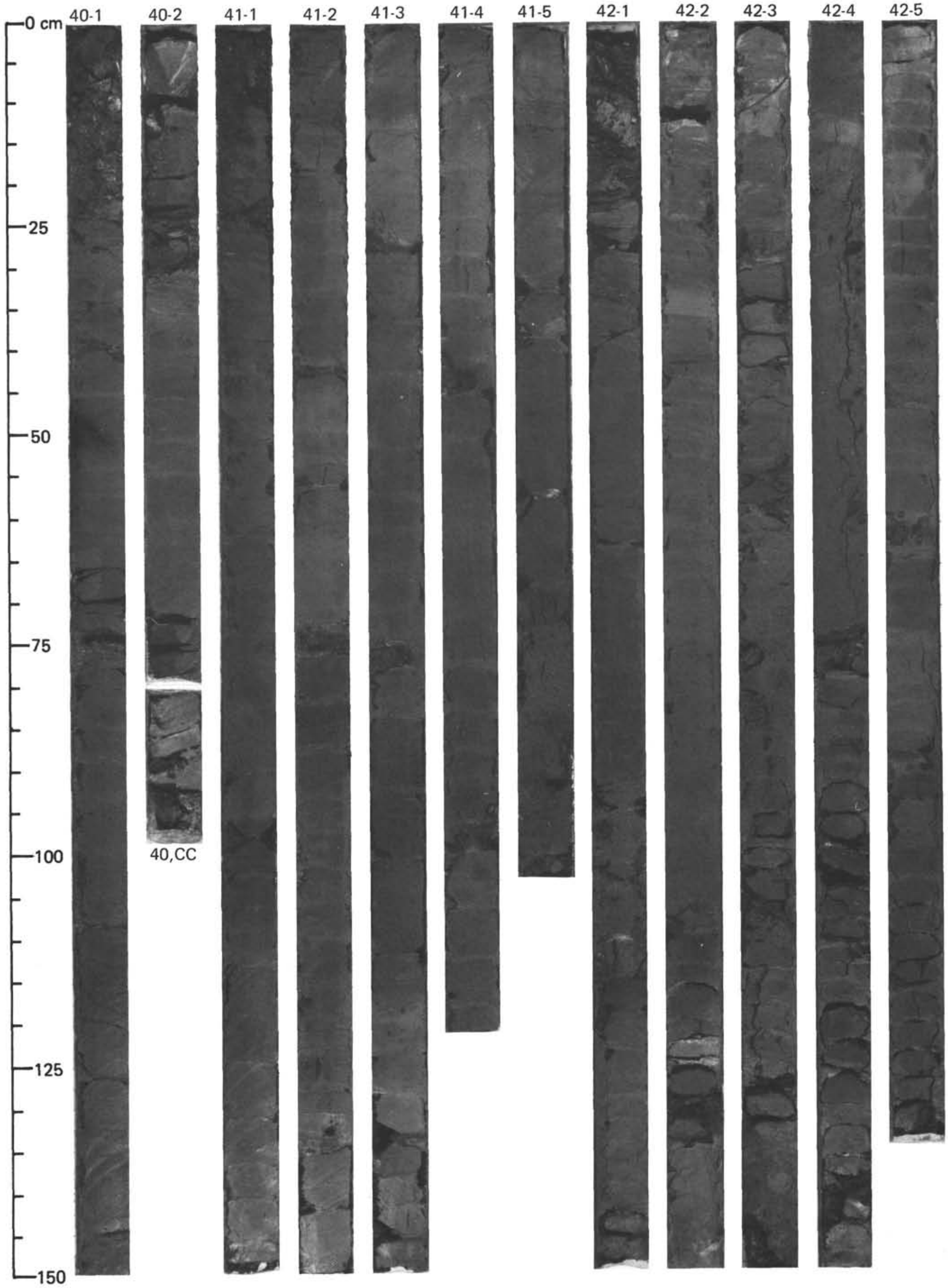
0 cm
25
50
75
100
125
150
40-1
40-2
40,CC
41-1
41-2
41-3
41-4
41-5
42-1
42-2
42-3
42-4
42-5

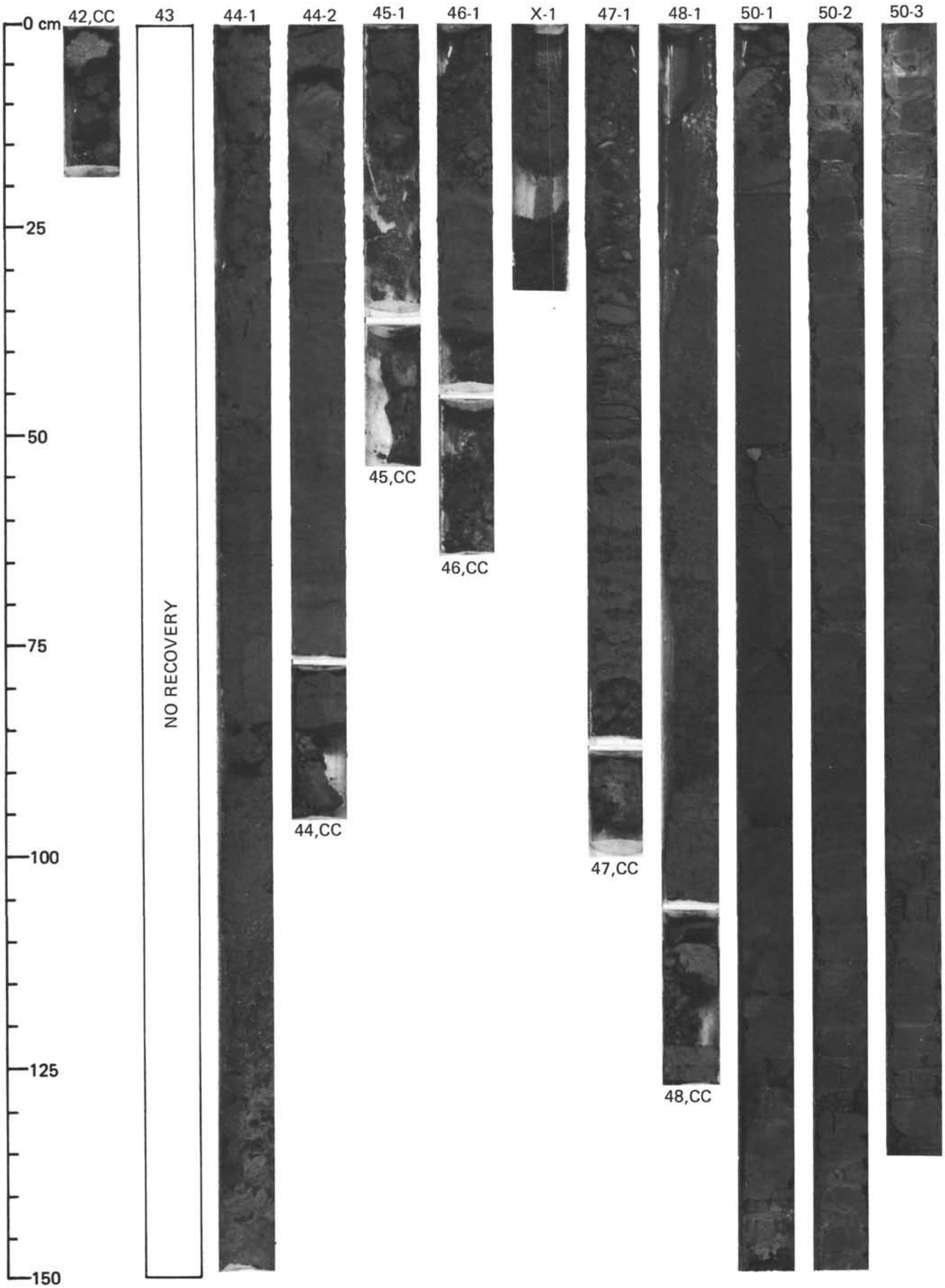
0 cm
25
50
75
100
125
150
42,CC
43
NO RECOVERY
44-1
44-2
44,CC
45-1
45,CC
46-1
46,CC
X-1
47-1
47,CC
48-1
48,CC
50-1
50-2
50-3

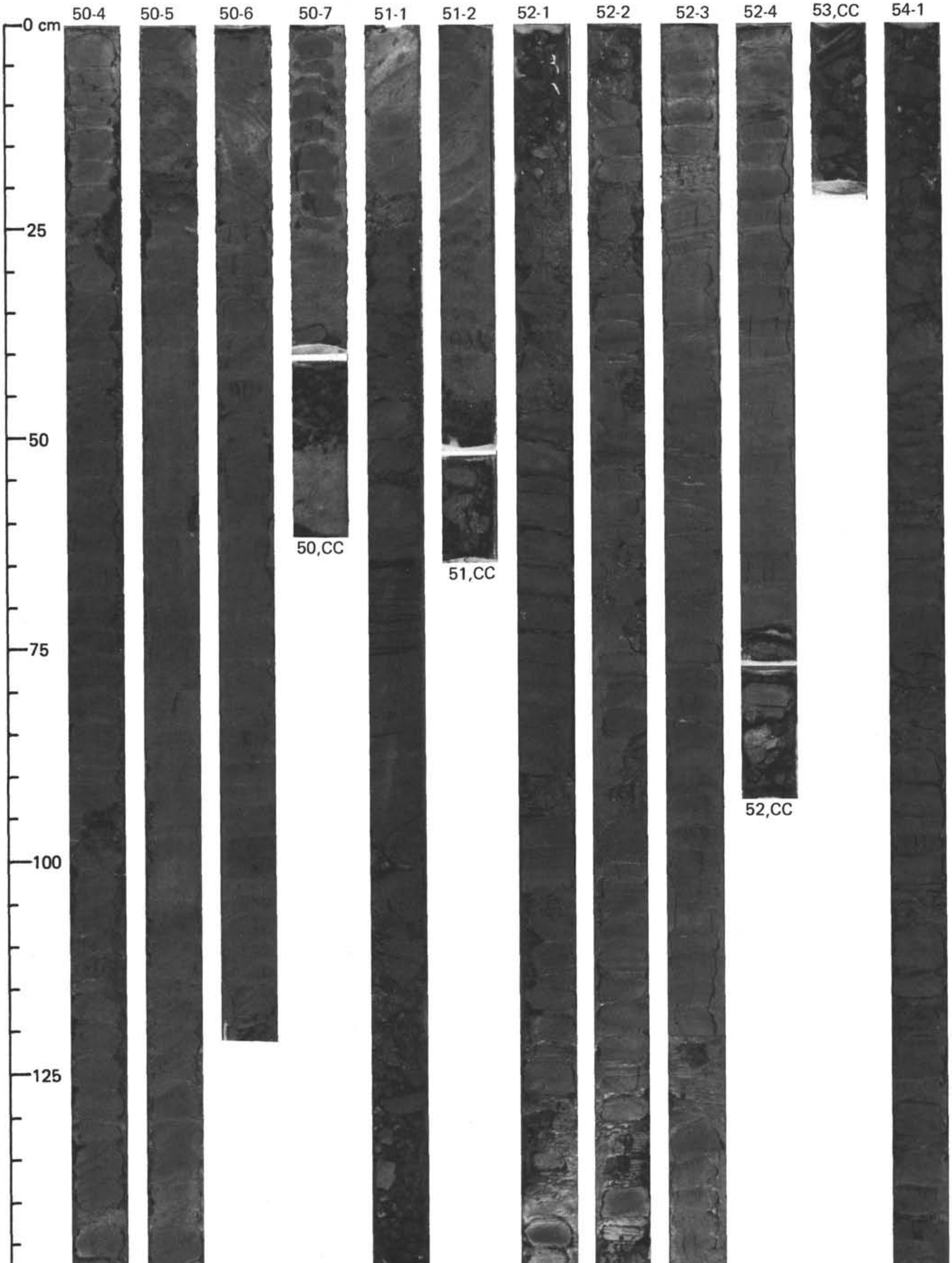
50-4
50-5
50-6
50-7
51-1
51-2
52-1
52-2
52-3
52-4
53,CC
54-1
50,CC
51,CC
52,CC
0 cm
25
50
75
100
125
150

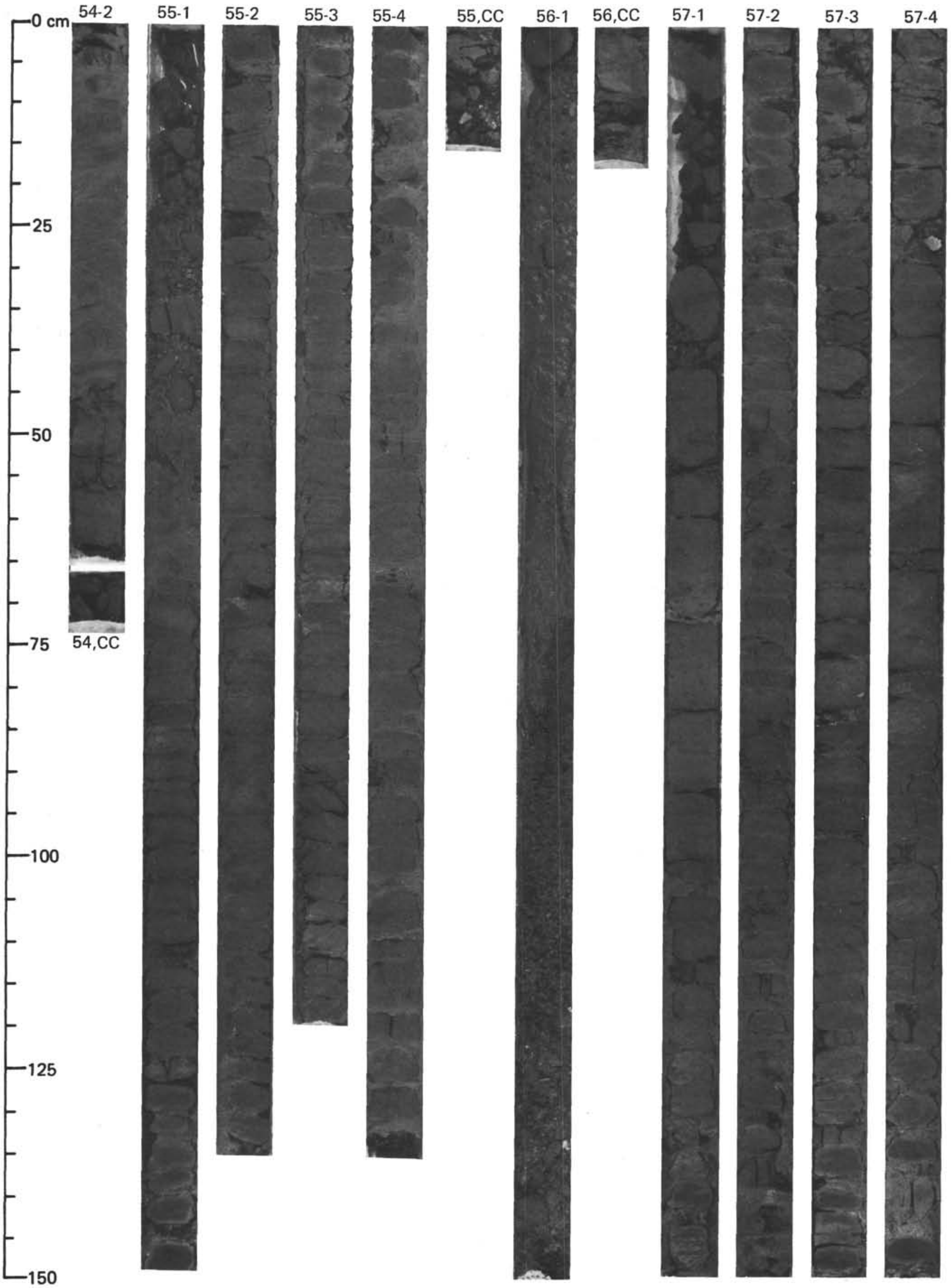
0 cm
25
50
75
100
125
150
54-2
54,CC
55-1
55-2
55-3
55-4
55,CC
56-1
56,CC
57-1
57-2
57-3
57-4

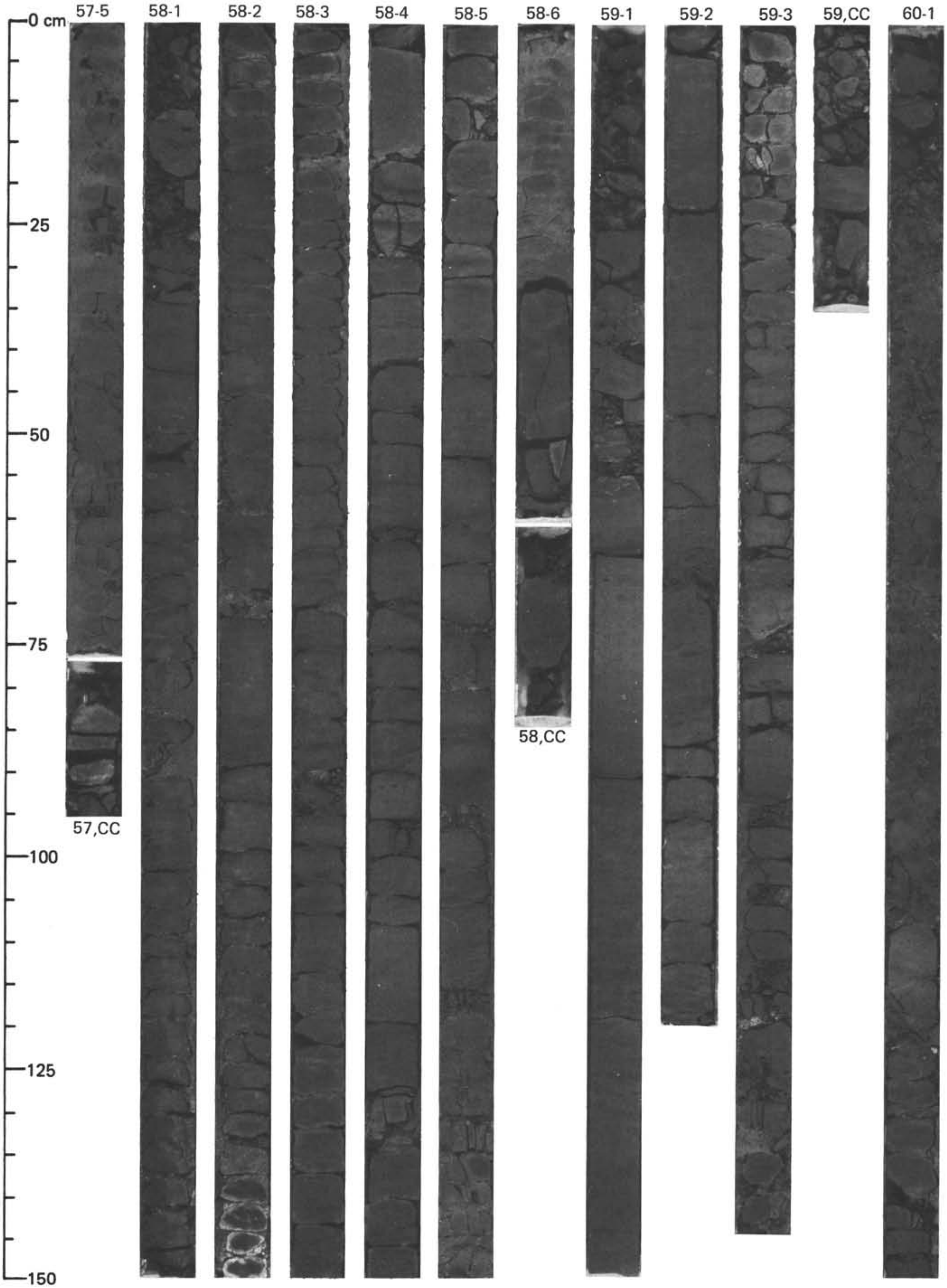
0 cm
25
50
75
100
125
150
57-5
58-1
58-2
58-3
58-4
58-5
58-6
59-1
59-2
59-3
59,CC
60-1
57,CC
58,CC

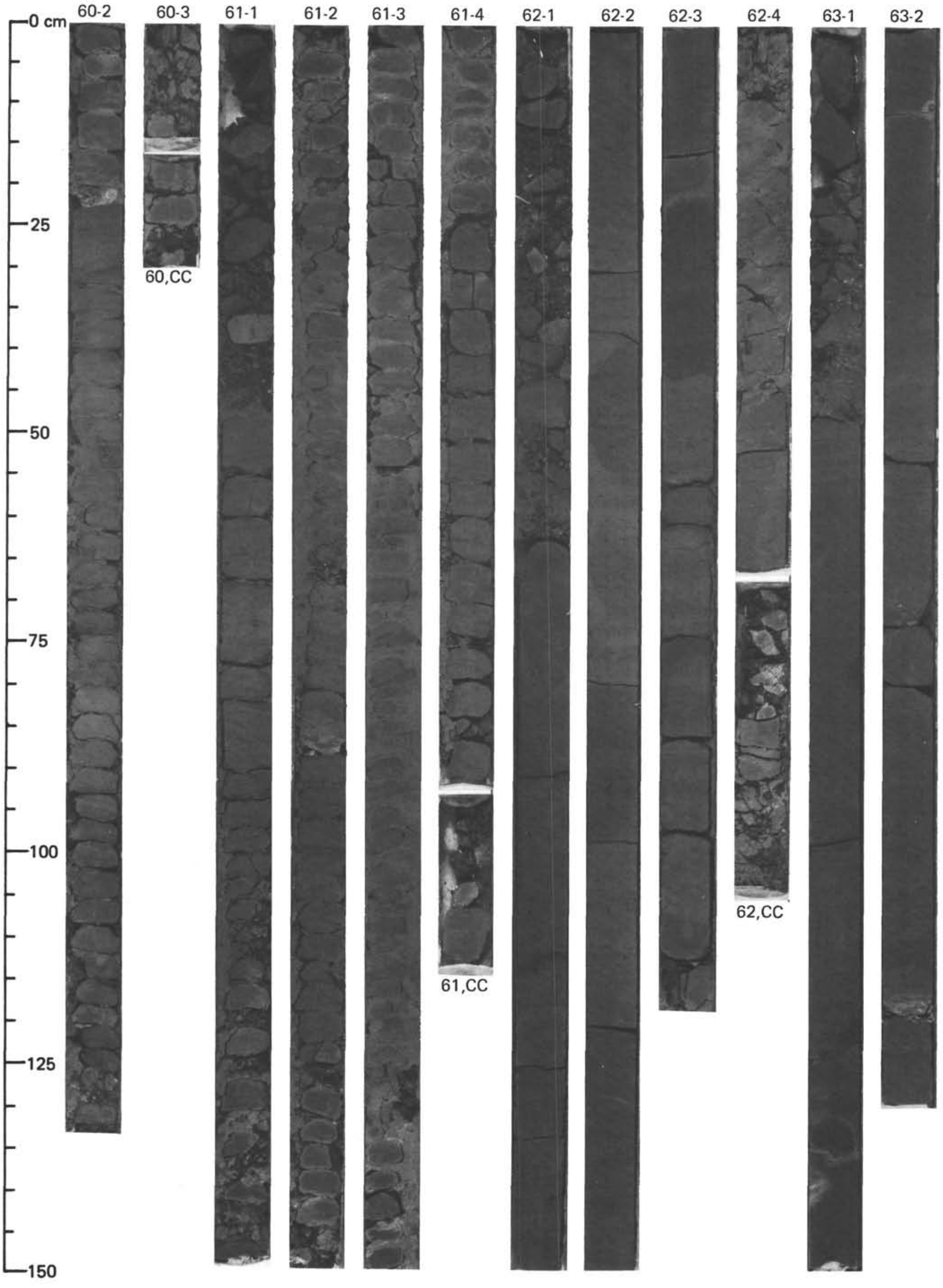

0 cm
25
50
75
100
125
150
60-2
60-3
60,CC
61-1
61-2
61-3
61-4
61,CC
62-1
62-2
62-3
62-4
62,CC
63-1
63-2

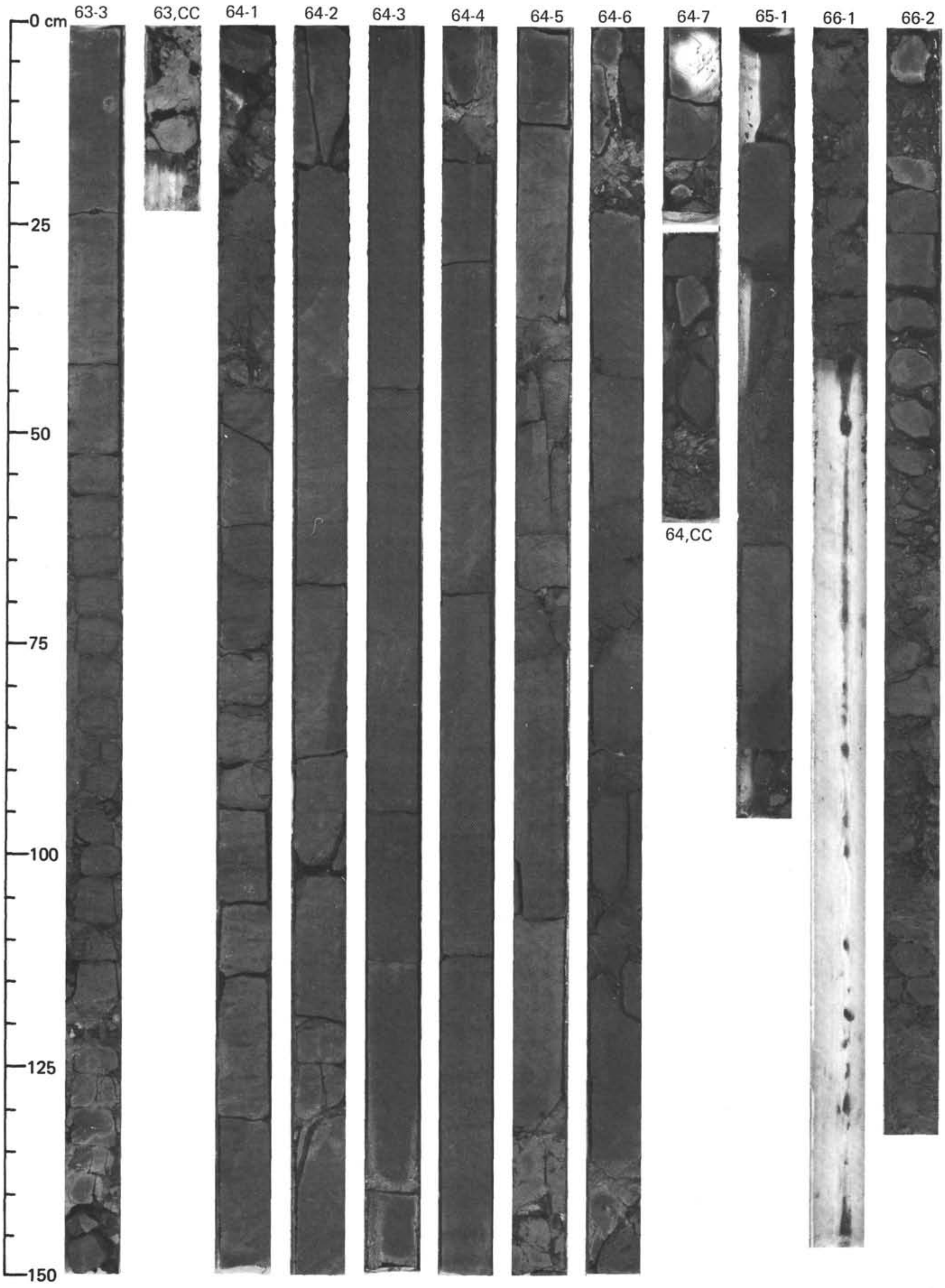
0 cm
25
50
75
100
125
150
63-3
63,CC
64-1
64-2
64-3
64-4
64-5
64-6
64-7
64,CC
65-1
66-1
66-2

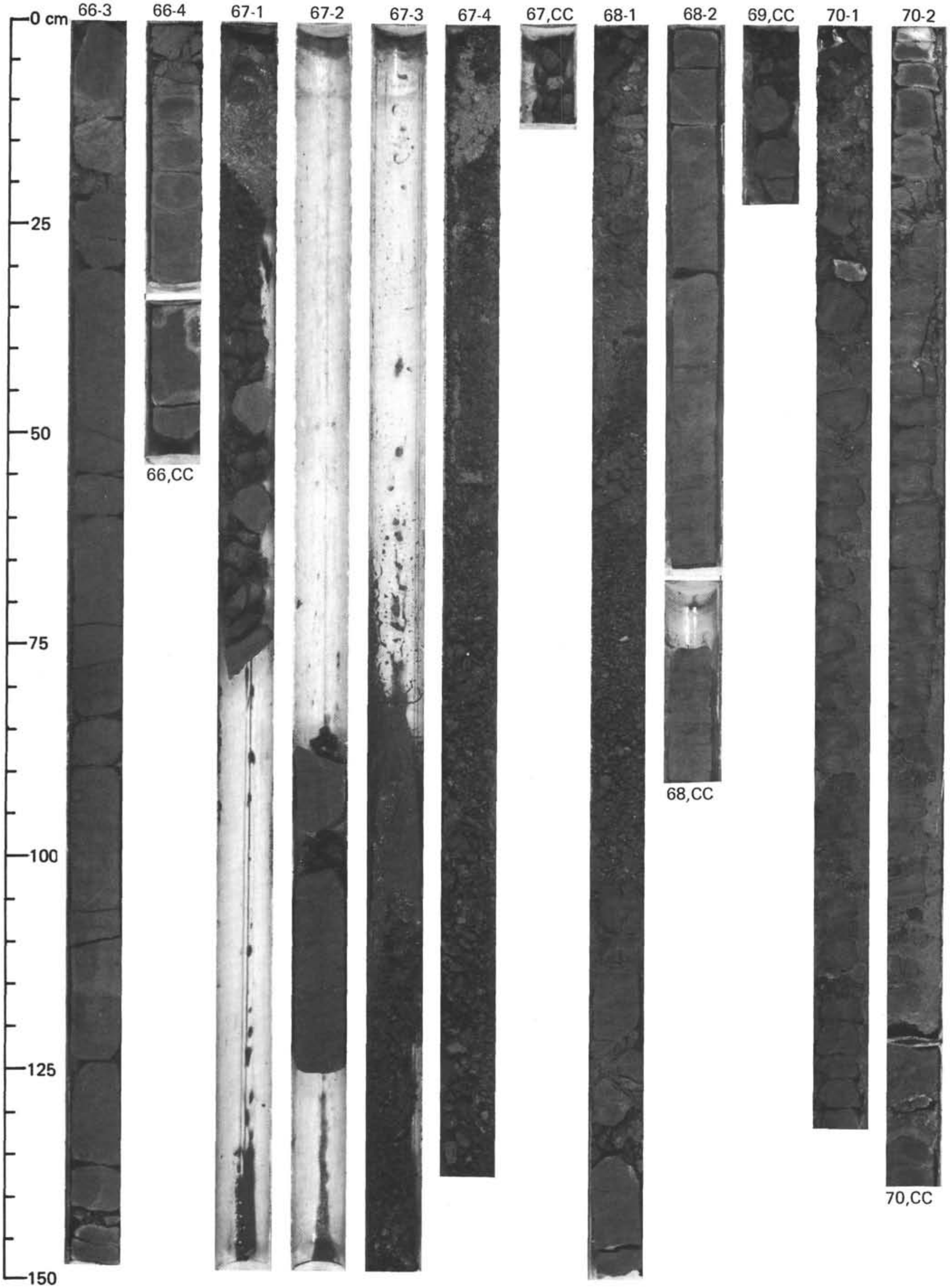
0 cm
25
50
75
100
125
150
66-3
66-4
66,CC
67-1
67-2
67-3
67-4
67,CC
68-1
68-2
68,CC
69,CC
70-1
70-2
70,CC

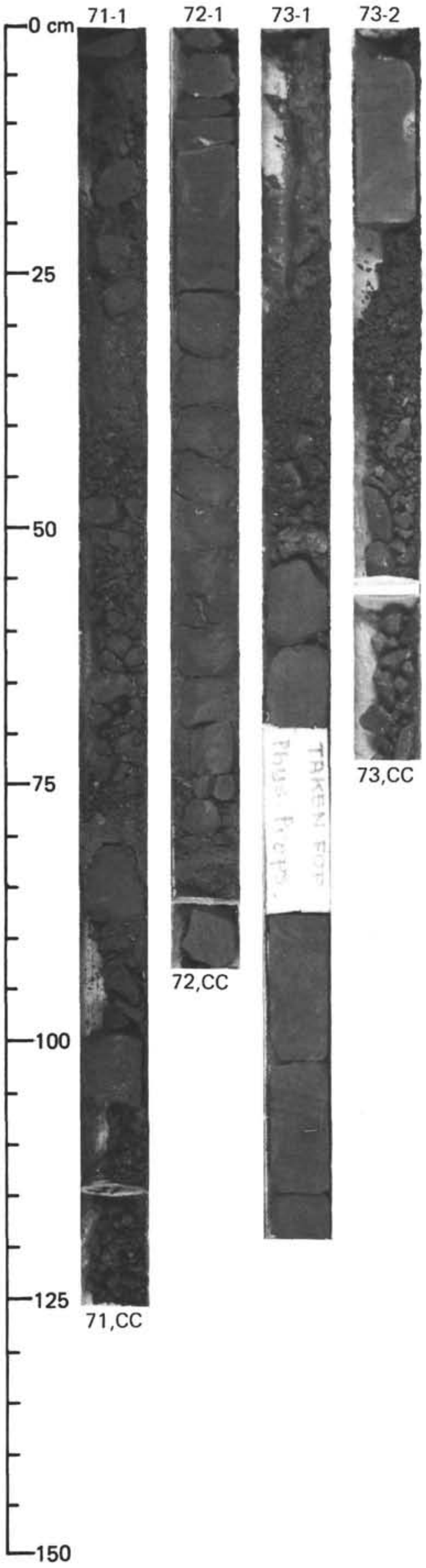
71-1
72-1
73-1
73-2
0 cm
25
50
75
100
125
150
71,CC
72,CC
73,CC
TAKEN FOR
Phys Props.